INFORMATION TO USERS

University of Alberta

Hydraulic Flood Routing with Minimal Channel Data

by

Kristi Ann McKay   ©

A thesis submitted to the Faculty of Graduate Studies and Research in partial

fulfillment of the requirements for the degree of Master of Science

in

Water Resources Engineering

Department of Civil and Environmental Engineering

Edmonton, Alberta

Spring 1997

National Library
of Canada

Bibliothèque nationale
du Canada

Acquisitions and
Bibliographic Services

Acquisitions et
services bibliographiques

395 Wellington Street
Ottawa ON K1A 0N4
Canada

395, rue Wellington
Ottawa ON K1A 0N4
Canada

Your file Votre référence

Our file Notre référence

The author has granted a non-exclusive licence allowing the National Library of Canada to reproduce, loan, distribute or sell copies of his/her thesis by any means and in any form or format, making this thesis available to interested persons.

L'auteur a accordé une licence non exclusive permettant à la Bibliothèque nationale du Canada de reproduire, prêter, distribuer ou vendre des copies de sa thèse de quelque manière et sous quelque forme que ce soit pour mettre des exemplaires de cette thèse à la disposition des personnes intéressées.

The author retains ownership of the copyright in his/her thesis. Neither the thesis nor substantial extracts from it may be printed or otherwise reproduced with the author's permission.

L'auteur conserve la propriété du droit d'auteur qui protège sa thèse. Ni la thèse ni des extraits substantiels de celle-ci ne doivent être imprimés ou autrement reproduits sans son autorisation.

0-612-21190-8

Canada

University of Alberta

Library Release Form

Name of author: Kristi Ann McKay
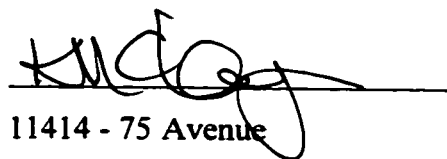
Title of Thesis: Hydraulic Flood Routing with Minimal Channel Data

Degree: Master of Science

Year this Degree Granted: 1997

Permission is hereby granted to the University of Alberta Library to reproduce single copies of this thesis and to lend or sell such copies for private, scholarly, or scientific research purposes only.

The author reserves all other publication and other rights in association with the copyright in the thesis, and except as hereinbefore provided, neither the thesis nor any substantial portion thereof may be printed or otherwise reproduced in any material form whatever without the author's prior written permission.

11414 - 75 Avenue

Edmonton, Alberta

T6G OH7

Date: JANUARY 29, 1997

University of Alberta

Faculty of Graduate Research
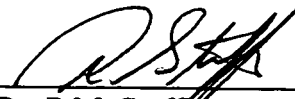
The undersigned certify that they have read, and recommend to the Faculty of Graduate Studies and Research for acceptance, a thesis entitled submitted by Kristi Ann McKay in partial fulfillment of the requirements for the degree of Master of Science in Water Resources Engineering.

F.E. Hicks
Dr. F.E. Hicks (Supervisor)

John Shaw
Dr. John Shaw (External Examiner)

P.M. Steffer
Dr. P.M. Steffler

Date: _JANUARY 27, 1997_

To Jamie and Oma,

who taught me the importance of

fantasy and reality

ABSTRACT

Flood forecasting involves the use of flood routing techniques in order to model the propagation of a flood wave, knowing the inflow into the study reach. It is important to the population residing and working along the river banks as it provides information regarding the river flow which is required for the design and maintenance of various structures located along the banks as well as for establishing a flood warning system.

When an hydraulic flood routing technique is applied for flood forecasting, topographic data describing the study reach is required in addition to the hydrologic data. Obtaining sufficient data to adequately define the channel geometry is costly. Since a decrease in government funding has lead (and will continue to lead) to the closure of streamflow gauges, the hydrologic data is not always available and the use of a hydraulic model becomes important in predicting flows between the existing gauges. Therefore, this study reviews the minimal channel data required in order to use an hydraulic flood routing model.

ACKNOWLEDGMENTS

On a more personal note, I would like to thank my parents and my brothers, Jason and John Allan for their love, support, and encouragement through the last two years (John Allan, I promise I will come home soon!), as well as the rest of my family who have been behind the scenes offering their encouragement (Opa and Grammy). I would also like to thank Jocelyn, Michel, and Greg, for being there with me almost every day; Michelle, for her love, support, encouragement, and typing skills; Christine, for the moral support throughout; Michelle (red), for the hideout and the thoughtful ear; Sheldon and Arbind, for the encouraging words and e-mails; as well as all of their families and significant others (Edie, Nathalie, Corbin, and Mavis).

TABLE OF CONTENTS

LIST OF TABLES

LIST OF FIGURES

LIST OF SYMBOLS

A = cross sectional area perpendicular to the flow

A_{HS} = area of the basin above the hydrometric station

A_P = area of the basin above the project station

B = width of rectangular cross section

b = the pack width

c = flood wave celerity

C_r = Courant number

g = acceleration due to gravity

H = depth of flow to the phreatic surface

H_0 = depth of flow downstream of the jam, prior to its release

H_1 = depth of flow including the surge

I_1 = inflow at time t_1

I_2 = inflow at time t_2

k = the composite roughness

k_i = the ice roughness

k_b = the bed roughness

m = coefficient between -1.0 and 1.0

O_1 = outflow at time t_1

O_2 = outflow at time t_2

Q = discharge

q = the discharge per unit width of channel

Q_{HS} = outflow from the basin at the hydrometric station

Q_P = outflow from the basin at the project station

S = the slope of the water surface (approximating the slope of the energy grade line)

S_f = longitudinal boundary friction slope

S_o = longitudinal channel bed slope

S_w = water surface slope

S_1 = storage at time t_1

S_2 = storage at time t_2

T_s = time storage of water

t = temporal coordinate

U = cross sectionally averaged longitudinal velocity

U_0 = cross sectionally averaged longitudinal velocity downstream of the jam, prior to its release

U_1 = cross sectionally averaged longitudinal velocity after the jam failure

V_w = the wave speed

x = longitudinal coordinate

α = kinematic wave speed coefficient

β = numerical constant determined by trial and error

μ = an internal friction - porosity coefficient

ρ_w = density of water

τ_o = bed shear stress

CHAPTER 1

INTRODUCTION

Flood forecasting involves using flood routing techniques to trace the propagation of a flood wave throughout a channel reach. This requires knowledge of the inflows to the reach from the upstream boundary and from the tributaries. The majority of communities are constructed along the river banks for water supply and sanitation, power, and transportation purposes. Therefore, the timing and magnitude of flood water levels is important to the residents of these communities.

There are two techniques currently available for flood routing: hydrologic flood routing and hydraulic flood routing. Hydrologic models have traditionally been used for flood routing. These models are based solely on the conservation of mass, with momentum effects handled only in a conceptual way. Therefore, the only data they require is streamflow data at the upstream and downstream ends of the reach as well as from the tributaries. These types of models are quite attractive since they are economical. However, due to their neglect of the conservation of momentum, they are not appropriate for modelling more dynamic events such as ice jam surge releases.

Hydraulic flood routing models provide a practical alternative to the hydrologic models as they consider the conservation of both mass and momentum. Their greatest limitation stems from the fact that they require geometric data describing the study reach as well as the hydrologic data required for hydrologic modelling.

1

Obtaining survey information is quite costly, particularly considering the long distances involved in flood routing (hundreds of kilometres), therefore the economical value of hydraulic models is often questioned.

The objective of this study was to determine the minimal amount of data required for the construction of a reliable hydraulic model. Therefore, where limited hydrologic and geometric data were available an approximation to the missing data was adapted. A mathematical simulation was conducted using this approximated data and the results were compared to hydrographs which had been measured during various events along the study reach.

Chapter 2 provides a description of the modelling techniques available, in order to demonstrate the difference between hydrologic and hydraulic models and to justify the use of an hydraulic flood routing technique in the case studies which follow. It also explains how ice cover is handled in flood routing. Finally, it presents the methodology used in assessing the data requirement for an hydraulic model.

Chapter 3 presents two open water flood routing scenarios where minimal physical data was available. It describes the geometric database employed for the Peace and Oldman/South Saskatchewan Rivers in Alberta. As well, it compares the events computed by the hydraulic model to those measured on these rivers in order to verify the accuracy of the limited geometry approximation for moderate and more extreme events.

Approximations for both geometric and hydrologic data for a large ice related event are discussed in Chapter 4. A large snowmelt runoff event and its associated ice jam surge releases provide the flood wave modelled on the Porcupine River, Yukon. It describes the geometric database, and the approximations to the tributary inflows and the ice effects used for this case study for which both geometric and hydrologic data was extremely limited. Once again the results were compared to the measured values in order to verify the accuracy of the input database.

The final case study involves modelling the propagation of a surge resulting from an ice jam on the Saint John River, New Brunswick. Chapter 5 provides verification of hydraulic flood routing techniques and the approximations used in the previous case studies for a well defined study reach. It verifies whether a rectangular channel approximation is justified. As well, it reviews the accuracy of predicting water levels where channel geometry is detailed and of assuming an equilibrium ice jam configuration where the ice jam profile is unknown.

CHAPTER 2

BACKGROUND AND METHODOLOGY

2.1   INTRODUCTION

Flood forecasting involves the use flood routing techniques to determine flood wave characteristics (stage and discharge) at sites of interest along a river reach, knowing the inflows to that reach at the upstream end and from its tributaries. Flood forecasting is important to the population residing and working near the river banks. It provides the information regarding peak water levels and discharges, which are necessary in the design and operation and/or maintenance of various structures (bridges, dams, culverts, water intakes) and industrial plants located near the river banks. It also allows the determination of the flood affected areas and the timing of the incoming flood wave, thus enabling the establishment of a warning system.

A flood most often results from an increase in the volume of water entering a river channel over a short period of time, which in turn causes the propagation of a flood wave in the downstream direction. A high intensity rainfall during the summer, or a rapid snowmelt in the spring, may lead to a substantial increase in runoff and eventually to a flood event as the excess water enters the river channel. Flood routing techniques can be used to model the movement of any flood wave regardless of their cause. The simplifications made to the governing equations will control the accuracy

4

of the flood routing techniques.

Traditionally, hydrologic flood routing models have been used for flood forecasting (Amein, 1968). These models are primarily based on the conservation of mass. They treat the channel region as a lumped system in which the conservation of longitudinal momentum equation is replaced by a conceptual model (Dooge, 1986). They are practical and economical, as the only input data they require are streamflow hydrographs. However, hydrologic flood routing models have limitations as well. For example, the application of these models to dynamic events, such as ice jam surge releases, is not appropriate because of their conceptual approach to momentum conservation. As well, the only output they provide are discharge hydrographs at the gauge sites used in their calibration.

Hydraulic flood routing techniques provide a practical alternative to hydrologic flood routing. They are based on the conservation of both mass and longitudinal momentum. Therefore, they require detailed data describing the topographic and hydraulic characteristics of the river reach being modelled. Their greatest limitation is the cost required to obtain survey data to define long study reaches (Cunge, Holly, Verwey, 1980). However, in a recent study (Hicks, Yasmin and Chen, 1994), hydraulic flood routing techniques have been successfully applied to determine discharge hydrographs on the Peace River, where the available channel geometry data was limited. This was accomplished by assuming a rectangular channel, and developing a geometric database using the available survey data, supplemented with

5

topographic map data.

The following chapter describes the theory behind flood forecasting for both open channel and ice related events. It looks in detail at the solution techniques used, namely: hydrologic and hydraulic flood routing. Then, it presents the objectives to be accomplished in each case study used in this investigation, and, finally, the numerical technique used for flood forecasting.

2.2   EQUATIONS OF UNSTEADY OPEN CHANNEL FLOW

2.2.1   ST. VENANT EQUATIONS

Flood routing models for river channels are based on the one-dimensional equations of unsteady open channel flow, the St. Venant equations (Cunge *et al.*, 1980). These equations assume:

1) the flow is one-dimensional;

2) the pressure distribution is hydrostatic;

3) the boundary and turbulence effects can be accounted for in the roughness coefficient used for steady state flow; and

4) the bed slope is small.

The one-dimensional flow approximation is reasonable in flood forecasting as the characteristics of flood waves are considered to be largely influenced by their movement in the direction of flow (Fread, 1976). Chow (1959) shows that the pressure head at any depth within the river channel is equal to the depth times a

6

correction factor, $\cos^2\theta$, where θ is the angle of the bed slope to the horizontal. As long as θ is less than 6° the error in pressure head will be less than 1% and the pressure distribution can be assumed to be hydrostatic. As well, for a bed slope at an angle of 16°, which is extremely steep in open channels, the error in the gravity term in the St. Venant equations is only 2%, thus assuming a small bed slope is reasonable (Liggett, 1975).

Assuming a rectangular channel approximation, the St. Venant equations include the continuity equation, which is written in its differential form as:

$$\frac{\partial A}{\partial t} + \frac{\partial Q}{\partial x} = 0 \qquad [2.1]$$

where:

A = cross sectional area perpendicular to the flow;

Q = discharge;

t = temporal coordinate; and

x = longitudinal coordinate,

and the momentum equation:

$$\frac{\partial Q}{\partial t} + \alpha U \frac{\partial Q}{\partial x} + gA \frac{\partial H}{\partial x} = gA(S_o - S_f) \qquad [2.2]$$
$$\Rightarrow \quad inertial \quad \Leftrightarrow \quad pressure \Leftrightarrow friction\ and\ gravity \Leftarrow$$

where:

α = kinematic wave speed coefficient;

7

U = cross sectionally averaged longitudinal velocity;

H = depth of flow;

S_o = longitudinal channel bed slope;

S_f = longitudinal boundary friction slope; and

g = acceleration due to gravity.

2.2.2 FLOW APPROXIMATIONS

The most complete model for flood routing is known as the dynamic wave, which is described by the St. Venant equations as they are shown above. A dynamic wave. may propagate in either the upstream or downstream direction with a wave speed of (U-c) or (U+c), respectively, where

$$c = \sqrt{gH}$$ [2.3]

is the celerity of a shallow water wave (Henderson, 1966). This type of wave must be considered when modelling an ice jam surge release especially within the first few kilometers of its release.

Generally, the complete open channel unsteady flow equations would be preferable in routing any flood. However, in some situations, such as for summer rainfall events, a simplified version of the St. Venant equations is sufficient.

When the inertial terms in the momentum equation are negligible in size compared to the remaining terms, the flood wave is referred to as diffusive (Ferrick, 1985). It is

8

described by the continuity equation and the following form of the momentum equation:

$$\frac{\partial H}{\partial x} = (S_o - S_f) \qquad [2.4]$$

A diffusive wave travels in the downstream direction only, with a wave speed of αU where α is $^3/_2$ or $^5/_3$ depending on whether Chezy's or Manning's equation is used to quantify the friction slope (Chow, 1959).

The most dramatic simplification to the St. Venant equations is the one in which the momentum equation is replaced with a conceptual model. This is called an hydrologic model (Miller and Cunge, 1975). It will be examined in more detail in section 2.3.2.

2.2.3 APPLICABILITY OF THE VARIOUS FLOW APPROXIMATIONS

In this section, the wave progression from dynamic to diffusive is shown. The majority of flood waves are diffusive (i.e. the acceleration terms are small compared to the pressure, gravity and friction terms). However, in some cases, such as for ice jam surge releases, the acceleration terms are important for a short distance following the wave release.

The progression from dynamic to diffusive waves can be seen on an assembly of discharge hydrographs for various points along a study reach, on a phase diagram of wave location versus time, or on a stage-discharge rating curve. On a discharge

9

hydrograph, the dynamic wave will be characterized by a high peak with a steep rising limb. The amplitude of a diffusive wave will diminish as it travels downstream, thus, on a discharge hydrograph, the wave will be dispersed and diffused compared to the initial dynamic wave. The change from dynamic to diffusive is also shown by the change in slope of the line on the plot of the location of the wave peak versus time from $1:(U\pm c)$ for dynamic waves to $1:\alpha U$ for diffusive waves. However, tributary inflows and rapid changes in channel geometry may make it difficult to determine the exact point where the slope change occurs, therefore another option would be to study stage-discharge rating curves at various locations along a river reach. The wider the loop on a rating curve, the more dynamic the flood wave.

2.3   FLOOD ROUTING TECHNIQUES

2.3.1   HYDROLOGIC FLOOD ROUTING

As mentioned earlier, hydrologic flood routing models include all models which are based primarily on the continuity equation and which use a conceptual model in place of the longitudinal momentum equation. For their calibration, these models require only streamflow data from previous events at the upstream and downstream ends of the modelled reach, as well as any tributary inflows into the reach. Geometric and hydraulic information is not required when using this modelling technique.

The Streamflow Synthesis and Reservoir Regulation (SSARR) model, developed by the U.S. Army Corps of Engineers (beginning in 1956), is frequently used by Alberta

10

Environment Protection (Taggart, 1995). This model is based on the following form
of the continuity equation, which simply states that the difference between the inflow
(I_t) and outflow (O_t) is equal to the rate of change of storage (S) in the reach (Bedient
and Huber, 1988).

$$I_t - O_t = \frac{ds}{dt}$$

[2.5]

in which:

$$I_t = \frac{1}{2}(I_1 + I_2)$$

[2.7]

$$O_t = \frac{1}{2}(O_1 + O_2)$$

[2.7]

$$\frac{ds}{dt} = \frac{1}{2}(S_2 - S_1)$$

[2.8]

where:

I_1 = inflow at time t_1;

I_2 = inflow at time t_2;

O_1 = outflow at time t_1;

O_2 = outflow at time t_2

S_1 = storage at time t_1; and

S_2 = storage at time t_2.

A study reach on which this method is used is divided into sub-reaches. Channel
routing is therefore treated as a series of small successive increments of lake-type
storage which provide the delay in flood wave propagation between the upstream and

11

downstream boundaries. Based on this assumption, the SSARR model computes the outflow at the end of a given time period, knowing the inflow and outflow at the beginning of that time period, using the following equation:

$$O_2 = \left| \frac{I_1 - O_1}{T_s + \frac{\Delta t}{2}} \right| \Delta t + O_1$$

[2.9]

where:

$T_s =$ time storage of water ($= \beta Q/m$); [2.10]

β = numerical constant determined by trial and error; and

m = coefficient between -1.0 and 1.0.

The outflow, O_2, becomes the outflow, O_1, for the new routing period. (Brooks, Davis, and Kuehl, 1972)

The calibration of the SSARR model requires the development of travel times for each sub-reach within the study reach. The "time-of-storage" is the term used by the SSARR model to describe the total travel time for a given discharge. Once the initial travel times have been determined the calibration simply involves varying those times until modelled discharge hydrographs match those measured during various events.

As evidenced by the SSARR model, hydrologic flood routing techniques are economical in that the only data they require for their calibration is streamflow data. They are not practical however for modelling dynamic events such as ice jam

12

releases. Since SSARR and other hydrologic models are based solely on the continuity equation, they are linear models. The river flow is non-linear as described by the unsteady flow equations. Therefore, the best predictions given by these models are for flood flow conditions which can reasonably ignore the momentum equation such as floods which have nearly steady flows. The dynamic wave is a very unsteady flow which can therefore not realistically be modelled using hydrologic flood routing techniques. Furthermore, dynamic surges propagate in the upstream and downstream directions, hydrologic models only account for wave movement in the downstream direction (Miller and Cunge, 1975).

2.3.2 HYDRAULIC FLOOD ROUTING

Hydraulic flood routing is the technique which uses both the continuity and longitudinal momentum equations thus providing a method of relating hydraulic phenomena, such as flow and storage, to channel geometry and resistance, in the prediction of natural flood events. The dynamic wave, described by the complete St. Venant equations, is the most thorough model of this type. It may reproduce hydrographs which have been measured for past flood events and extrapolate hydrographs at key sites between them provided sufficient hydrologic and geometric data are available for its calibration.

Calibration of hydraulic models involves adjusting hydraulic parameters to obtain an agreement between measured and simulated hydrographs. This is accomplished by varying the resistance coefficient to account for bed, bank, and floodplain roughness

13

and storage. The complete unsteady flow equations are used because an increase in roughness increases the unsteadiness of the flow. Since the resistance coefficient must define the roughness for the entire channel, the topographic aspects throughout the entire reach must be specified in the calibration.

A properly calibrated hydraulic model provides a practical replacement for hydrologic flood routing techniques, however the key problem arises in obtaining sufficient geometric data to describe the topography of the study reach. In previous studies, survey data was used to provide this description as it can be obtained with accuracy and completeness. However the cost of acquiring these surveys can be astronomical (Cunge *et al.*, 1980). Therefore, Hicks *et al.* (1994) reviewed a method of describing the geometry of a river reach with limited survey data. They found that defining a study reach using the available cross sectional surveys, supplemented with data from topographic maps, provided a reasonable description of the reach's topography, creating a more economical alternative to obtaining survey data.

Various hydraulic models have been developed to date. The few that will be described here are unsteady flow models which can model rapidly changing flow conditions through the use of the complete St. Venant equations (CSCE Task Force on River Models, 1987). They are ONE-D, DAMBRK, MOBED, and cdg1-D.

The majority of the existing unsteady flow models use finite difference schemes to solve the St. Venant equations. Environment Canada's ONE-D model, (One Dimensional Hydrodynamic Model) is a six point finite difference model

14

(Gunaratnam and Perkins, 1970). DAMBRK (or DWOPER) developed by the U.S. National Weather Service (NWS) and MOBED, a sediment transport model with a fixed bed option, created by the National Hydrology Research Institute, use a four point finite difference scheme, the box scheme (Fread, 1988 and Krishnappan, 1983, respectively).

Finite element schemes have also been used in hydraulic flood routing models. The cdg1-D model, developed in the Civil Engineering Department at the University of Alberta, is one such model. This model employs a Petrov-Galerkin finite element scheme called the characteristic-dissipative-Galerkin scheme (Hicks and Steffler. 1990, 1992) to solve the one-dimensional unsteady open channel flow equations.

The cdg1-D model was chosen for this study as comparisons to other model has shown that it is accurate and robust (Hicks and Steffler, 1995). As well. the model was readily available to the author.

2.4   ICE CONSIDERATIONS

2.4.1   INTRODUCTION

During the spring, a high runoff causes a rapid increase in water level and discharge under the intact ice cover which creates the fragmented ice floes, typical of a dynamic breakup. As these floes travel downstream they may encounter an obstruction or contraction in the river, such as a solid ice cover, a change in river geometry, an island, or a bridge, which halts their movement thus beginning the formation

15

of an ice jam (Gerard, Jasek, and Hicks, 1992). The jam may block a substantial portion of the river flow, resulting in a rise in water level behind it. When the ice jam releases a strong, high velocity surge, containing large ice blocks, can lead to considerable increases in water level and discharge downstream of the jam site (Gerard, 1979). For the first few kilometers from its origin, the ice jam release surge is dynamic and therefore requires the complete St. Venant equations to model its propagation.

2.4.2 MODELLING ICE JAM SURGE RELEASES

A number of studies have been carried out to include the effects of ice with the one-dimensional unsteady flow equations previously presented. This section concentrates on techniques developed for modelling the dynamic surges caused when an ice jam releases, including both the wave propagation and the ice movement.

Henderson and Gerard (1981)

Henderson and Gerard (1981) developed an explicit analytical solution for ice jam release. They assumed that the formation of an ice jam was equivalent to the insertion of a resistant baffle (of zero volume) into the river flow, and its release to the removal of that block. In addition to assuming that ice effects were negligible once the jam releases, Henderson and Gerard (1981) assumed a classic dambreak scenario, in which the bed is assumed to be horizontal and frictionless for the initial release of the jam; thus, the momentum equation for this dynamic wave became:

$$\frac{\partial Q}{\partial t} + \beta U \frac{\partial Q}{\partial x} + gA \frac{\partial H}{\partial x} = 0.$$ [2.11]

The continuity equation, which will apply throughout this section, remained as shown in equation 2.1.

Henderson and Gerard assumed the flood wave scenario shown in Figure 2.1 after the release of the ice jam. Conservation of momentum and mass were then written as:

$$\frac{(c - U_0)^2}{gH_0} = \frac{1}{2} \frac{H_1}{H_0} \left[\frac{H_1}{H_0} + 1 \right]$$ [2.12]

$$c(H_1 - H_0) = U_1 H_1 - U_0 H_0$$ [2.13]

where:

c = flood wave celerity;

U_0 = cross sectionally averaged longitudinal velocity downstream of the jam. prior to its release;

U_1 = cross sectionally averaged longitudinal velocity after the jam failure;

H_0 = depth of flow downstream of the jam, prior to its release; and

H_1 = depth of flow within the surge.

Data collected by Doyle and Andres (1979) on the Athabasca River which provided data for verifying the solutions, which gave encouraging results. Thus, using the St. Venant equations while neglecting ice effects, friction, and bed slope seemed to produce adequate results. However, ice blocks carried by the flow are presumed to slow it down and cause a rise in water level therefore Henderson and Gerard (1981)

recommended further research.

Beltaos and Krishnappan (1982)

Beltaos and Krishnappan (1982) discovered that the unsteady flow equations for open water may be applied to ice jam surge releases provided that one dimensional flow approximations are valid and that the speed of the ice cover is fully developed (i.e. the speed of the ice cover has reached 95% of the river velocity). The initial water depth is assumed to be the depth of flow to the phreatic surface when an ice cover is present. In this case, the momentum equation governing the ice and water movement was taken as:

$$\rho_w H\left(\frac{\partial U}{\partial t} + U\frac{\partial U}{\partial x}\right) = \rho_w g H S_w - \tau_o$$

[2.14]

(which can be rearranged to give equation 2.2)

where:

ρ_w = density of water;

S_w = water surface slope; and

τ_o = bed shear stress.

They found that the time required for the speed of the ice cover to become fully developed was small and, therefore, that these equations could be applied from the moment of jam failure.

Beltaos and Krishnappan (1982) applied an algorithm, developed by Krishnappan

and Snider (1977) for unsteady one dimensional flow with variable channel width to the Athabasca River data presented by Doyle and Andres (1979). The algorithm used an four point (box) finite difference scheme with a double sweep method. The roughness was accounted for in a constant friction factor, which was assumed to include bed and ice jam roughness, as well as any additional conditions which may impede the propagation of the flood wave, such as a competent ice cover downstream of the jam. This assumption was considered the greatest limitation of the model.

In applying Krishnappan and Snider's algorithm, Beltaos and Krishnappan (1982) used a rectangular approximation which they deemed sufficient to describe the geometry despite the capability of the algorithm to handle irregular shaped cross sections. Each surveyed cross section was approximated by a trapezoidal shape of depth equal to the average channel depth. The rectangular shape was then determined by averaging the channel width of the trapezoid.

The results obtained, by Beltaos and Krishnappan, using this method, were quite promising. They demonstrated that ice effects may be neglected in modelling ice jam surge releases and that assuming a rectangular cross section for an arbitrary channel shape is a valid approximation.

Joliffe and Gerard (1982)

In 1982, Joliffe and Gerard conducted laboratory experiments using a sluice gate as the ice jam toe and polyethylene pellets as the artificial ice forming the jam, to

examine the effects of the ice in the jam on flow conditions immediately following jam failure and on the surge as it moved downstream. They found that the presence of ice had little impact on the flow conditions or on the surge profile following the jam failure. As well, they discovered that ice floes, resulting from the jam release, traveled at the average river velocity, which is much slower than the surge celerity. Therefore, the ice in the flow does not affect the surge propagation and the unsteady flow equations for open water can be used when modelling ice jam surge releases.

Joliffe and Gerard (1982) also conducted a computational study to review the importance of bed slope, friction, and ice jam profiles in modelling surge propagation following an ice jam release. They used a box finite difference model which used a Newton-Raphson iteration procedure (Joliffe, 1982) to solve the St. Venant equations for the sudden release of an assumed ice jam profile.

The "flat" ice jam profile assumed for this release was located in a rectangular channel of significant bed slope and low flow. Therefore, in contrast to the classic dam break scenario the channel could not be assumed frictionless or horizontal and the profile did not have a step change at its toe.

The results found using the above scenario showed that steep channel slope, and high roughness, along with the ice jam configuration are significant in determining the flow depths of the modelled wave. Since the dynamic form of the unsteady open channel flow equations allows for the inclusion of these channel and jam

characteristics, they are recommended over the classic dam break equations when modelling ice jam surge releases.

Wong, Beltaos and Krishnappan (1985)

Laboratory tests were conducted in 1985 by Wong, Beltaos and Krishnappan to confirm the validity of assuming one dimensional flow and of neglecting ice effects in the studies conducted by Henderson and Gerard (1981) and Beltaos and Krishnappan (1982). In order to accomplish this, a sluice gate was used to create the increase in water level found behind a jam and polyethylene blocks made up the artificial ice. The jams were released by suddenly lifting the gate. The water levels were recorded at various locations along the channel and compared to the predictions from the numerical models developed by Henderson and Gerard (1981), and Beltaos and Krishnappan (1982).

The results using both of these numerical models were promising. The water levels modelled using Beltaos and Krishnappan's method (1982) gave a good approximation to the measured levels throughout the ice jam release event. The analytical model developed by Henderson and Gerard (1981) was able to predict the peak water level with accuracy. Therefore, Wong *et al.* (1985) confirmed that moving ice following a jam release has minimal impact on the characteristics of the resulting surge. They also reinforced the validity of assuming one dimensional flow and full development of ice velocity.

Hicks, Steffler, and Gerard (1992)

Hicks, Steffler, and Gerard (1992) used a finite element model of the St. Venant equations, which used the characteristic-dissipative-Galerkin scheme, to simulate ice jam surge propagations on the Hay River in Northern Canada. A number of simplifications were made to the initial jam profile and failure mechanism in modelling the surge release. First, the ice jam in this investigation was assumed to have a toe length equal to the spatial discretization used in the geometric database input to the model. The gradually varied profile upstream of the jam was assumed to follow an M1 backwater curve, which was approximated by a horizontal line extending upstream until it intersected the water surface slope for the established initial conditions. The ice jam itself was assumed to follow an equilibrium jam profile and to release instantaneously. The effect of the ice pack on the flow was assumed negligible, as it was to move with the surge being released. Finally, the open water conditions were assumed downstream of the jam.

The results of this study showed that mathematical models which use the full dynamic equations of unsteady flow successfully simulate ice jam surge releases, which vary from dynamic to diffusive during their propagation. Since there was no available field data for model verification, the accuracy of assuming an equilibrium ice jam profile will be further discussed in Chapter 5. As well, this study presents the idea of establishing a limited geometry hydraulic flood routing model.

22

Saade, Sarraf, and El-Jabi (1993)

Saade, Sarraf, and El-Jabi (1993) developed a two dimensional numerical model, which uses the Modified explicit MacCormick scheme (a two step finite difference scheme), applied to the two-dimensional shallow water equations, for predicting the propagation of surges resulting from the failure of ice jams. The numerical simulation accounted for an ice jam by imposing one on the initial flow conditions and running the computational model until steady state conditions were achieved. The initial conditions for the surge propagation were then taken as the steady state conditions previously calculated.

The laboratory tests conducted by Saade, *et al.* (1993) to verify the accuracy of the model studied the surge movement immediately following the jam release. Once again the jam was formed of polyethylene blocks with a retaining gate forming the toe of the jam. The experimental ice jam was released suddenly by lifting the gate and the water levels were recorded at various locations along the flume for comparison to the water levels computed using the mathematical model developed by Saade *et al.* (1993).

The results of the laboratory experiments showed once again that the presence of ice had little effect on the characteristics of the surge. The two-dimensional numerical scheme used in this study was able to simulate the rapidly varied flow conditions immediately following an ice jam surge release. The scheme introduced numerical oscillations which Saade, et al. (1993) have stated can be reduced by modifying

23

the approximation of the spatial derivative.

2.4.3 DISCUSSION

Since the majority of hydraulic models still employ the one-dimensional unsteady open channel flow equations and it is these models which are used for routing the surge resulting from an ice jam release, the majority of the assumptions made in the studies listed in Section 2.4.2. still apply. These assumptions include:

1) all the assumptions which apply to using the St. Venant equations, made in Section 2.2.1, including one-dimensional flow;

2) the effect of the ice pack on the flow is negligible; and

3) open water conditions exist downstream of the ice jam.

The assumptions made by Hicks *et al.* (1992) regarding ice jam profiles will be reviewed later in this study.

2.5 PROPOSED METHODOLOGY

2.5.1 OUTLINE OF OBJECTIVES

As mentioned previously, the data required for the development of an hydraulic model includes both hydrological and geometrical data. The hydrological data required may include: stage and discharge hydrographs, site measurements of stage and discharge, high water marks, rating curves and flood area limits and depths. The necessary geometric data required may include: the channel width and cross sectional area, the volumes of inundated floodplains and the storage areas. Since obtaining this

data may not always be economical, this thesis reviews methods by which hydraulic flood routing techniques may accurately predict natural flood events, using the cdg1-D model, when minimal hydrologic and geometric data are available.

The first studies involved in this thesis look at modelling open channel flow events on two rivers where limited survey data is available. For the first river reach, the Peace River, the hydrologic data is abundant, however the geometric data is lacking and would be quite costly to obtain with surveys, due to the length of the reach. Therefore, the accuracy of the hydraulic flood routing model based on a geometric database from the available survey data and topographical maps, is reviewed. Since the hydrological data available for the Peace River study is for small to moderate events, the effect of the synthesized geometric database for more extreme events is unknown. Therefore, the second case study evaluates the accuracy of establishing a geometric database, similar to that established on the Peace River, for modelling events on the Oldman/South Saskatchewan River, which recently experienced a flood in the order of a 1:100 year event.

Next, the investigation is expanded to include more extreme ice related events. The first study in this area (the Porcupine River), once again reviews the minimal amount of survey data required to establish an adequate hydraulic model. As well, it looks at two methods of quantifying tributary inflows where hydrologic data was unavailable.

Finally, a study reach along which geometric and hydrologic data are abundant, the Saint John River, is reviewed. This study verifies the validity of the

approximations used in defining the channel geometry and the ice jam configuration in the previous studies.

2.5.2 NUMERICAL TECHNIQUES USED

As mentioned, the cdg1-D model, developed at the University of Alberta, is the model used in this study. The cdg1-D model uses the finite element method to describe the conservation form of the St. Venant equations. Although many previous methods have favored the non conservation form of the governing equations and used a finite difference model, comparisons to the numerical scheme used in the cdg1-D model have confirmed that its approach is superior in terms of solution accuracy and numerical stability (Hicks and Steffler, 1990, 1995).

The friction slope used in this model was computed based on Manning's equation. The hydraulic model assumed a rectangular cross section therefore the St. Venant equations were adapted to provide a conservation formulation which can be applied to rectangular channels of varying width (Hicks and Steffler, 1990). The continuity equation modelled was:

$$\frac{\partial A}{\partial t} + \frac{\partial Q}{\partial x} = 0$$
[2.15]

and the adapted momentum equation was:

$$\frac{\partial Q}{\partial t} + \frac{\partial QU}{\partial x} + \frac{\partial}{\partial x}\left(\frac{gAH}{2}\right) - \frac{gAH}{2B}\frac{dB}{dx} = gA(S_o - S_f)$$
[2.16]

where:

26

A = cross sectional area perpendicular to flow;

Q = discharge;

U = cross sectionally averaged longitudinal velocity;

H = depth of flow;

B = width of rectangular cross section;

S_f = longitudinal boundary friction slope;

S_o = longitudinal channel bed slope;

g = acceleration due to gravity;

t = temporal coordinate; and

x = longitudinal coordinate.

This system of equations describing one-dimensional, unsteady open channel flow may also be written in matrix notation:

$$\frac{\partial \{\phi\}}{\partial t} + \frac{\partial \{F\}}{\partial x} + \{f_c\} = \{0\} \qquad [2.17]$$

where

$$\{\phi\} \equiv \begin{Bmatrix} A \\ Q \end{Bmatrix} \quad ; \quad \{F\} \equiv \begin{Bmatrix} Q \\ \left(UQ + \dfrac{gAH}{2}\right) \end{Bmatrix} \quad ; and, \quad \{f_c\} \equiv \begin{Bmatrix} 0 \\ -gA\left(S_0 + \dfrac{H}{2B}\dfrac{dB}{dx} - S_f\right) \end{Bmatrix}$$

$$[2.18]$$

with the Petrov-Galerkin upwinding terms based on a non-conservation form of the system (St. Venant equations):

$$\frac{\partial \{\phi\}}{\partial t} + [A]\frac{\partial \{\phi\}}{\partial x} + \{f_n\} = \{0\} \qquad [2.19]$$

where

27

$$[A] \equiv \frac{\partial \{F\}}{\partial \{\phi\}} = \begin{bmatrix} 0 & 1 \\ c^2 - U^2 & 2U \end{bmatrix}$$ [2.20]

and,

$$\{f_n\} \equiv \left\{ \begin{array}{c} 0 \\ -gA\left(S_0 + \frac{H}{B}\frac{dB}{dx} - S_f\right) \end{array} \right\}$$ [2.21]

Hicks and Steffler (1990) showed that the most accurate results obtained using the CDG scheme were obtained for a Courant number less than or equal to 0.5, where:

$$C_r = V_w \frac{\Delta t}{\Delta x}$$ [2.22]

in which V_w is the wave propagation speed.

2.5.3   ICE JAM COMPONENT OF cdg1-D

Ice jam releases can be considered in two ways with the cdg1-D model. The first method is using an option built into the model. When chosen this option requires the specification of ice jam location, length, and roughness. A number of simplifying assumptions regarding the initial jam shape and the failure mechanism are made when this approach is used. These assumptions are shown in Figure 2.2. The ice jam is assumed to have a toe length equal to the spatial discretization chosen in establishing the geometric database. The gradually varied profile upstream of the jam is an M1 backwater curve. The cdg1-D model approximates it by projecting a horizontal line from the jam to an intersection with the upstream water level. The flow depth to the

28

phreatic surface within the jam is determined based on an equilibrium section of a fully developed jam, using the following relationship developed from an approach suggested by Beltaos (1983).

$$\eta = 0.38\zeta + \frac{5.75}{\mu}\left\{1 + \sqrt{1 + 0.07\mu\zeta\left(\frac{k_i}{k}\right)^{\frac{1}{4}}}\right\}$$ [2.23]

in which

$$\eta \equiv \frac{H}{Sb}$$ [2.24]

and,

$$\zeta \equiv \frac{\left(qk^{\frac{1}{6}} / \sqrt{gS}\right)^{\frac{3}{5}}}{Sb}$$ [2.25]

where:

    μ = an internal friction - porosity coefficient (taken as 1.0 for this investigation);

    S = the slope of the water surface (approximating the slope of the energy grade line);

    q = the discharge per unit width of channel;

    b = the pack width;

    k = the composite roughness;

    k_i = the ice roughness; and

    k_b = the bed roughness.

The composite roughness is defined as:

$$k = \left(\frac{k_i^{\frac{1}{4}} + k_b^{\frac{1}{4}}}{2}\right)^4$$ [2.26]

The second method which can be used involves inserting a measured ice jam profile on the established steady flow conditions. In this case, as with the previous one, the M1 backwater curve is approximated by extending the most upstream measured water level in the jam horizontally to intersect with the previously calculated steady flow water levels.

In both cases, the jam is assumed to release instantaneously along its entire length, resulting in a uniform acceleration of stored water. In addition, the ice pack is assumed to have no resistance effect on the flow after the release of the jam.

2.5.4 CHARACTERIZATION OF THE SIMPLIFIED CHANNEL FOR HYDRAULIC FLOOD ROUTING

2.5.4.1 Introduction

A fundamental assumption behind the application of the hydraulic model is that an adequate representation of the river geometry can be developed from limited survey data, supplemented with topographic map data. The ability of the limited geometry modelling approach to provide accurate flood routing results has been confirmed by Hicks, Yasmin, and Chen (1994). As well, this limited data approach has also been applied to dynamic events, specifically for modelling ice jam release surges on the Hay River, NWT (Hicks et al., 1992), which was mentioned in Section 2.4.2. However, in that case, no verification data was available.

Local geometry is not significant to the model, in terms of its ability to successfully

30

route moderate floods over long reaches (Hicks *et al.*, 1994) as the primary influence on the hydraulic model, in the context of flood routing over long distances, is the accuracy with which the gradient of the river is represented as this is the driving force behind flood wave propagation. However, this may not be the case when overbank flooding is significant. Therefore, one of the objectives of this study was to examine this question. The geometric databases, established for each river reach involved in this study, were developed from the available survey data supplemented with topographic map data, as in the earlier study, in order to obtain the most accurate representation possible with the available data. The channel geometry was described based on the channel top width and the bed profile at given increments along the study reaches.

2.5.4.2 Channel Distances

River stations, or locations along the channel length, were obtained by marking out one kilometre intervals on 1:250,000 or 1:50,000 scale National Topographic Series (N.T.S.) maps, depending on the size of the river channel, with dividers. Stations were specified in kilometers (km) downstream of a given origin. For consistency, the stations were measured along the channel centreline, rather than along the thalweg as the latter is a more subjective criteria when limited cross section data are available. The difference between the channel stations obtained using these two criteria was marginal in this case, and the choice of channel centreline as the longitudinal axis was consistent with the assumption of a rectangular cross section shape. Each of the

31

surveyed cross sections was referenced to this stationing system. as were all major tributaries and key sites of interest.

2.5.4.3 Water Surface Slopes from the N.T.S. maps

A water surface profile was obtained from 1:250,000 or 1:50,000 scale N.T.S. maps by identifying locations where the topographic contours intersected the river channel. The corresponding stations, in terms of distance downstream of the origin, were then used to determine water surface slopes.

2.5.4.4 Effective Bed Profile

The effective bed level is defined as the elevation of an equivalent rectangular section approximating the actual channel geometry.   Effective bed elevations were determined at each of the surveyed cross sections, by measuring the flow area and top width for a specified water level, either the computed (HEC-2) 1:2 year water surface elevation or the water level on the day of survey. These measurements were done graphically: the area of the cross-section was determined using a planimeter; and the top width was measured with a scale. With the area and top width determined, the effective bed for each of the cross sections was found by calculating the average water depth (area/top width) and subtracting it from the specified water level.

There is some inconsistency in using the water level on the day of survey over the 1:2 year computed water surface elevation because of the fact that cross sections were surveyed at different times (and, therefore, at different flows). However, the effective

bed elevations obtained were found to provide a good representation of the mean bed level. That is, the effective bed elevation was not found to be sensitive to the water level used.

The effective bed profile was established at even 1 km increments, corresponding to the stationing system, for each case study. A best fit line was drawn through the effective bed points from the surveyed cross sections. Effective bed levels between the surveyed reaches were estimated by projecting values in the surveyed reaches using the water surface slopes obtained from the 1:250,000 and 1:50,000 N.T.S. maps. The absolute value of the bed elevations is estimated as the objective is to provide as accurate an estimate of the channel gradient as possible.

2.5.4.5 Channel Widths

The channel widths used in the hydraulic model were obtained from the 1:250,000 and 1:50,000 scale N.T.S. maps, by measuring the channel top width with scale and dividers at one kilometer intervals along the channel centreline. Although more accurate results could have been obtained from larger maps, the number of maps required would have been excessive and the cost high. This was not considered necessary as a previous study (Hicks *et al.*, 1994) had indicated that the flood routing results for moderate events are not particularly sensitive to the accuracy of the width variable. However, for events where overbank flooding occurs, this channel width may not adequately represent the effects of floodplain storage and roughness on the flow, since the cdg1-D model neglects compound channels in its rectangular

33

channel approximation. Therefore, the importance of channel width will be evaluated for more extreme events.

2.5.4.6 Channel Resistance

Channel resistance, specifically Mannings n, is the only calibration parameter required for the hydraulic flood routing model. This resistance factor must take into consideration the effects of both roughness and form drag on the flow. In the context of the limited geometry model, it must also include the effects of storage associated with floodplain inundation, if it occurs, as the floodplain hydraulics are not considered.
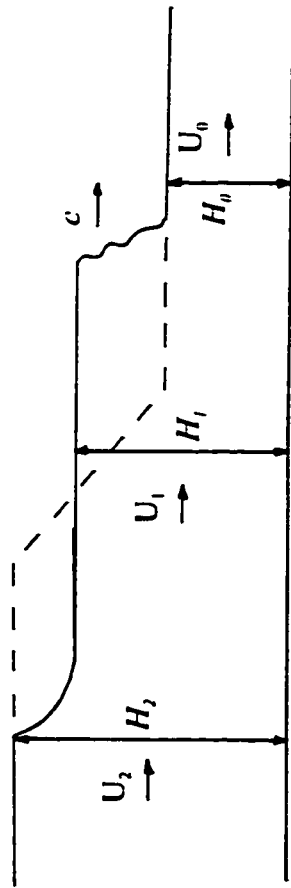
Figure 2.1. Surge formation after the release of an ice jam.

Adapted from Henderson and Gerard (1981).
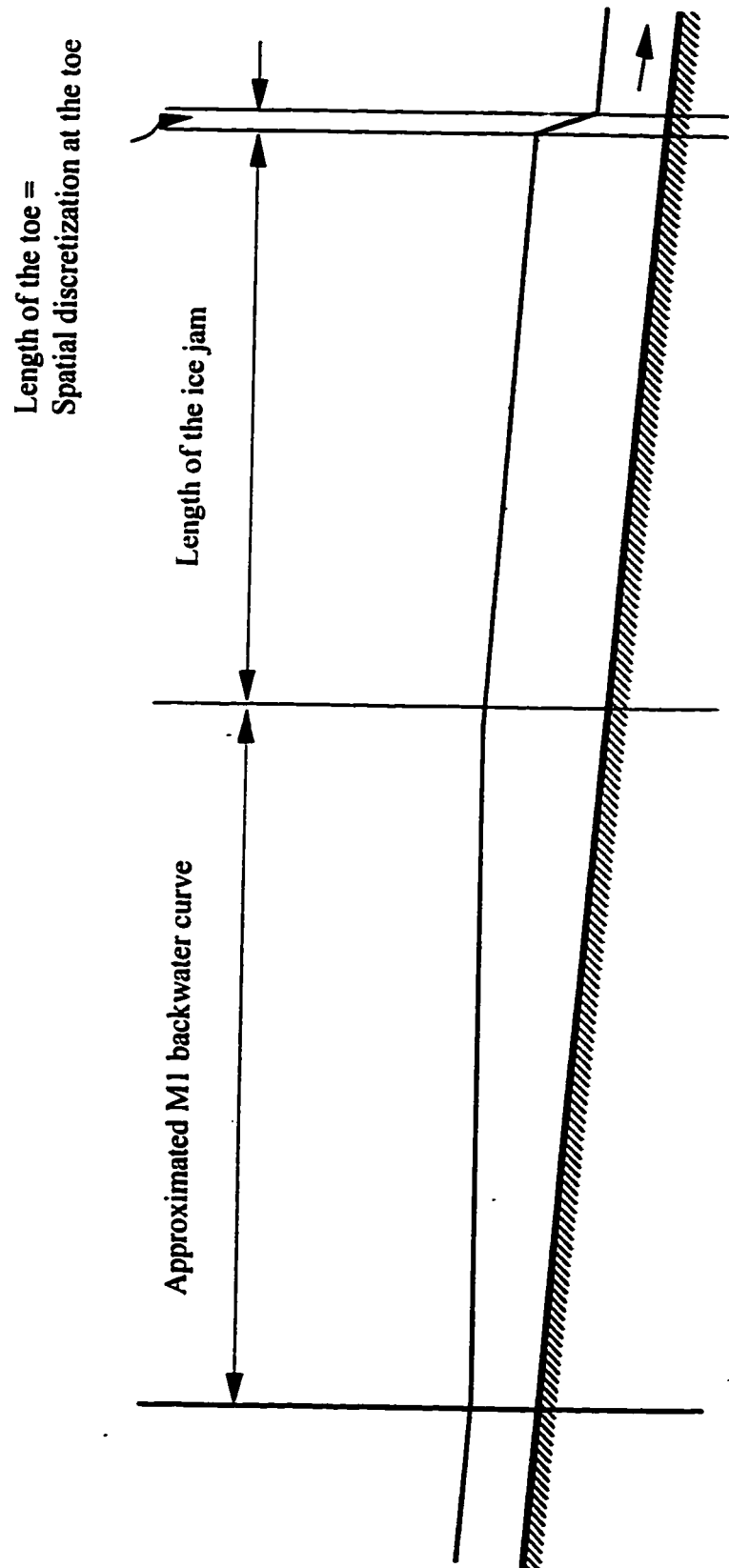
Figure 2.4. Schematic describing ice jam prior to failure for cdg1-D model.

CHAPTER 3

VERIFICATION OF FLOOD ROUTING WITH MINIMAL PHYSICAL DATA UNDER OPEN WATER CONDITIONS

3.1 INTRODUCTION

In the absence of survey data to define a study reach for an hydraulic flood routing model a geometric database can be created based on the available survey data supplemented with topographic map data. The purpose of this chapter is therefore to demonstrate that this synthesized geometry provides a reliable estimate of channel topography when routing moderate to more extreme flood events.

This investigation reviews two case studies: the Peace River and the Oldman/South Saskatchewan River. For the Peace River study, the events modelled were small to moderate, 1:2 year events or less. The Oldman/South Saskatchewan River Study allowed for the constructed database to be tested for events in the order of 1:100 year events, where overbank flooding is known to have occurred. In both cases, the simulated results were compared to those measured during the events to verify the accuracy of their geometric databases, which were created as described in Section 2.5.4.

37

3.2   PEACE RIVER[1]

3.2.1   INTRODUCTION

Figure 3.1 illustrates the Peace River study reach, which extends from the Water Survey of Canada (WSC) gauge at Hudson Hope (28 km downstream of W.A.C. Bennett Dam) to Peace Point in Wood Buffalo National Park, a distance of 1107 km in terms of length measured along the channel centerline. The actual model extends downstream an additional 93 km (to station 1200 km) to minimize the influence of boundary effects on the calculations at Peace Point.

The bed material and the river type vary along the length of the Peace River reach. In the upstream portion of the study reach the river is straight with occasional islands and has a gravel bed. The bed material turns to sand further downstream and the river begins to have both irregular and sinuous meanders. The river valley is stream cut throughout the entire reach. It is fragmentary and narrow with partially cultivated flood plains. The river is partly entrenched and confined (Kellerhals, Neill, and Bray, 1972).

The objective of this case study was to assess the exactitude of a geometric database, established with the available survey data, supplemented with topographic map data,

---

[1] This section is adapted from Hicks, F.E., and K. McKay. 1995. Peace/Slave River Flow Modelling. (NRBS project 1154-D1) Water Resources Engineering Report 95-H3, Civil Engineering Department, University of Alberta, Edmonton, Alberta, Canada.

(Hicks, Yasmin, Chen, 1994) in routing various moderate flood events which occurred along the Peace River. The available survey data for the study reach was scarce. The channel geometry within British Columbia was well defined; however, in Alberta hundreds of kilometres in intermediate reaches between key sites: Dunvegan; Peace River; Fort Vermilion; and Peace Point, contained few surveyed cross sections. The hydrologic data was available at various locations along the study reach: Hudson Hope; Taylor; Dunvegan; Peace River; and Peace Point, to provide a comparison to the modelled output. Since there was an absence of cross sectional data and an abundance of hydrologic data within this lengthy study reach, this investigation provided a valuable assessment of the importance of both the geometric and hydrologic data components to hydraulic flood routing.

3.2.2 INPUT DATA

3.2.2.1 Introduction

The hydraulic flood routing model implemented for this reach required two types of input data: geometric data and hydrologic data. The geometric data requirements for the model include details of the effective bed profile, channel widths, and hydraulic resistance characteristics of the river channel, which were obtained from available cross section surveys, 1:250,000 scale N.T.S. maps, and documented observations. The hydrologic input data was based solely on discharge data available from the various WSC gauges along the study reach.

39

3.2.2.2 Available Geometric Data

N.T.S Map Data

The origin was specified as the downstream face of the W.A.C. Bennett Dam for the stationing system used in this case study. Table 3.1 presents the location of these key sites along the Peace River, in terms of their distances downstream of this origin. Table 3.2 provides the water surface elevations obtained from the 1:250,000 scale N.T.S. maps and Table 3.3 presents the estimates of the water surface slope obtained from the data in Table 3.2.

Available Survey Data

As previously mentioned, detailed survey data was available upstream of the B.C./ Alberta border. However, in Alberta, cross section surveys were much more dispersed. The original cross section data in Alberta was available only at Dunvegan. Peace River, Fort Vermilion and Peace Point. Virtually hundreds of kilometers of river remained unsurveyed in the intermediate reaches. In 1982, the Alberta Research Council (ARC) collected additional surveys. Water Survey of Canada (WSC) surveyed one cross section at Carcajou in 1994. An additional six cross sections were surveyed downstream of Peace Point in 1995. Figure 3.2 illustrates the survey data currently available on the Peace River.

Table 3.1. Location of key sites along the Peace and Slave Rivers.

Location	Station (km)
Peace River at Hudson Hope	*28*
Halfway River confluence	65
Moberly River confluence	103
Peace River at Fort St. John	110
Pine River confluence	120
Peace River at Taylor	**121**
Beaton River confluence	141
Kiskatinaw River confluence	154
British Columbia-Alberta Border	*166*
Clear River confluence	186
Peace River at Dunvegan Bridge	**295**
Smoky River confluence	388
Heart River confluence	394
Peace River at Peace River	**395**
Notikewin River confluence	558
Peace River near Carcajou	650
Peace River at Fort Vermilion	808
Boyer River confluence	819
Wabasca River confluence	865
Peace River at Peace Point	*1107*
Chenal des Quatres Fourches confluence	1199
Riviere des Rochers confluence	1216

† *measured along the main channel through the delta*

Effective Beds Calculated from Surveys

The effective beds were determined for this case study using the flow area and top width for the 1:2 year (naturalized) flood level. The flow area and water surface top widths were determined based on a steady, gradually varied flow analysis of each surveyed reach. These analyses were done using the U.S. Army Corps of Engineers HEC-2 model, and were based on the Mannings resistance values reported by

Kellerhals, *et al.*, (1972), as shown in Table 3.4. No refinement of these Mannings *n* values were considered warranted at this early stage, given the purpose of this analysis. Figure 3.3 shows the effective bed profile for the entire study reach.

Table 3.2. Water surface elevations from the N.T.S. maps.

Station (km)	Contour Elevation
24	1500 ft (460 m)
72	1400 ft (430 m)
127	1300 ft (400 m)
221	1200 ft (370 m)
323	1100 ft (340 m)
425	1000 ft (300 m)
542	900 ft (270 m)
893	800 ft (240 m)
1089	220 m
1487	160 m

Table 3.3. Water surface slopes based on the N.T.S. map data.

Reach (km)	Water Surface Slope
24 to 72	0.00064
72 to 127	0.00055
127 to 221	0.00032
221 to 323	0.00030
323 to 425	0.00030
425 to 542	0.00026
542 to 893	0.00009
893 to 1089	0.00012
1089 to 1487	0.00015

Table 3.4. Mannings *n* values used in the preliminary hydraulic analysis.

(after Kellerhals, et al., 1972)

Location (km)	Mannings *n*
Peace River at Hudson Hope (28 km)	0.031
Peace River at Taylor (121 km)	0.049
Peace River at Dunvegan Bridge (295 km)	0.021
Peace River at Peace River (395 km)	0.022
Peace River near Carcajou (650 km)	0.023
Peace River at Fort Vermilion (808 km)	0.017
Peace River at Peace Point (1107 km)	0.023

Channel Widths

The top widths obtained from the N.T.S. maps are compared to the measured top widths at the surveyed cross sections in Figure 3.4. Although the computational model is robust enough to allow for the use of such varying widths, such noise in the data does dramatically increase computational effort. Therefore, the channel top widths were smoothed, as shown in Figure 3.4.

As illustrated in Figure 3.4, the widths used in the model were different from those based on surveyed cross sections. There are two reasons for these differences. First, the top widths from the surveyed cross sections were based on the flow top width of an irregular section at the 1:2 year (naturalized) flood level. However, given the limited amount of data, the N.T.S. map values had to be used, for consistency in the model. Second, the river size on the 1:250,000 scale maps was quite small.

As a result of these differences, it was desirable to evaluate the sensitivity of the

model to the width variable. This assessment was achieved by developing the simple width model illustrated in Figure 3.5. A simulation of the 1987 flood event using this simple width model produced discharge hydrographs within 3% of those obtained with the smoothed widths, at Taylor, Dunvegan Bridge, Peace River and Peace Point. Output at intermediate stations were similarly close with the exception of the Fort Vermilion station, where the hydrographs obtained with the two width models were 12 hours out of phase. Nevertheless, the peak discharges were still within 4% of each other. Based on these results it is concluded that the hydraulic flood routing model is not particularly sensitive to the accuracy of the width variable. Therefore, the use of small scale maps and smoothed widths are justified.

Channel Resistance

The channel resistance must account for the bed material, the channel type, and any overbank flooding should it occur. The Peace River bed is gravel in the upstream portion of the reach and sand in the downstream section. It varies from straight with occasional islands to meandering (Kellerhals, *et al.*, 1972). The base values for channel resistance for the Peace River reach were estimated from the values presented by Kellerhals, *et al.* (1972) for 1:2 year flood events, as summarized in Table 3.4. Table 3.5 presents the values used in the various Peace River sub-reaches (obtained assuming the local values cited in Table 3.4 were valid halfway to each adjacent site).

Table 3.5. Mannings *n* values used in the Peace River hydraulic flood routing model.

(based on the data from Kellerhals, et al., 1972)

Location (km)	Mannings *n*
28 to 75	0.030
75 to 210	0.045
210 to 345	0.025
345 to 1107	0.020

3.2.2.3 Available Hydrologic Data

The National Topographic Series 1:250,000 scale maps show a total of more than 80 tributaries for the Peace River. However, only a fraction of these streams are gauged. This means that flood routing models, both hydrologic and hydraulic are constrained by a lack of hydrologic data. Consequently, it is impossible to assess the magnitude of the error in modelling the Peace River in certain reaches, because the difference between modelled and observed streamflows are comprised of both model errors and ungauged (unquantified) lateral inflows. In this section the available data is discussed, including details of how the lateral inflows were quantified, as well as information on the sites along the Peace River for which gauge data was available for comparison to the computed results.

WSC Gauge Data Available on the Peace River

Data from five streamflow gauges were used for graphical comparison to computed output for the Peace River, including: the Peace River at Hudson Hope (which was

used as the upstream boundary condition for the flood routing computations since dam outflows are not published) at station 28 km; the Peace River near Taylor, at station 122 km; the Peace River at Dunvegan Bridge, at station 295 km; the Peace River at the town of Peace River, at station 395 km; and the Peace River at Peace Point, located at station 1107 km. Data for the discontinued stations at Carcajou (650 km) and Fort Vermilion (808 km) were also employed. However, the records for these two gauges are limited.

WSC Gauge Data Available on the Peace River Tributaries

Table 3.6 presents the tributaries considered in this analysis, the numbers of the WSC gauges from which the data were obtained, and the multiplication factor used by Alberta Environment Protection (AEP) in a previous study to transpose the tributary gauge data downstream to the confluence with the Peace River (Taggart, 1995). Since the gauges are located relatively close to their confluences, a simple linear adjustment was done. That is, the multiplication factor is simply the ratio of the catchment area at the confluence to the catchment area at the gauge (Taggart, 1995).

Additional tributary inflow data were available from gauges on the Alces River (at the 22nd Baseline), the Saddle River (near Woking), and the Whitemud River (near Dixonville). However, as these data were not used in the prior AEP study, no multiplication factors were provided to transpose the gauge data downstream to the confluence in a manner consistent with the data from the other tributaries. Therefore, these tributaries were not considered in the hydraulic model simulations. As these

tributaries have limited flow records, and relatively small contributions, this is not considered significant to the model. Of far greater importance are the ungauged inflow from major tributaries, such as the Wabasca River, downstream of Fort Vermilion. When relatively large flows occur on these tributaries, these ungauged inflows introduce significant errors in the hydrographs predicted at the gauges downstream of their confluence with the Peace River.

It was possible to run historical flows from 1961 to 1993, inclusively, based on inflow (Hudson Hope) and tributary data available from the current issue of the WSC records on the HYDAT CD-ROM. It is important to note, however, that not all of the tributaries listed in Table 3.6 contain complete records during this extensive period.

Table 3.6. Peace River tributaries considered in the flood routing models.

Location	WSC	Factor
Halfway River near Farrell Creek	07FA006 (1987)	1.00
Halfway River near Farrell Creek (lower)	07FA001 (1980)	1.00
Moberly River near Fort St. John	07FB008	1.40
Pine River at East Pine	07FB001	1.00
Beaton River near Fort St. John	07FC001	1.03
Kiskatinaw River near Farmington	07FD001	1.26
Clear River near Bear Canyon	07FD009	1.00
Smoky River near Watino	07GJ001	1.02
Heart River near Mampa	07HA003	1.00
Notikewin River at Manning	07HC001	1.39
Boyer River near Fort Vermilion	07JF002	1.00
Ponton River above Boyer River	07JF003	1.26
Wabasca River at Walden Lake Road	07JD002	1.10

3.2.3 MODEL RESULTS

The hydraulic model developed for the Peace River allowed for the comparison of modelled to measured discharge, water level, and average channel velocity in order to evaluate its reliability. The following section presents the results of these comparisons.

3.2.3.1 Modelling Discharge Hydrographs: Flood Routing

As a part of the study, historical flows from 1961 to 1993 were run from May 15 to October 15 every year. Input data for each simulation included the geometric data describing the channel as well as lateral inflow (tributary) hydrographs. In addition, two boundary conditions (discharge upstream, and stage downstream) and initial conditions at every computational node (stage and discharge) had to be specified for each event. The gauge site at Hudson Hope was taken as the upstream boundary of the computational domain, with the WSC data from the gauge providing the inflow boundary condition. The model was extended 100 km downstream of Peace Point (assuming a constant width and slope) to allow for an estimated stage as the downstream boundary condition. The numerical model was used to calculate the initial conditions for each steady flow test, by calculating a gradually varied flow profile for constant inflow and tributary discharges, based on observed flows on the day the simulation started. A time step of 6 hours was used for these simulations as a sensitivity analysis showed that for small to moderate events a larger temporal discretization could be used with negligible effect on the results. For each event,

48

calculated results were output at select sites, to facilitate a comparison to WSC gauge data.

As a part of the model evaluation, historical runs were conducted for the pre-regulation period for which sufficient tributary data was available, specifically 1965 to 1968, inclusively. These tests are extremely valuable because of the fact that the gauge at Fort Vermilion was operational during this period. The historical runs for the post-regulation period, when the Fort Vermilion gauge was operational are 1970 through 1976, and 1978. The results of these runs for the Peace River, Fort Vermilion, and Peace Point stations are compared to gauge records for each of these years in Figures 3.6 through 3.17, respectively. As the figures illustrate, the model consistently provides a good match to the gauge data at Fort Vermilion, despite the fact that there is virtually no geometric data over the 400 km reach in between Peace River and Fort Vermilion. These results clearly illustrate the validity of the approximate geometry model where the tributary data is available for all major tributaries. Also, the chosen values of Mannings n, based solely on the experience of earlier investigators, are reasonable and require no further calibration.

Figure 3.18 illustrates the results obtained for the 1987, the second largest event on record. For this year the gauge at Fort Vermilion was not operational thus the model results are shown at the Dunvegan Bridge gauge. Peak discharge magnitudes were only slightly higher than 1:2 year flood flows. Therefore, this event might be described as a "moderate" flood event. Again, general agreement between the

49

calculated historical flood and the WSC data measured at these sites was good.

3.2.3.2 Comparisons of Computed and Measured Water Levels

An hydraulic model provides details of both stage and discharge at any location along the study reach. Therefore, computed and measured water levels could be compared in the same manner as discharge was previously.

Figure 3.19 presents the stage hydrographs which were measured and modelled for the 1987 event on the Peace River. The timing of the computed flood wave propagation was consistent with the measured data however the magnitude of the flood peak is not. This may be explained by the variation between the effective bed profile used in the geometric database established for this study and the actual surveyed bed. For example, looking at Figure 3.20, which shows a section of the study reach near Peace River, the effective bed used in modelling this event was estimated graphically by fitting a line to the effective beds calculated from the surveyed cross sections. At any site along the study reach, the actual bed elevation may differ from the modelled bed elevation by several metres.

Since the population residing and working along the river banks is frequently concerned with the increase in water level, the computed and measured change in water level were plotted in Figure 3.21. The magnitude of the computed stage increase is more consistent with the measured stage increase than the computed and measured water levels were in Figure 3.19. However, the approximate channel

geometry still affects the accuracy of the modelled stage change. Therefore, it is recommended that water levels be computed at sites where detailed channel geometry is available using a model which can account for natural channel geometry.

3.2.3.3 Average Channel Velocity

Average channel velocity is a derivative output. That is to say, it is not a direct output of the model, but rather is determined from other variables. Specifically, average channel velocity is equal to the discharge divided by the flow area. The discharges computed in the model are considered to be very reliable. However, area, being a geometric variable, is not accurately reproduced in a limited geometry model. Therefore, the velocities output by the model must be considered to be very crude estimates. Therefore, it is also recommended that velocities be calculated only for reaches of detailed channel geometry or that the discharge hydrographs output from this model be used as input to another hydraulic model with site specific channel geometry.

3.2.4. DISCUSSION OF RESULTS

The objective of this study was to establish the reliability of hydraulic models which use a geometric database which was synthesized based on limited cross section data supplemented with topographic map data for small to moderate open channel events. The development of a model for the Peace River, between the W.A.C. Bennett Dam, British Columbia and Peace Point, Alberta, demonstrated the validity of this

51

approach, provided that ungauged tributary inflows are not significant. However, this limitation is independent of the flood routing technique used. The key advantage of this hydraulic flood routing approach over traditional hydrologic flood routing methods is that output describing flood hydrographs between gauge sites is provided.

The only calibration parameter involved in the development of the hydraulic model was the channel resistance coefficient, specifically Mannings n. It has been shown that base values for this parameter derived from the data provided by Kellerhals, *et al.* (1972) for 1:2 year flood pre-regulation events at gauge sites give good agreement between measured and computed flood hydrographs on the Peace River.

Because the program developed here employs hydraulic flood routing techniques. water level and velocity output can be extracted from the model, as well. However. unlike the predicted discharge hydrographs, the quality of the water level and velocity output is heavily dependent upon channel geometry. Therefore, in this limited geometry flood routing application, the predicted stage changes and velocities are crudely estimated. Consequently, it is recommended that the discharges, which are accurately calculated with the flood routing model, be used as input to site specific hydraulic models which incorporate detailed geometry to determine accurate water levels and velocities.

3.3   OLDMAN AND SOUTH SASKATCHEWAN RIVERS[2]

3.3.1   INTRODUCTION

During June of 1995 and of 1975, major flooding occurred in southern Alberta. Flood forecasting plays a key role in serious flood events such as these, as people with homes, businesses, and property in the flood affected areas need to be advised of the timing and the magnitude of expected flooding early enough to facilitate safe evacuation of people and livestock.

The Oldman/South Saskatchewan River is a gravel bed river with irregular meanders and occasional islands, and mid-channel and diagonal bars. The channel is entrenched further downstream where the Oldman River becomes the South Saskatchewan River. In the upstream portion of the reach it is occasionally entrenched and confined. The valley is continuous and of moderate extent with some vegetation in the upstream section; downstream, it is fragmentary and narrow and covered with shrubs (Kellerhals, *et al.*, 1972).

The purpose of this investigation was to assess the reliability of this approximate geometry approach for severe flood events, ones for which overbank flooding is known to have occurred. The events considered in this case were more extreme than

---

[2] This section is expanded from McKay, K., S. Mikolajczyk, and F.E. Hicks. 1996. Application of Hydraulic Flood Routing Techniques to the 1995 Flood in Southern Alberta. Proc. of the CSCE Annual Conference, Edmonton, Alberta, Canada.

those reviewed on the Peace River. Flows from the Bow and Oldman Rivers to the South Saskatchewan River in southern Alberta were sufficient to generate two of the largest floods on record (June 1995 and 1975) in the city of Medicine Hat. Figure 3.21 illustrates the study reach. Initially, it was hoped that the model could be applied to the entire river reach between the Oldman River Dam and the city of Medicine Hat for the two events. However, lateral inflows from the Belly and St. Mary Rivers could not be accurately quantified, due to gauge failures during the 1995 flood. Therefore, the model was applied to this event on the Oldman and South Saskatchewan Rivers, between Lethbridge and Medicine Hat, Alberta. The 1975 flood was applied to the entire reach, as well as to the shortened reach.

3.3.2 INPUT DATA

3.3.2.1 Introduction

Both topographic and hydrologic data are required as input in order to route a flood using an hydraulic model. The hydrologic data on the Oldman/South Saskatchewan River was not as abundant as in the Peace River study therefore the length of the study reach changed with each modelled event and approximations to the tributary inflows from the Belly and Bow Rivers were used. The available data and the approximations used when geometric and hydrologic data was lacking are discussed here.

3.3.2.2 Available Geometric Data

N.T.S. Map and Survey Data

The origin for the Oldman/South Saskatchewan River case study was specified as the downstream side of the Oldman River Dam. The location of these key sites along the Oldman River are presented in Table 3.7, in terms of their distances downstream of the origin.

Table 3.7. Location of key sites along the Oldman and South Saskatchewan Rivers.

Location	Station (km)
Oldman River at Oldman River Dam	*0*
Belly River confluence	125
St. Mary River confluence	158
Oldman River at Lethbridge	**169**
Bow River confluence	325
South Saskatchewan River at Medicine Hat	**428**

The channel slopes, which were determined for the reach between Oldman River Dam and Medicine Hat based on the 1:50,000 scale N.T.S. map water surface slopes, are summarized in Table 3.8. The cross sectional data available for the study reach includes clusters of cross sections surveyed at Fort McLeod, Lethbridge, and Medicine Hat. Figure 3.23 illustrates the location of the available survey data along with the N.T.S. map water surface profile. The effective bed profile approximated using the data available for the study reach is shown Figure 3.23.

55

Table 3.8. Water surface slopes based on the N.T.S. map data

Reach (km)	Water Surface Slope
0 to 81	0.0015
169 to 205	0.0011
205 to 335	0.0007
335 to 550	0.0004

Channel Resistance

Channel resistance, specifically Mannings n, is the only calibration parameter required for this hydraulic flood routing model. In the context of this limited geometry model, it must represent a composite roughness of the channel and floodplain, including the effects of storage associated with floodplain inundation. The Oldman/South Saskatchewan River has a gravel bed, irregular meanders with occasional islands, and mid-channel and diagonal bars (Kellerhals *et al.*, 1972). Initially, a value of 0.030 was estimated for this parameter throughout the modelled reach, based on an average of channel roughness values reported by Kellerhals *et al.* (1972) for sites along the Oldman and South Saskatchewan Rivers.

3.3.2.3 Available Hydrologic Data

There are three main tributaries of the Oldman and the South Saskatchewan Rivers between the Oldman River Dam and Medicine Hat: the St. Mary River, the Belly River and the Bow River. There are also many small streams which provide lateral inflow to these two rivers. However, the inflows from these small tributaries were not

gauged and were considered negligible in comparison to the three main ones.

This study considered two flood events in the model evaluation. The first was the 1995 summer flood event and the second was the 1975 summer flood event. The hydrologic data available for these events will be discussed here.

The 1995 Summer Event

Although an inflow hydrograph could have been developed for a modelled reach beginning at the Oldman River Dam, the lateral inflow from the Belly River could not be accurately quantified, as the gauge (WSC05AD002) nearest the confluence with the Oldman River was not operational during the 1995 event. Data was available on the St. Mary River near Lethbridge (WSC05AE006) and at Glenwood on the Belly and Waterton Rivers (WSC05AD041 and WSC05AD028, respectively). However. this data did not adequately represent the lateral inflows from the Belly River. since the gauges at Glenwood were so far upstream of the confluence with the Oldman River.

Inflows for the Bow River were available from the Water Survey of Canada gauge located below the Bassano Dam (WSC05BM004), approximately 100 kilometres upstream of the confluence with the Oldman River. However, the Bow River gauge near the confluence with the Oldman River was not operational. As there are no major tributary inflows to the Bow River downstream of Bassano Dam, this gauge record was used for the lateral inflow condition from the Bow River.

Data from the streamflow gauge on the Oldman River at Lethbridge (WSC05AD007) were used to quantify the upstream boundary condition for the flood routing computations. Data from the streamflow gauge on the South Saskatchewan River at Medicine Hat (WSC05AJ001) were used to assess the results obtained with the flood routing model. The gauge data were provided at 6 hour intervals.

The 1975 Summer Event

For the 1975 event, lateral inflow data were available on the Belly River near Standoff (WSC05AD002) and the Waterton River near Glenwood (WSC05AD028), the gauges nearest the confluence of the Belly River with the Oldman River. In order to determine the inflow from the Belly River, the single station transfer method was used to transfer the flow data on the Waterton River from Glenwood to Standoff, where it was combined with the data from the Belly River gauge near Standoff (WSC05AD002). Finally, the combined flow at Standoff was transferred to the mouth of the Belly River using the same method. The equation for the single station transfer is given by Watt, *et al.* (1989) as:

$$Q_P = Q_{HS} \left(\frac{A_P}{A_{HS}} \right)^{0.8} \tag{3.1}$$

where: Q_P = Outflow from the basin at the project station;

Q_{HS} = Outflow from the basin at the hydrometric station;

A_P = Area of the basin above the project station; and

A_{HS} = Area of the basin above the hydrometric station.

58

The areas used to describe each basin were obtained from the WSC records on the HYDAT CD-ROM. They are shown in Table 3.9.

Tributary inflow data were also available on the St. Mary River near Lethbridge (WSC05AE006) and at the mouth of the Bow River (WSC05BN012) and on the Bow River below Bassano Dam (WSC05BM004). Therefore, for the 1975 event it was reasonable to develop a model of the Oldman/South Saskatchewan River beginning at the Oldman River Dam. The upstream boundary condition was determined from the streamflow gauge below the dam (WSC05AA024) for this event. Data from the streamflow gauge on the Oldman River at Lethbridge (WSC05AD007) and from the gauge on the South Saskatchewan River at Medicine Hat (WSC05AJ001) were used to evaluate the results obtained with the hydraulic flood routing model. The gauge data for the 1975 event, obtained from the WSC records on the HYDAT CD-ROM, were average daily flows.

Table 3.9. Basin areas for selected tributary gauges

Basin	Basin Area (km²)
Waterton River above Glenwood	1630
Waterton River above Standoff	1730
Belly River above Standoff	1210
Belly River at the mouth	3624
Bow River below Bassano Dam	20300
Bow River at the mouth	25300

3.3.3 MODEL RESULTS

The input data for the simulation included the geometric data describing the channel as well as the lateral inflow hydrographs from the tributaries. In addition, two boundary conditions (discharge upstream, and stage downstream) and initial conditions at every computational node (stage and discharge) had to be specified. The numerical model was used to calculate the initial conditions for each steady flow test, by calculating a gradually varied flow profile for constant inflow and tributary discharges, based on observed flows at the time the simulation started.

3.3.3.1. The 1995 Summer Event

As discussed above, the gauge site at Lethbridge (WSC05AD007) was taken as the upstream boundary of the computational domain for this event, with the WSC data from the gauge providing the inflow boundary condition. The model was extended 120 km downstream of Medicine Hat (assuming a constant channel width and slope) in order to allow for an estimated stage as the downstream boundary condition.

The 1995 flood event simulation extended from June 1 to 15. For maximum accuracy, the time step increment was based on an estimated peak travel time of approximately 1.5 days between Lethbridge and Medicine Hat and the distance increment of 1 km, to ensure a Courant number of 0.5 or less throughout the simulation. This required a time step increment of 4 minutes. A sensitivity analysis was conducted and it was found that a time step increment of one hour could be used

with no loss in accuracy, because of the length of the flood wave and the small distance increment used.

Figure 3.24 illustrates the results of the initial tests in which an attempt was made to calibrate Mannings n for the reach. For $n = 0.03$, the flood peak predicted by the model was 4.6% higher than the measured peak flow rate. The flood peak timing was early by 18 hours. This corresponds to a 50% error when the error is calculated based on the time of travel (36 hours), shown in Figure 3.25a, between Lethbridge and Medicine Hat. Increasing the value of Mannings n to 0.05 resulted in a better approximation of the magnitude of the peak (Figure 3.24). However, the difference was only 5% and the impact on the peak arrival time was marginal, as the predicted flood peak at Medicine Hat was still 12 hours early (33%).

There are two possible explanations for this difference in magnitude and timing. The first is the incorrect timing of the tributary inflow, since the gauge on the Bow River used in modelling the 1995 event is at Bassano Dam, approximately 100 km upstream of its confluence with the Oldman River. The second explanation is that the impact of floodplain storage has a significant effect on wave diffusion. Since there is insufficient information for quantifying the floodplain storage, the remainder of this section will focus on verifying the effect of the tributary inflow timing.

Based on gauge records for previous large floods, the average time taken for flood peaks on the Bow River to travel from the gauge below Bassano dam to the one near the mouth of the Bow River was approximately 22 hours. Therefore, the

61

timing of the inflow hydrograph from the Bow River was adjusted by 22 hours as shown in Figure 3.25b. No effort was made to adjust the magnitude of the flows for natural diffusion, or for additional inflows downstream of Bassano.

Figure 3.26 presents the results of this simulation for both estimates of Mannings n (0.03 and 0.05). The peak discharges were once again within 5% of the measured peak. The difference in the timing of the modelled flood waves using the adjusted inflow hydrograph was also negligible, in both cases, as the peak times were still off by 10 hours (28%) and 17 hours (47%), respectively. This clearly shows that the tributary inflow is not the problem in modelling this event. Therefore, floodplain storage effects can not be neglected for events where overbank flooding occurs.

3.3.3.2. The 1975 Summer Event

For the 1975 event, the upstream boundary was taken as the gauge site just below the Oldman River Dam (WSC05AA024), thus the gauge record provided the inflow boundary condition. The model was once again extended 120 kilometres downstream of Medicine Hat (assuming constant width and slope) in order for the downstream boundary condition to be an estimated stage.

The 1975 flood event simulation extended from June 1 to 30. For maximum accuracy, the time step increment was based on an estimated peak travel time of approximately 3 days between the Oldman River Dam and Medicine Hat and the distance increment of 1 km, to ensure a Courant number of 0.5 or less throughout the

62

simulation. This required a time step increment of 5 minutes.

The results of the model simulations for this event are shown in Figure 3.27 at Lethbridge and Medicine Hat for variable Mannings n. For $n=0.03$ the predicted flood peak was early by 12 hours in Lethbridge and 42 hours in Medicine Hat. As shown in Figure 3.28a, the travel time between the Oldman River Dam and Lethbridge for this event was 24 hours and between the dam and Medicine Hat it was 72 hours. Therefore, the error in timing based on these travel times was 50% and 58% respectively. The magnitude was overestimated by 19% in Lethbridge and 9% in Medicine Hat. Increasing Mannings n to 0.05 resulted in a better approximation of the timing of the peak, however, it had little effect on the prediction of its magnitude. The modelled peak for $n=0.05$ was early by 6 hours (25%) in Lethbridge and 24 hours (33%) in Medicine Hat. The difference in the magnitude of the peak was 19% and 11%, respectively.

For this event, which was modelled over a longer study reach, the differences in the magnitude and timing of the measured and modelled flood events is partially related to the tributary inflows. The inflow from the Belly River, in the reach between the Oldman River Dam and Lethbridge was estimated from WSC gauge records, which were measured over 40 km upstream of the confluence of the Oldman and Belly Rivers. The lag time was not accounted for in transferring the data from station to station. As well, the only hydrological data available for this event was the WSC data from the HYDAT CD-ROM. These are mean daily values, which average the

instantaneous discharges over the entire day. Therefore, the peak of the event would be underestimated and its exact timing unknown. Considering that the travel time for a flood wave between the dam and Medicine Hat during the 1975 event is 72 hours (3 days), the timing for the extended geometric model is undesirable.

In order to confirm whether the tributary inflows or the floodplain storage plays a more significant role in accurately modelling these flood events, the reach was shortened to match that used in modelling the 1995 event (Lethbridge to Medicine Hat) and the lateral boundary condition was varied. Initially, the flood was routed over this shortened reach using the WSC gauge at the mouth of the Bow River (WSC05BN012) as the tributary inflow. The results for this simulation are shown in Figure 3.29. The magnitude of the flood peak is predicted within 0.3% for $n=0.03$ and 0.5% for $n=0.05$. The arrival of the modelled flood peak at Medicine Hat is 18 hours and 12 hours early for the same Mannings n values. The travel time between Lethbridge and Medicine Hat is 48 hours. Therefore, the errors in timing are 38% and 25%, respectively.

Figure 3.28b compares the various approximations of the tributary inflow for the Bow River to that measured at the mouth. These include using the Bassano Dam gauge for the tributary inflow directly and lagged. Using the gauge data from below the Bassano Dam (WSC05BM004) directly, the magnitude of the wave peak was low by 1.9% and its timing was early by 24 hours (50%) for $n=0.03$. For $n=0.05$, the values were 3.1% and 18 hours (38%), respectively. These are shown in Figure 3.30. The

gauge record from below the Bassano Dam was then lagged by 24 hours as that was the travel time from the Bassano Dam to the mouth of the Bow River for this event. As shown in Figure 3.31, the flood wave peak in this case was 3.4% and 3.2% low for their respective roughnesses. The timing was, once again, 18 hours (38%) and 12 hours (25%) early.

These results indicate that using the gauge record at the mouth of the tributary or lagging the gauge data when the inflow is taken from further upstream provides a more precise simulation. However, the tributary inflow and the location of the gauge from which this data was taken is not the most important factor in routing overbank floods. In order to successfully route extreme flood events, floodplain storage cannot be neglected.

3.5   SUMMARY AND CONCLUSIONS

Based on the Peace River study, when a given reach lacks geometric data, a reliable geometric database may be created from the existing survey data supplemented with data from N.T.S. maps as this does not limit the simulation of moderate events. However, the limited geometry database should not be employed for more extreme events, such as those modelled on the Oldman River, where overbank flooding occurred. Since the limited geometry model assumes a rectangular channel of infinite height, flow and storage in the floodplain is considered negligible, which is not the case for the events modelled on the Oldman River.

65

As mentioned for moderate events like those on the Peace River, the limited geometry model is reliable. However, this is only valid for the simulation of flows. Additional survey data is required when the hydraulic flood routing model is used for predicting stages and average channel velocities, as these are quite dependent on the local channel geometry.
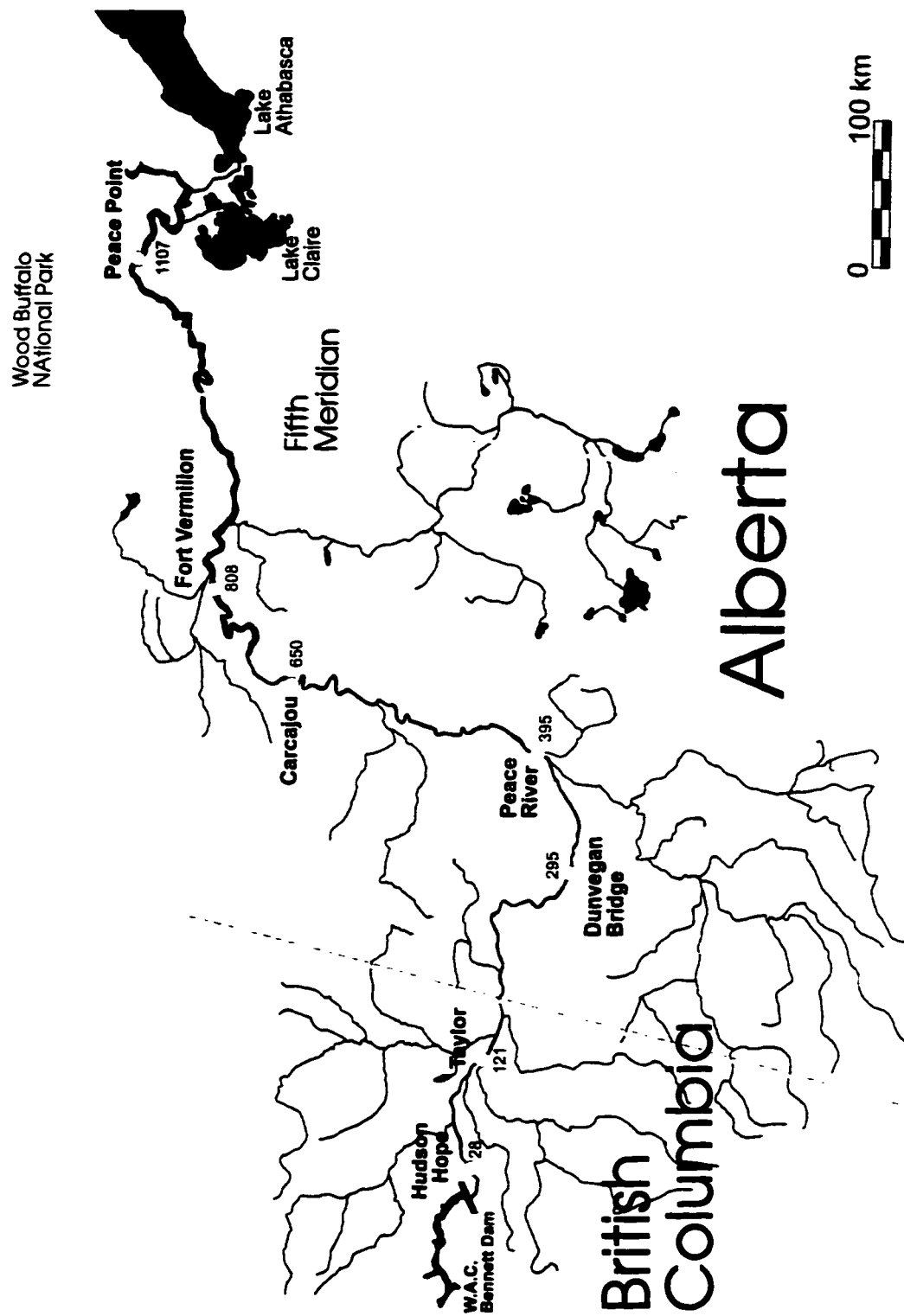
Figure 3.1. The Peace River study reach.
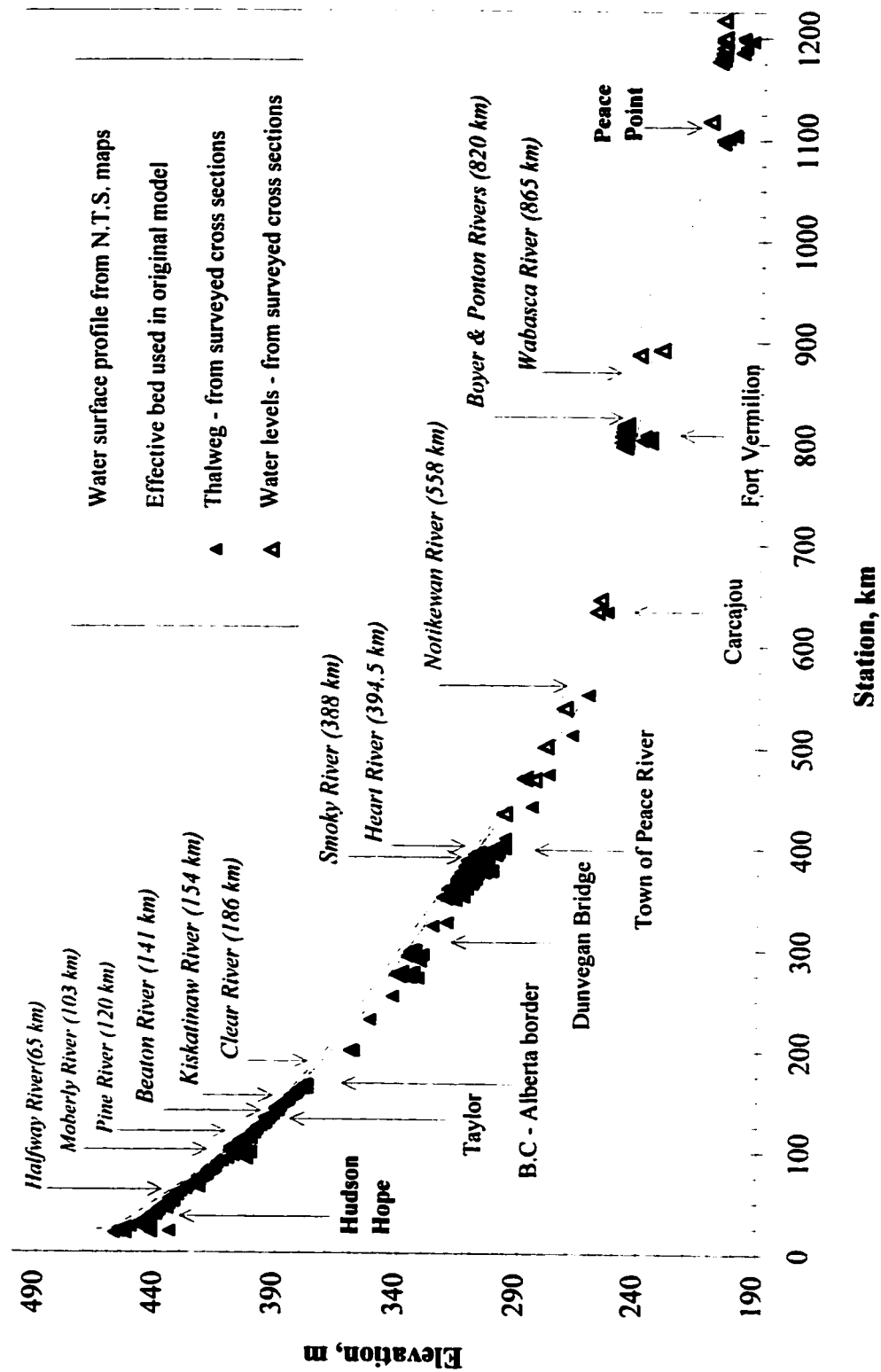
Figure 3.2. Available data for the Peace River reach.

68
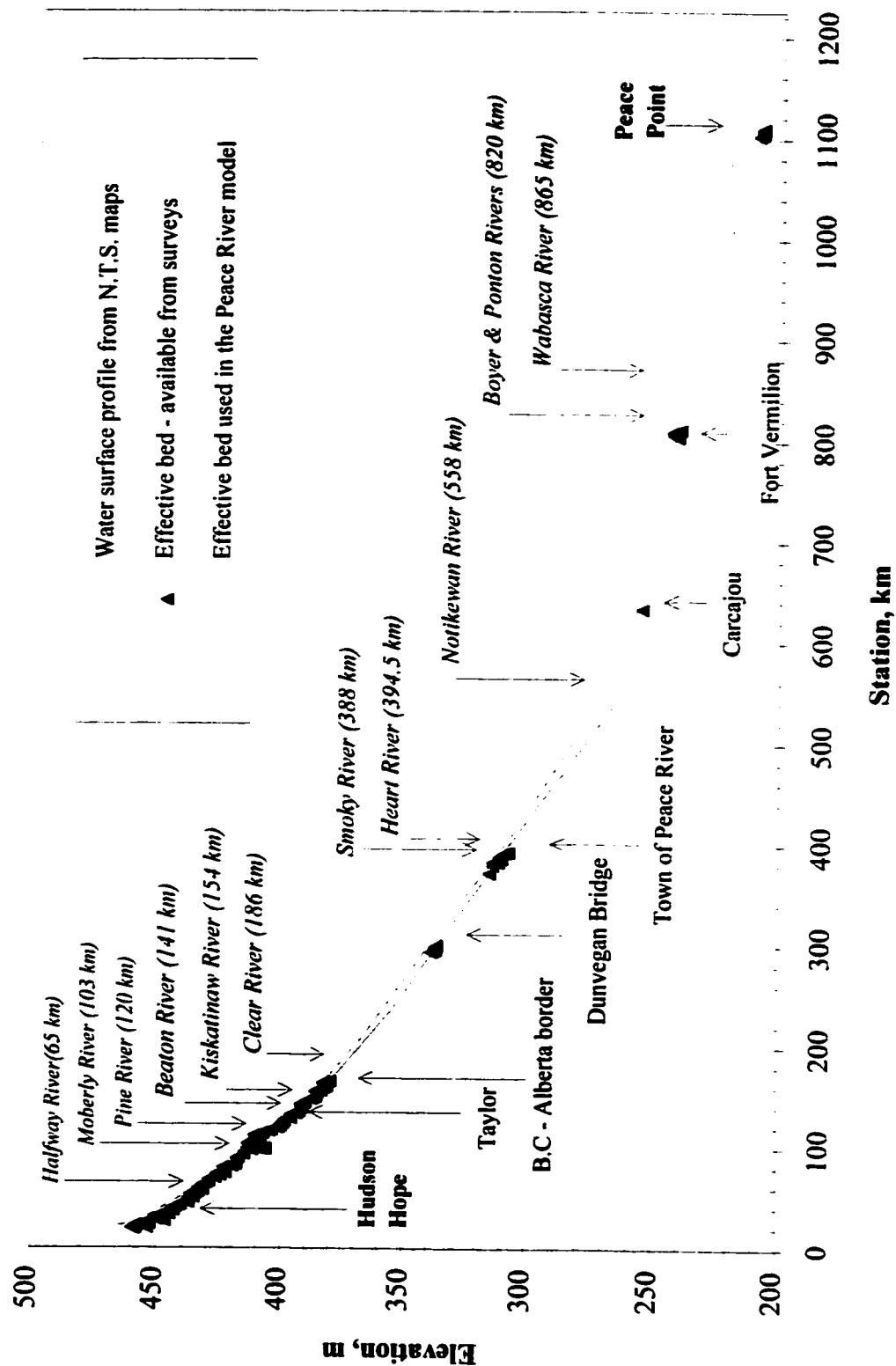
Figure 3.3. Effective bed profile used in the Peace River model.

69
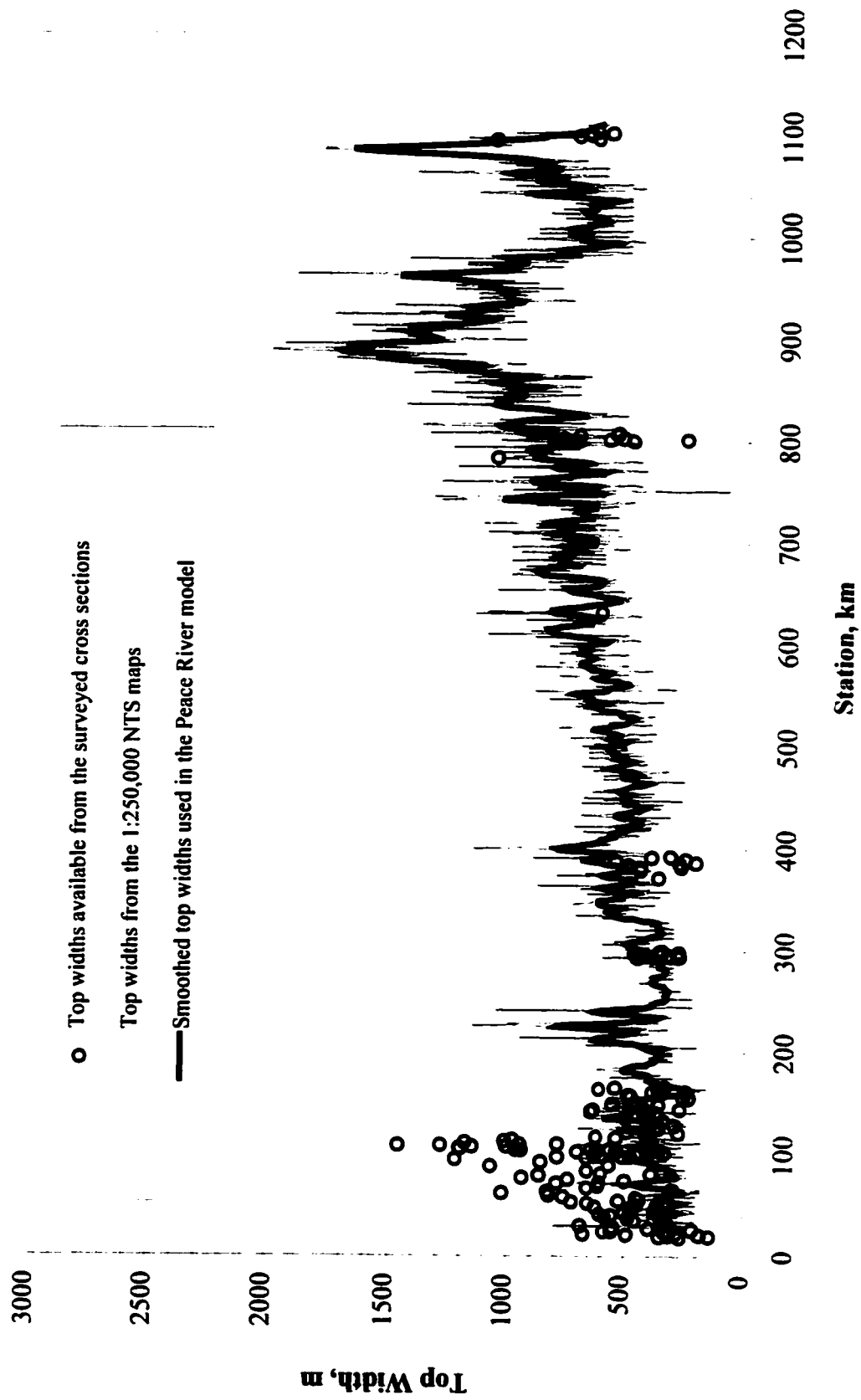
Figure 3.4. Top widths used in the Peace River model.

70
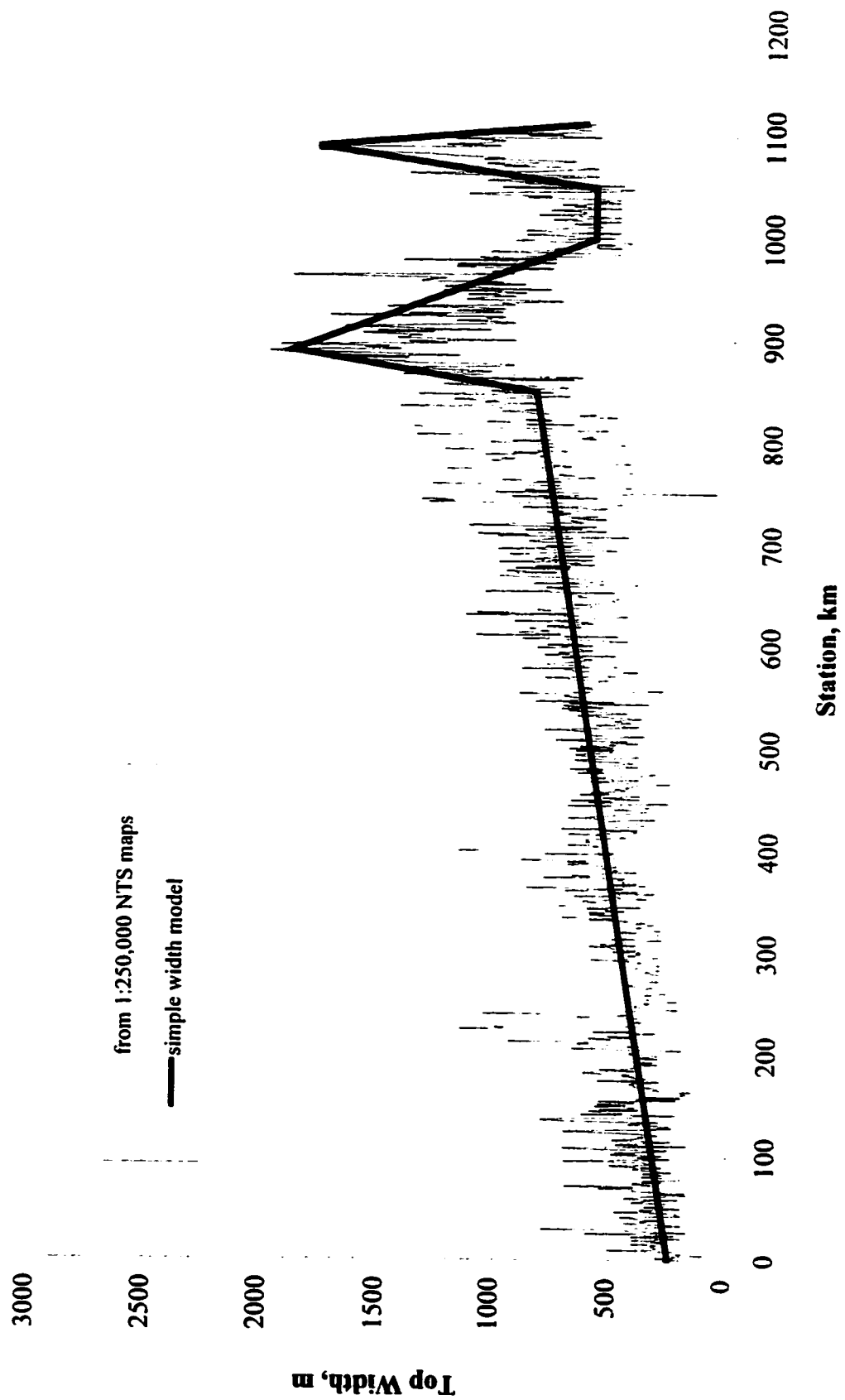
Figure 3.5. Top widths used to test the sensitivity of the Peace River model to the top widths used.

Figure 3.6. Simulation results for historical flows in the Peace River reach, May 15 to October 15, 1965.
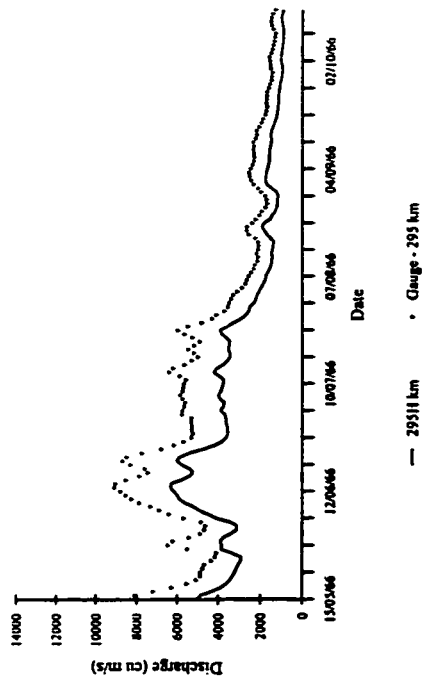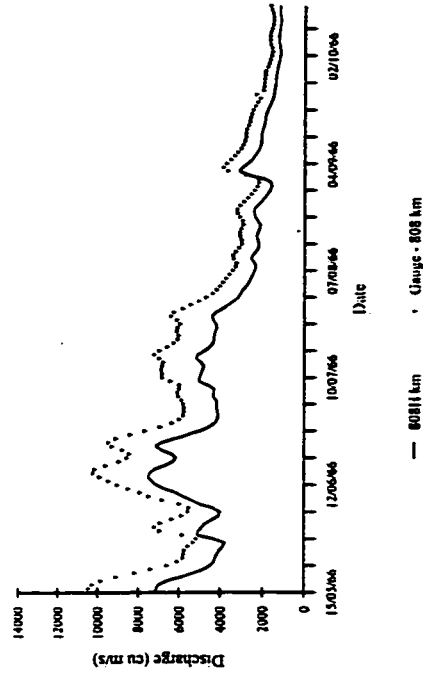
Figure 3.7. Simulation results for historical flows in the Peace River reach, May 15 to October 15, 1966.

73
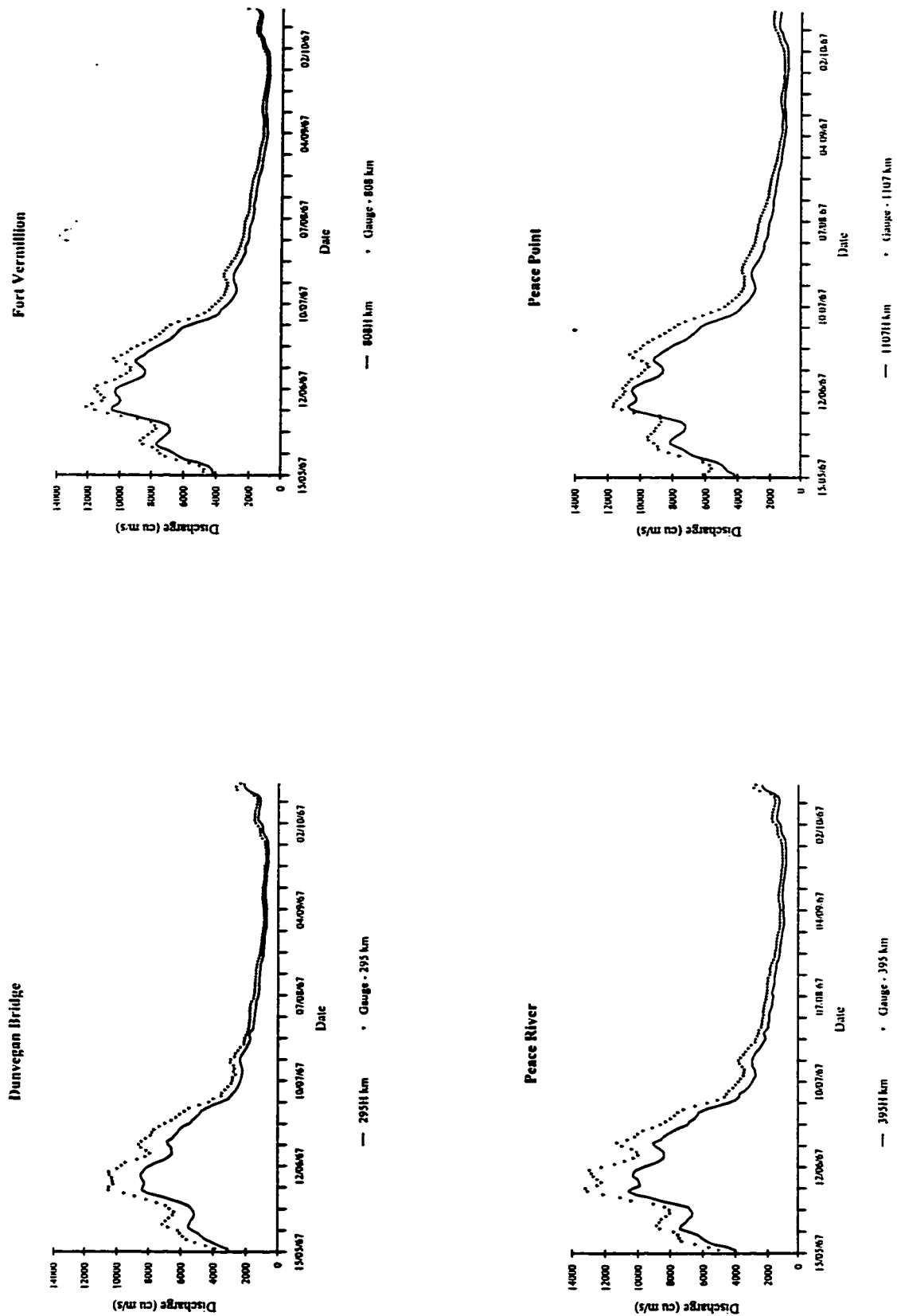
Figure 3.8. Simulation results for historical flows in the Peace River reach, May 15 to October 15, 1967.
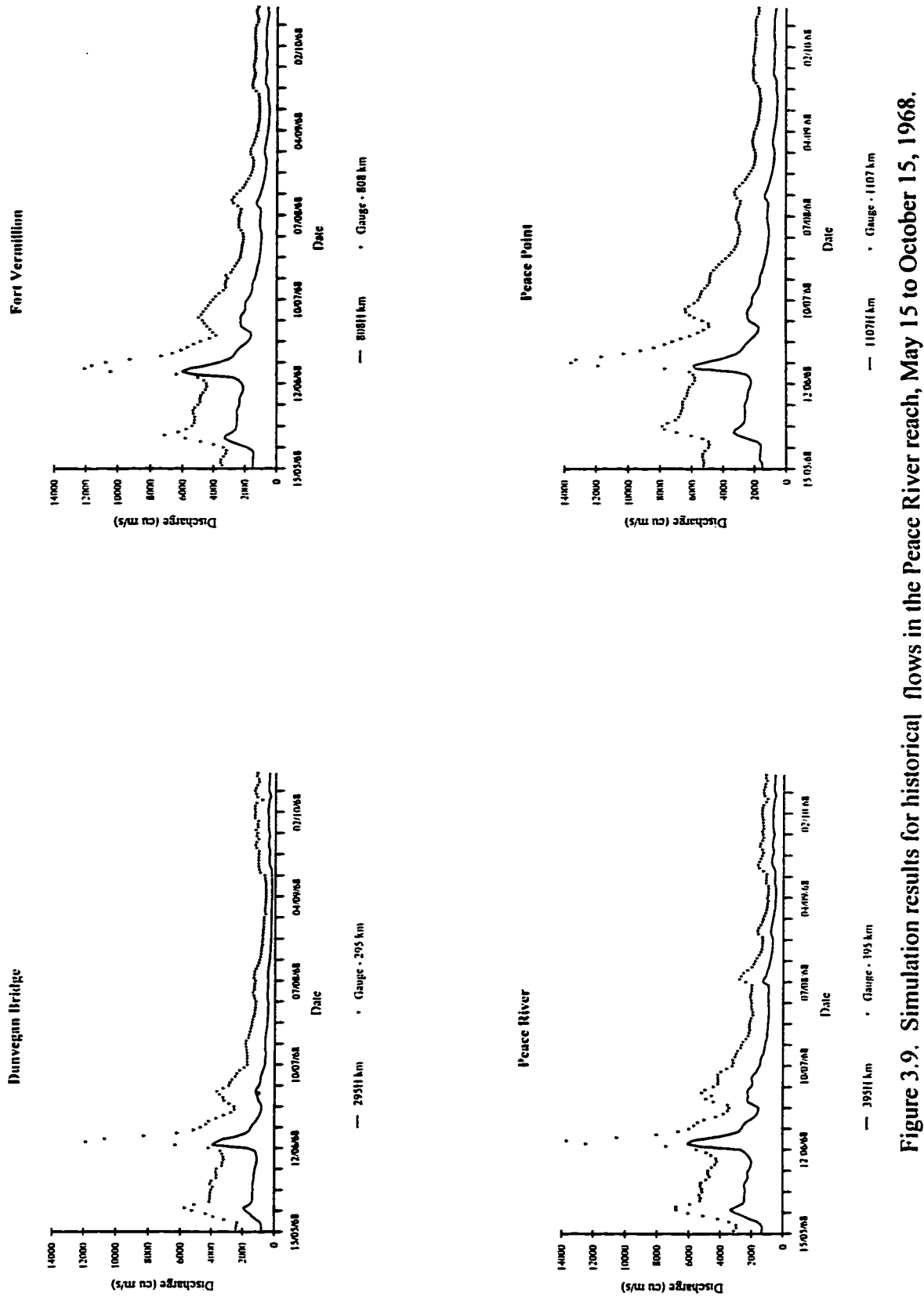
Figure 3.9. Simulation results for historical flows in the Peace River reach, May 15 to October 15, 1968.

75
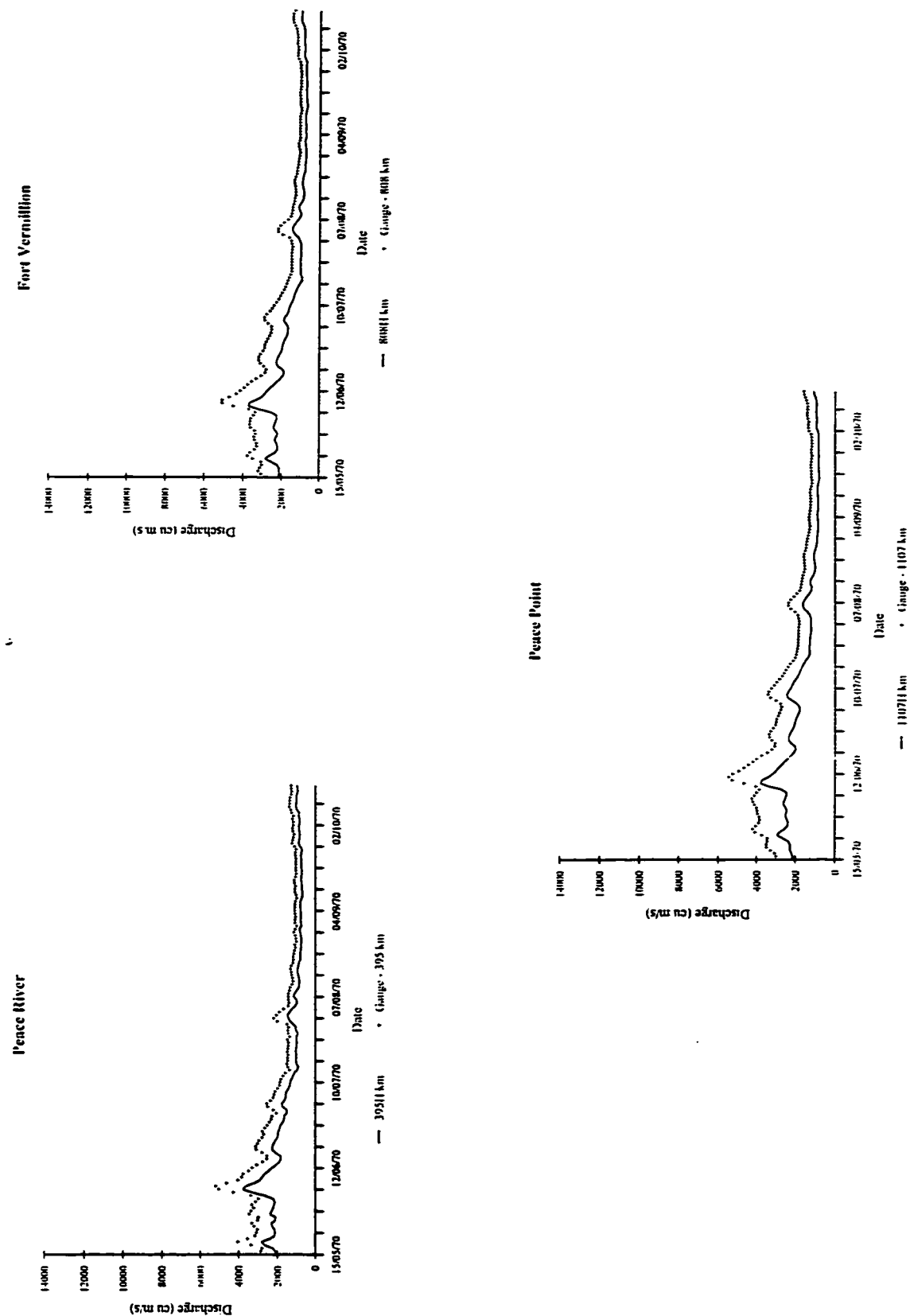
Figure 3.10. Simulation results for historical flows in the Peace River reach, May 15 to October 15, 1970.
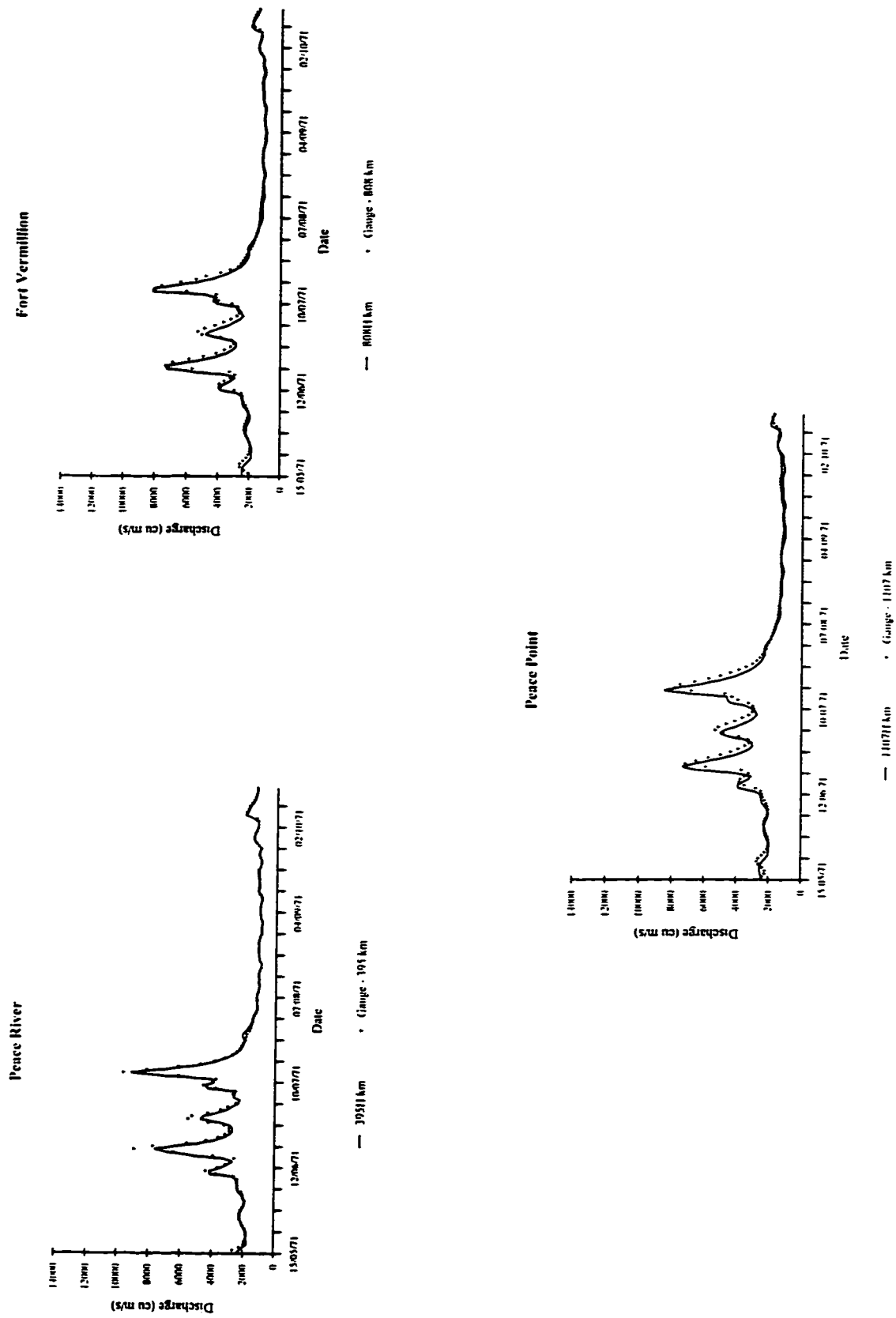
Figure 3.11. Simulation results for historical flows in the Peace River reach, May 15 to October 15, 1971.

77
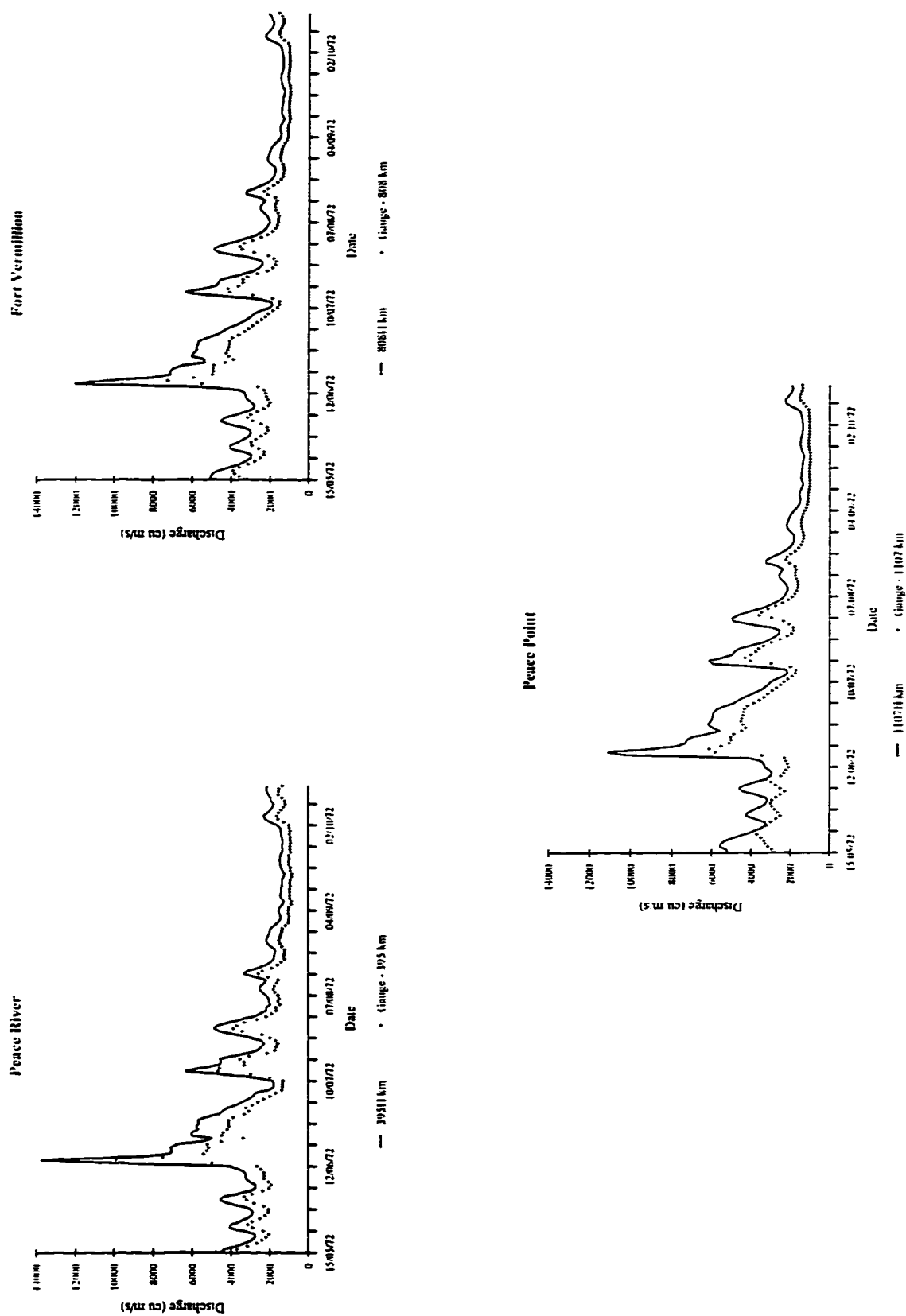
Figure 3.12. Simulation results for historical flows in the Peace River reach, May 15 to October 15, 1972.
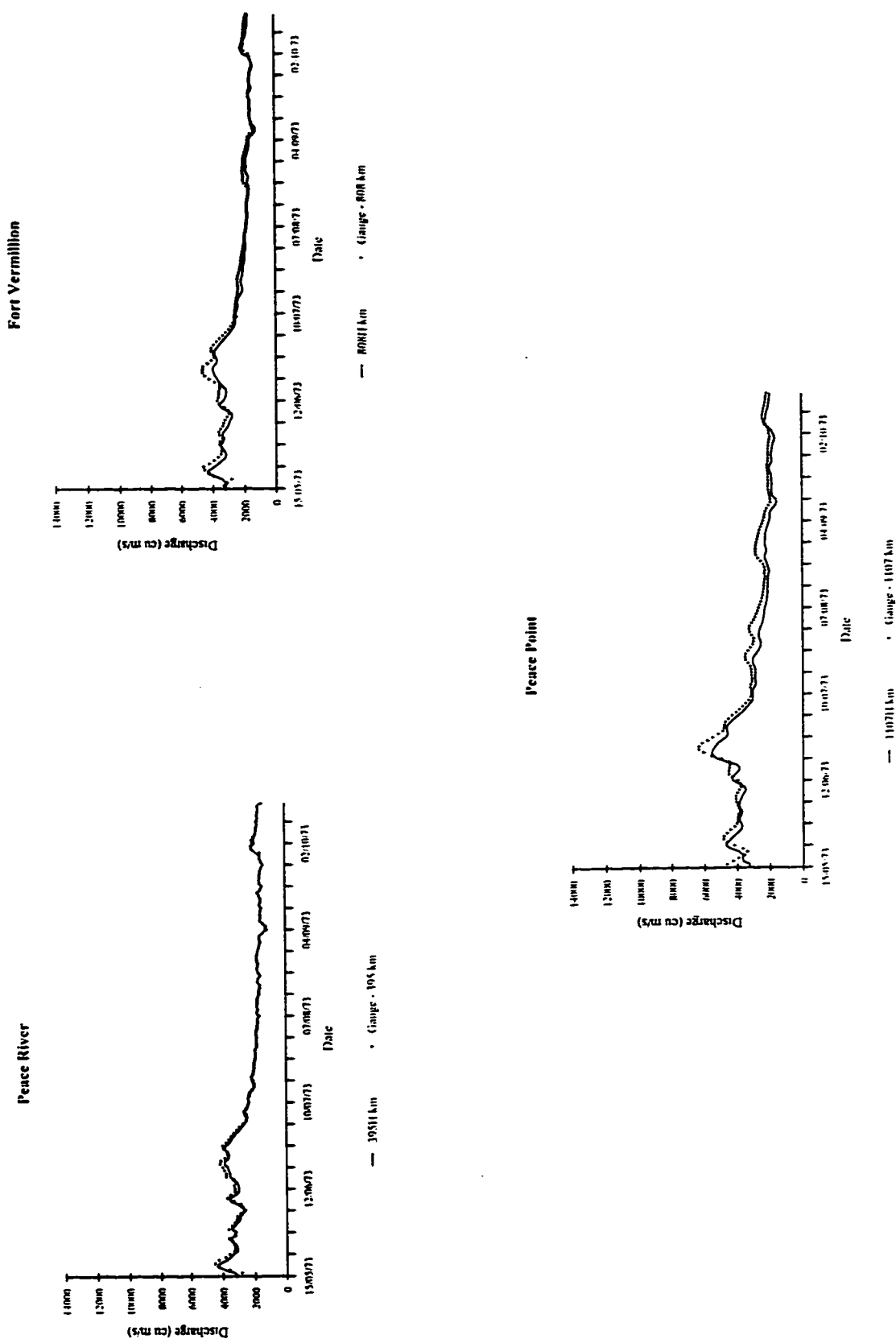
Figure 3.13. Simulation results for historical flows in the Peace River reach, May 15 to October 15, 1973.
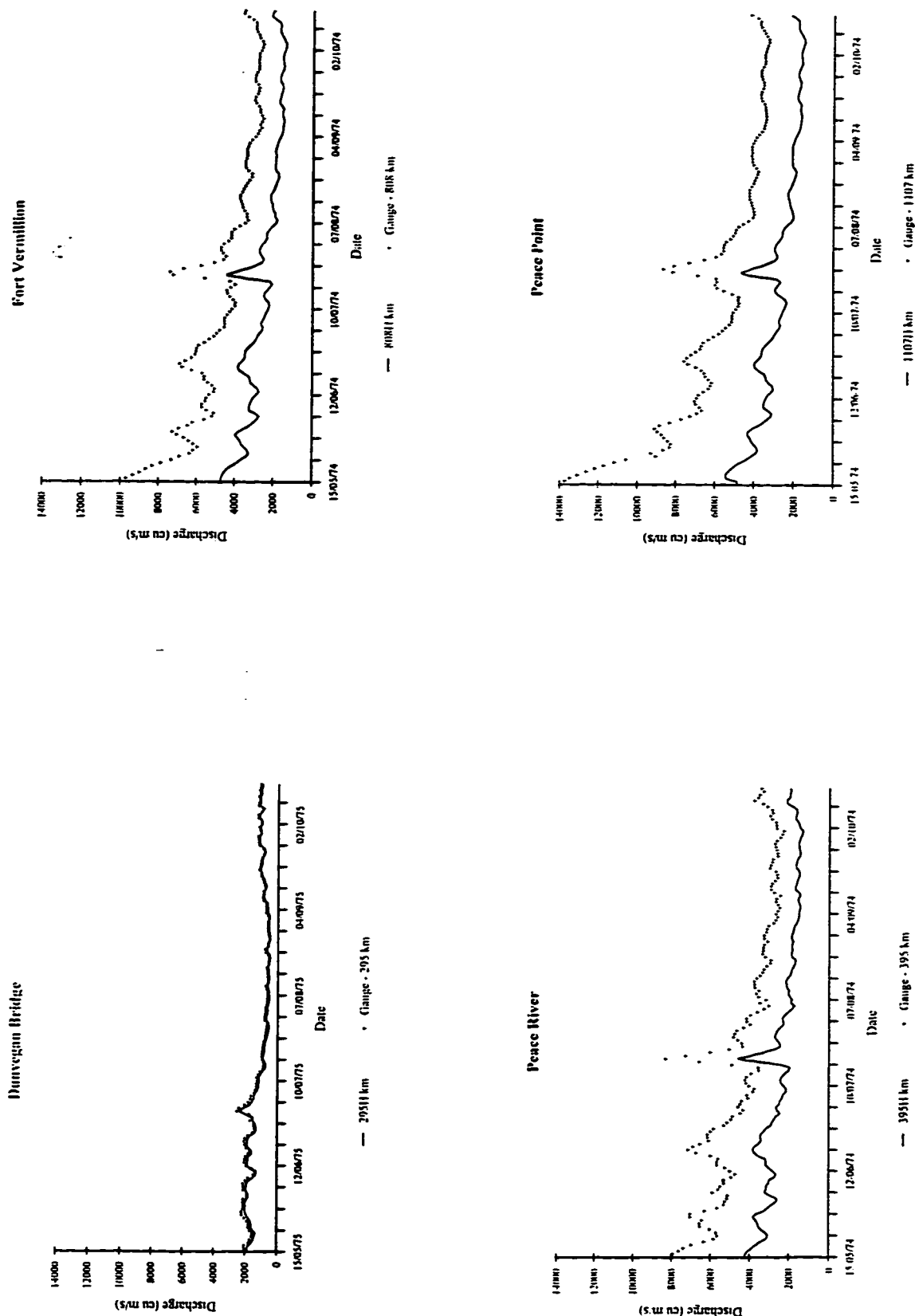
Figure 3.14. Simulation results for historical flows in the Peace River reach, May 15 to October 15, 1974.

80
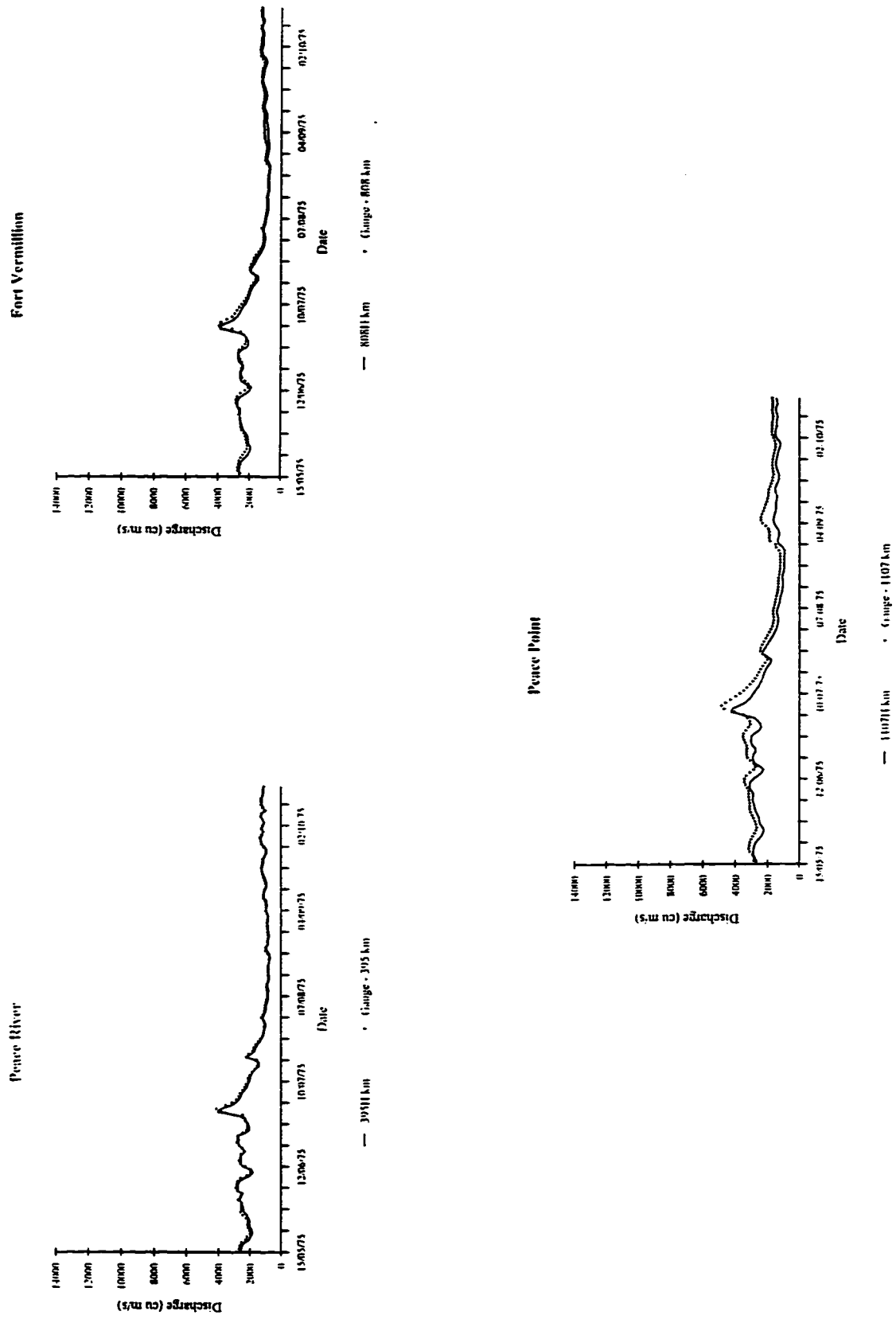
Figure 3.15. Simulation results for historical flows in the Peace River reach, May 15 to October 15, 1975.
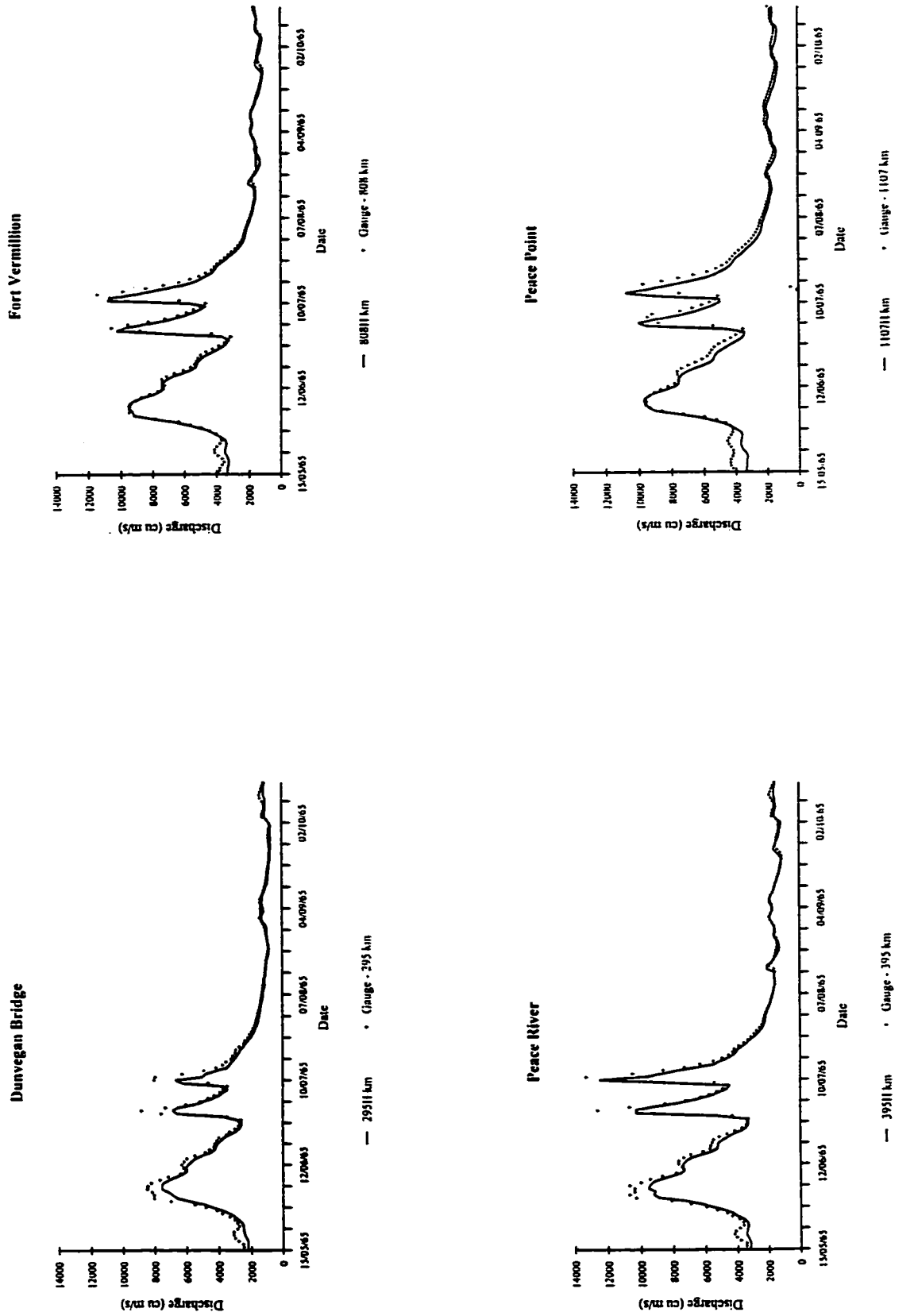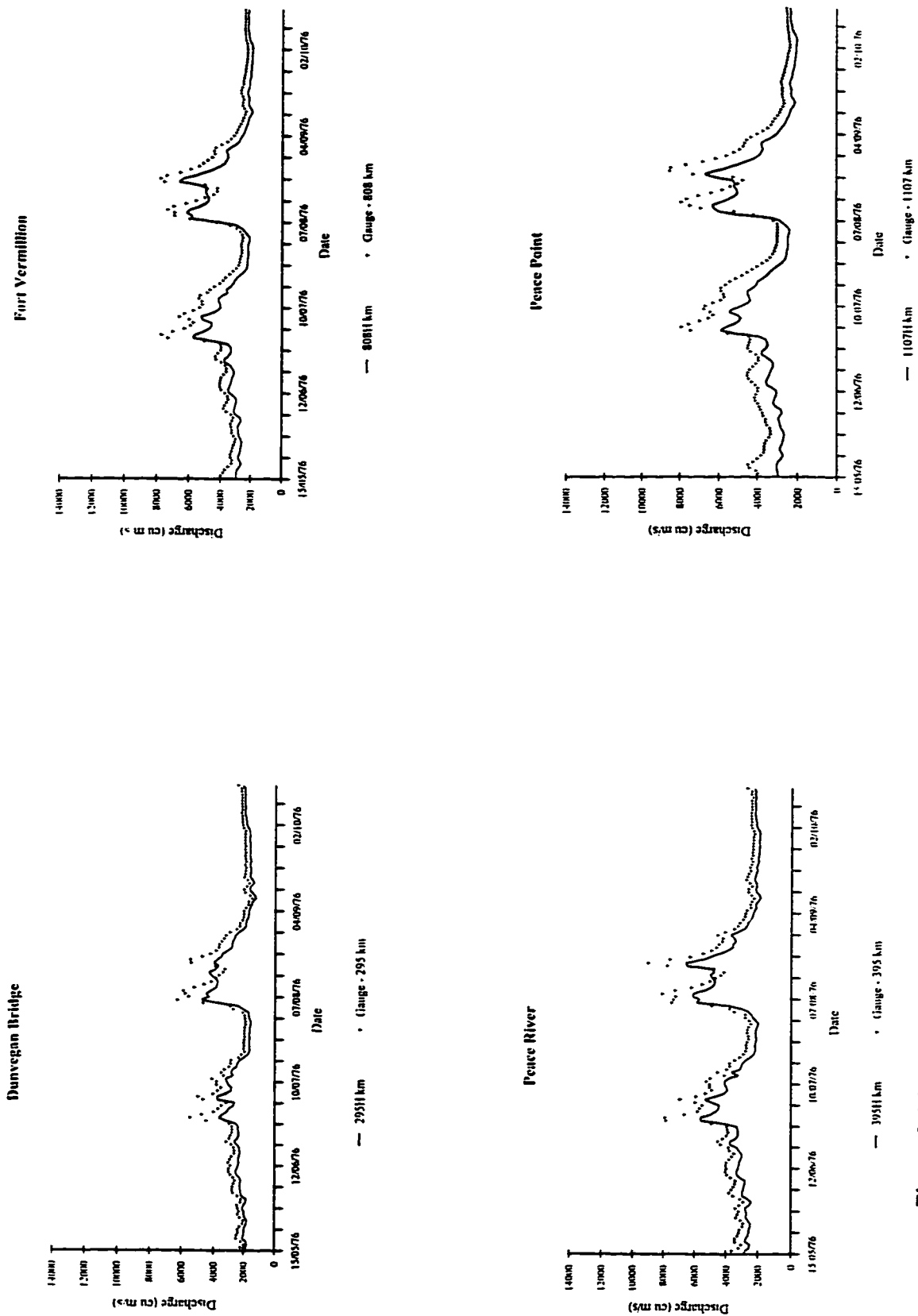
Figure 3.16. Simulation results for historical flows in the Peace River reach, May 15 to October 15, 1976.

82
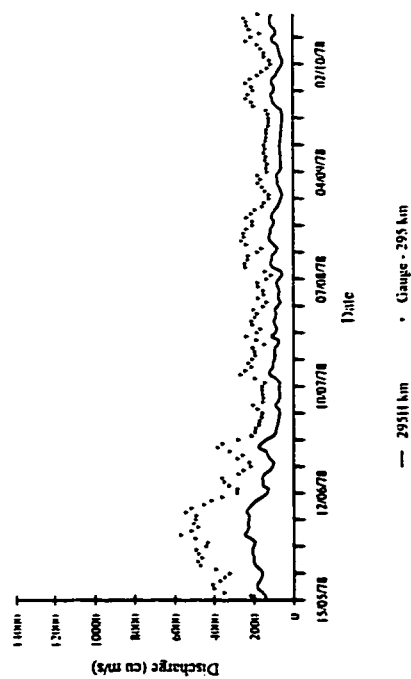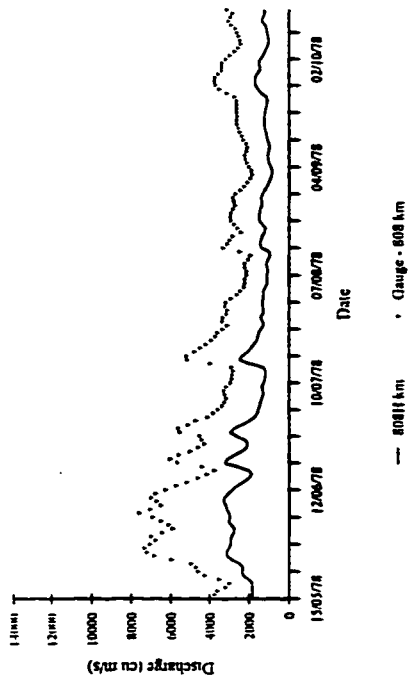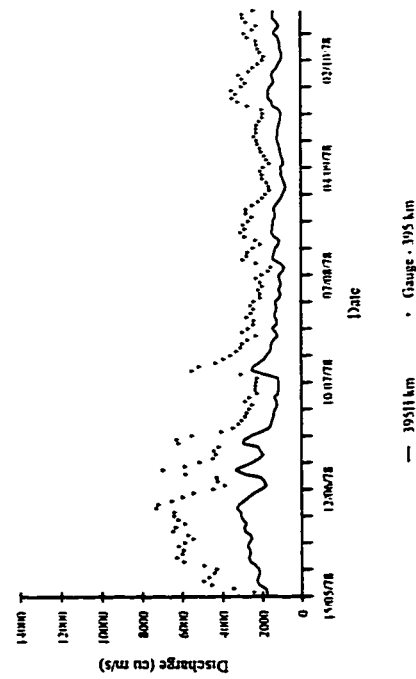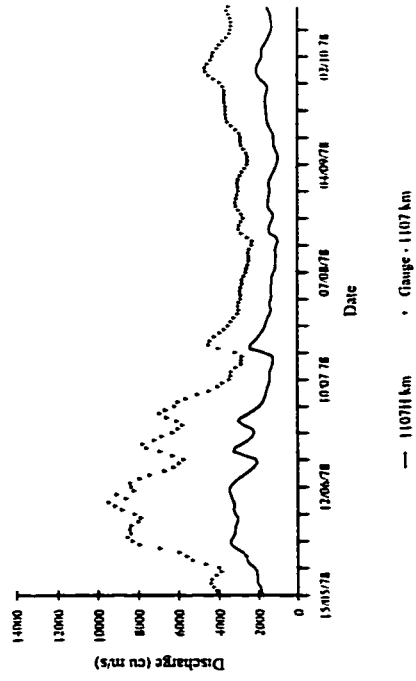
Figure 3.17. Simulation results for historical flows in the Peace River reach, May 15 to October 15, 1978.

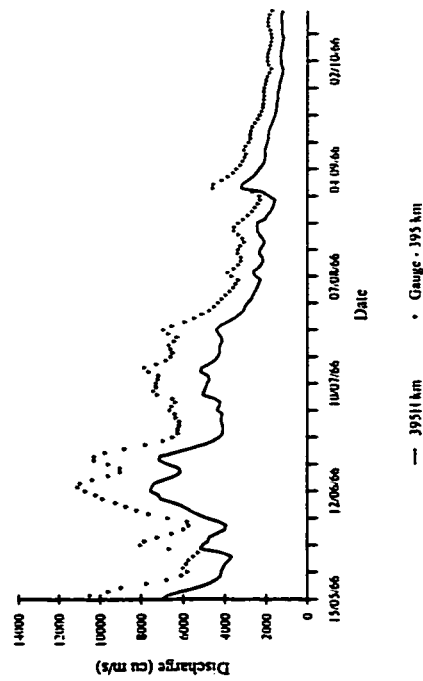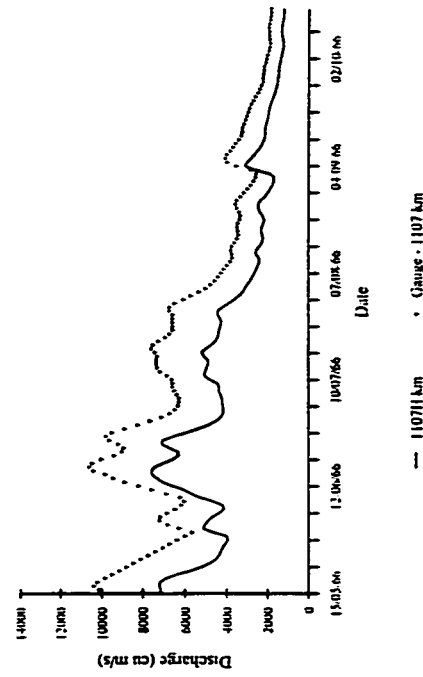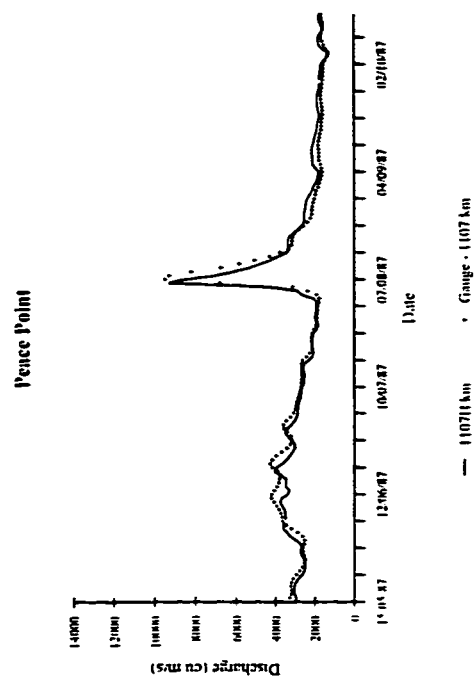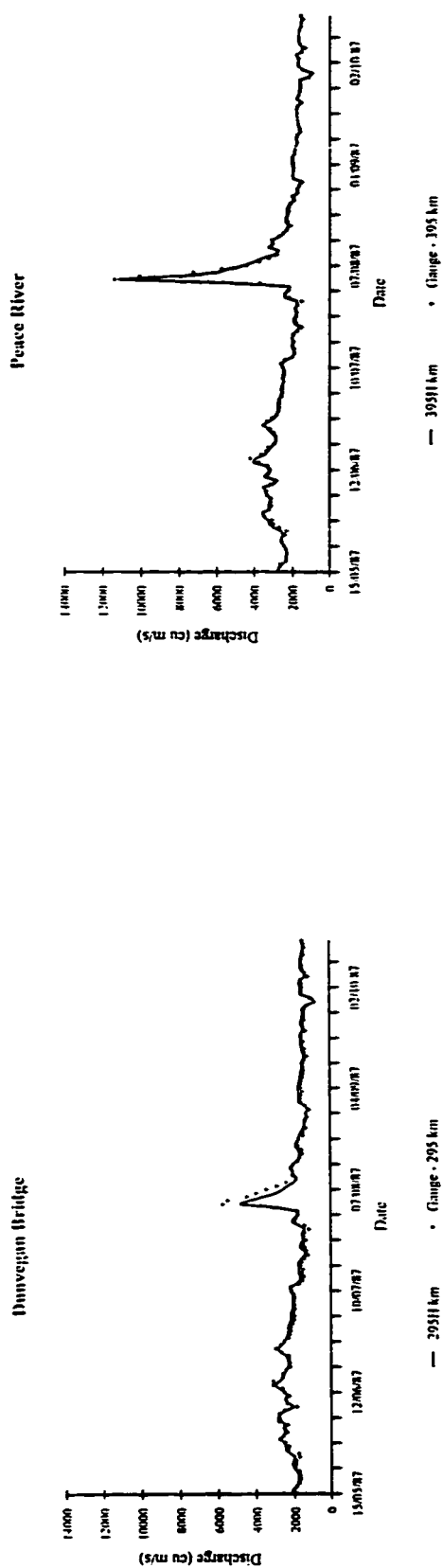Figure 3.18. Simulation results for historical flows in the Peace River reach, May 15 to October 15, 1987.

84
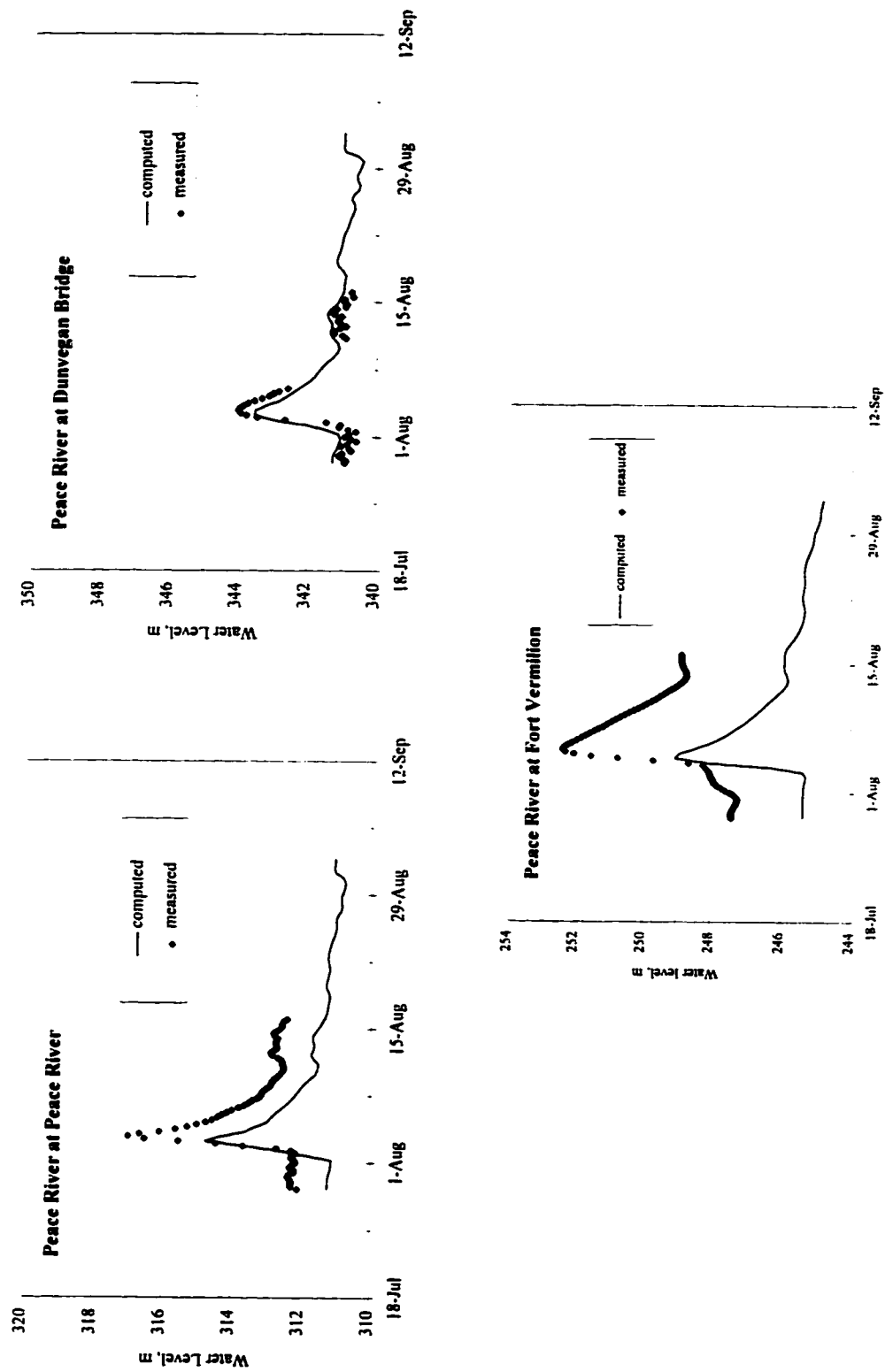
Figure 3.19. Comparison of measured and computed water levels for the Peace River reach, 1987 event.
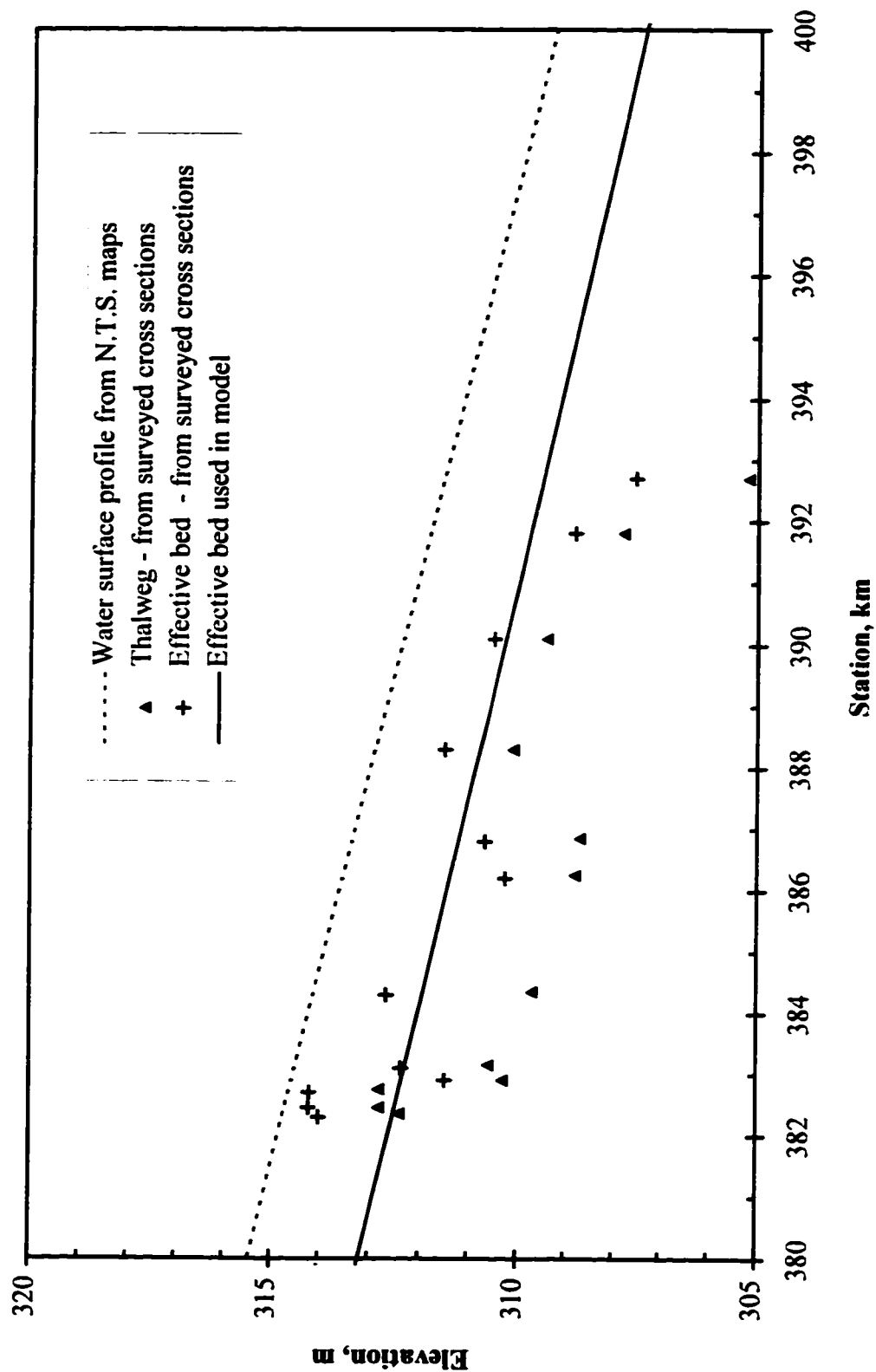
Figure 3.20. Comparison of measured and effective bed profiles in the vicinity of the town of Peace River.
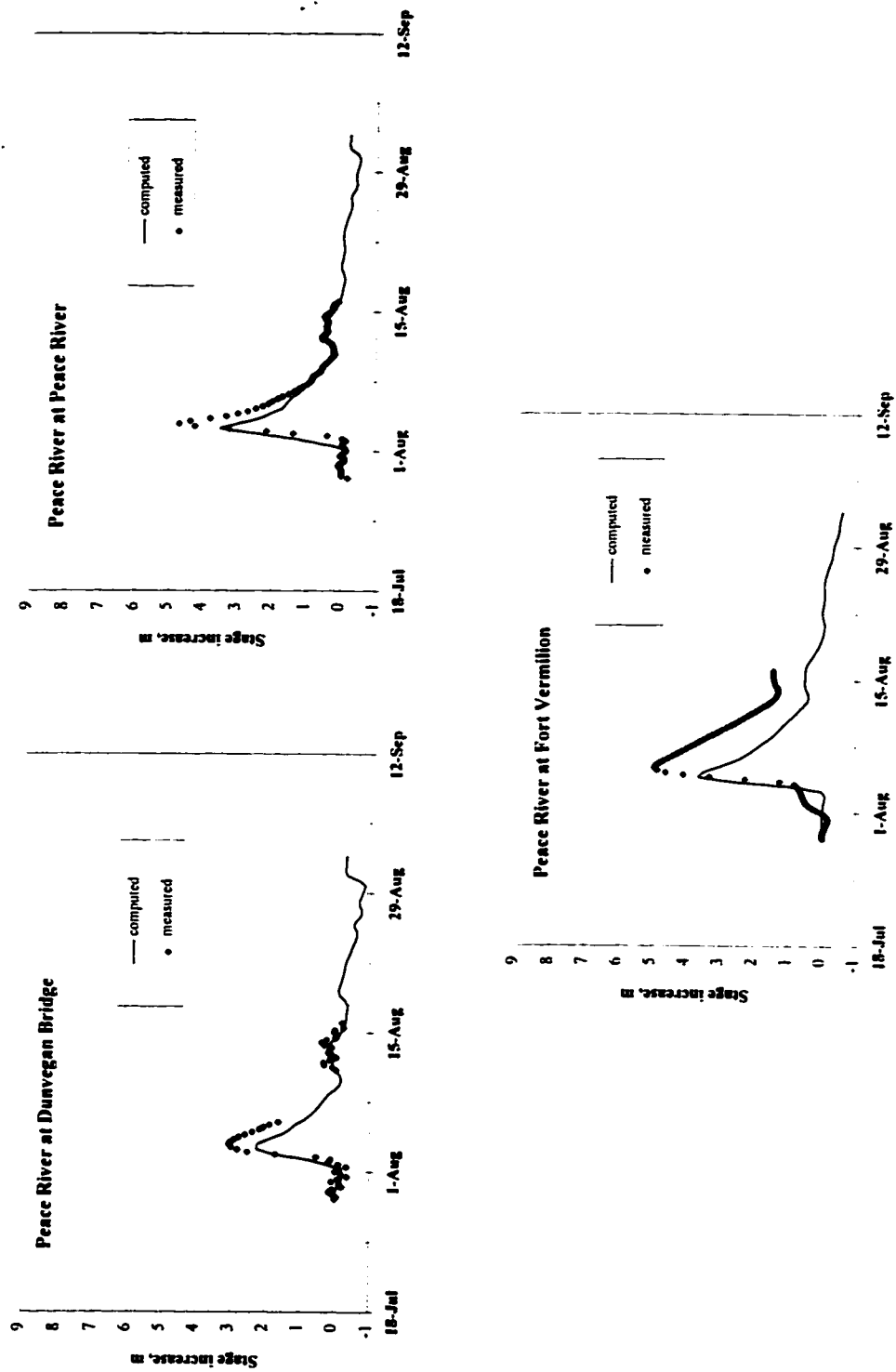
Figure 3.21. Comparison of measured and computed stage increases for the Peace River, 1987 event.
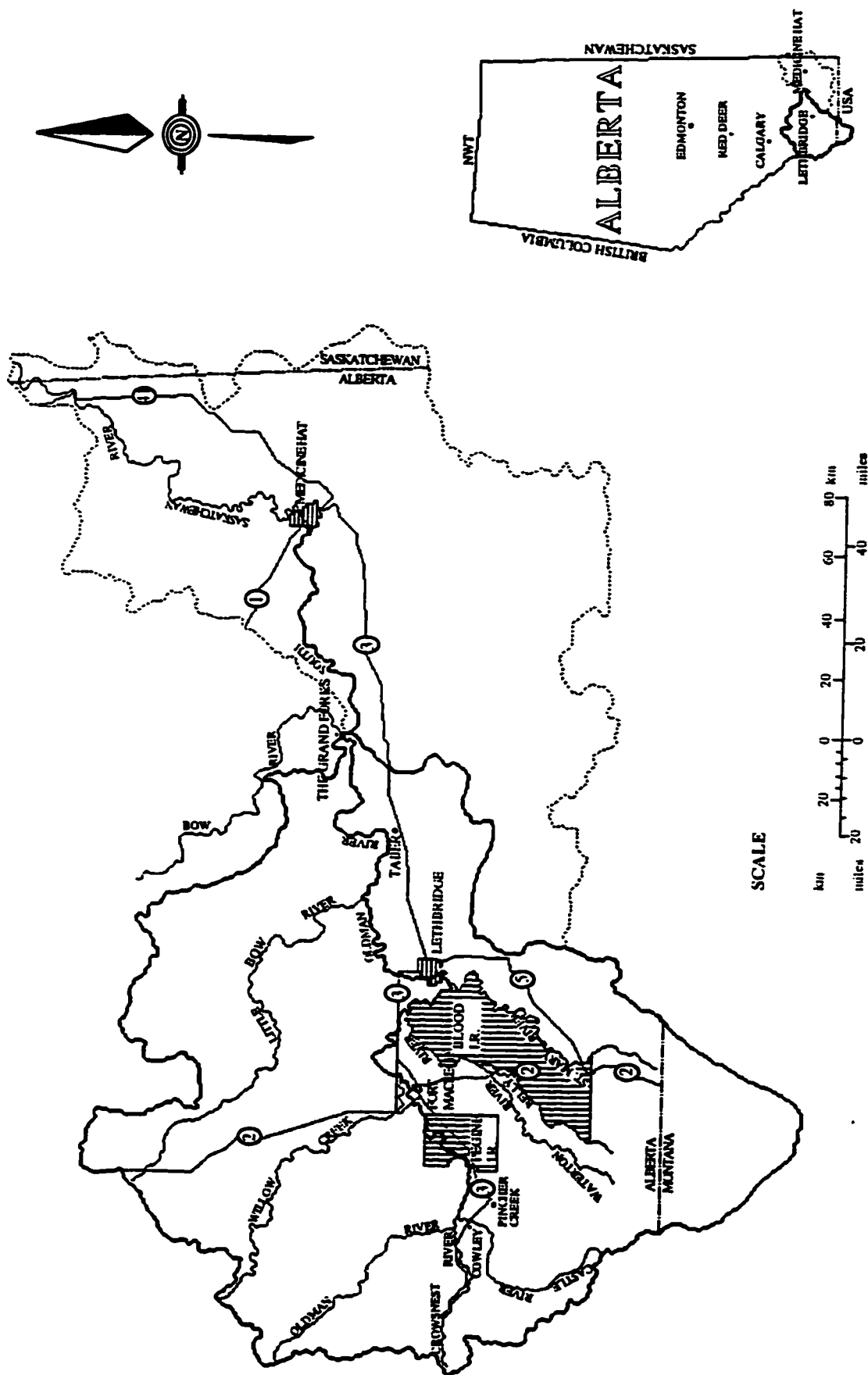
Figure 3.22. Location sketch for the Oldman/South Saskatchewan River study reach.
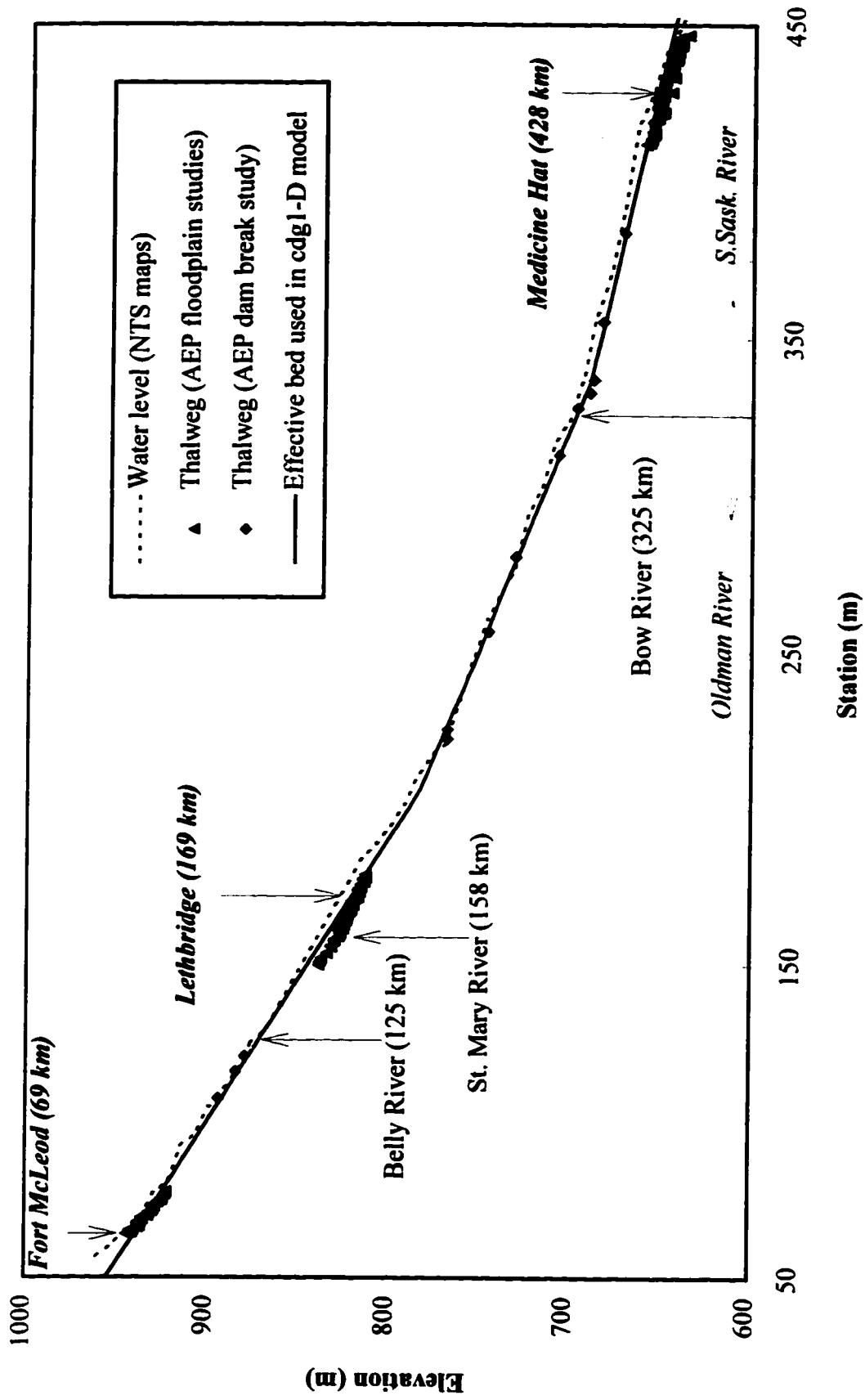
Figure 3.23. Effective bed profile developed from the available data for the Oldman/South Saskatchewan River.
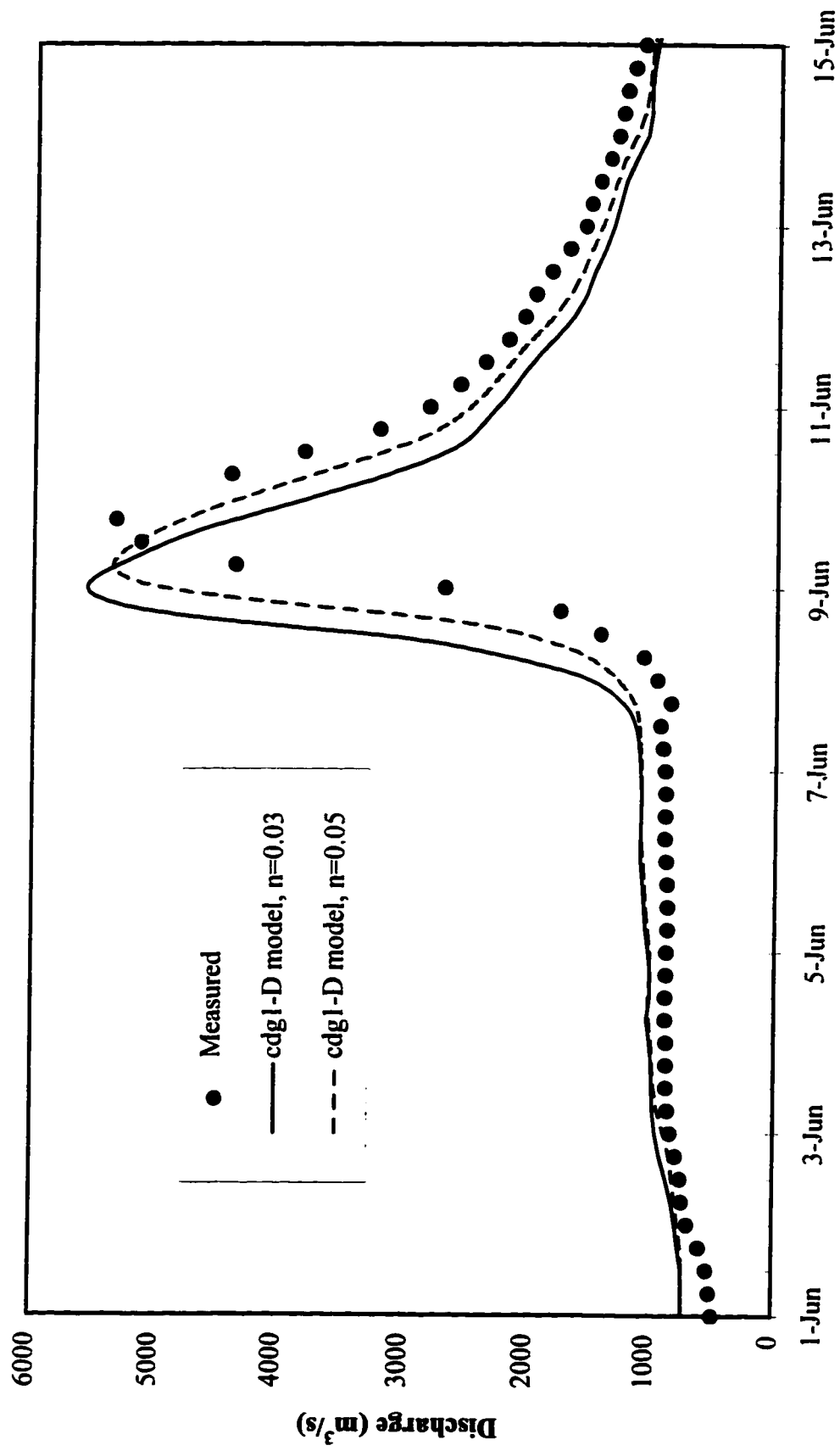
Figure 3.24. Comparison of measured and computed hydrographs at Medicine Hat for variable Mannings n for 1995 event on the Oldman/South Saskatchewan River.
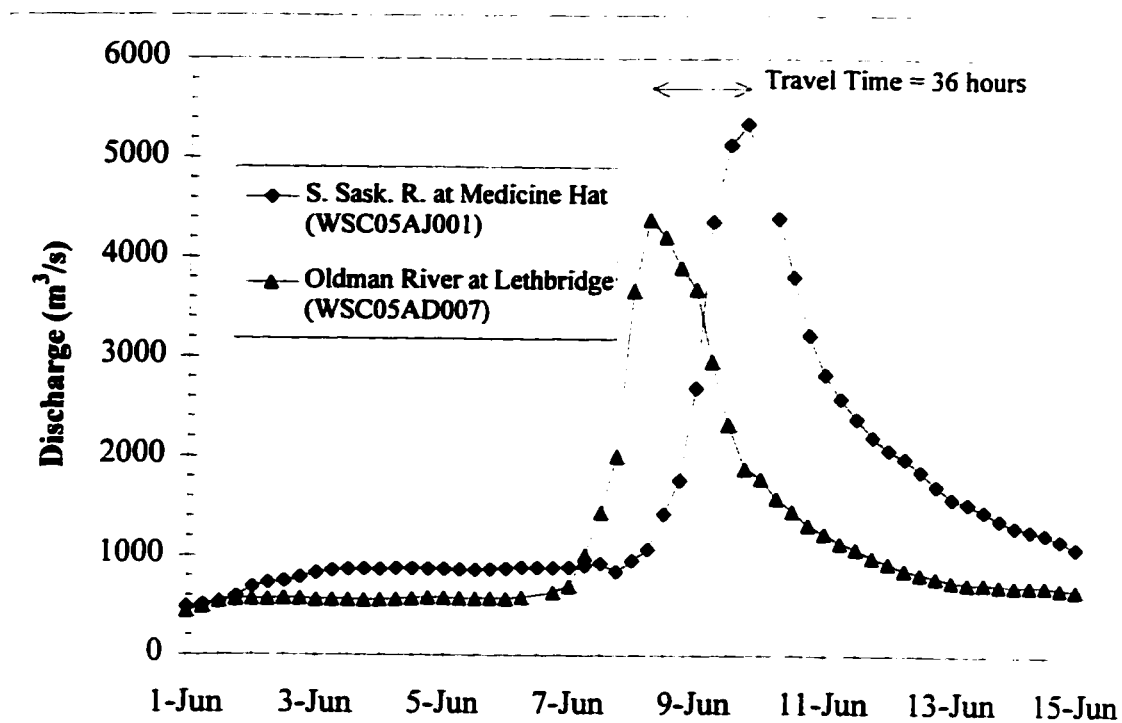
a) Travel Time between Lethbridge and Medicine Hat
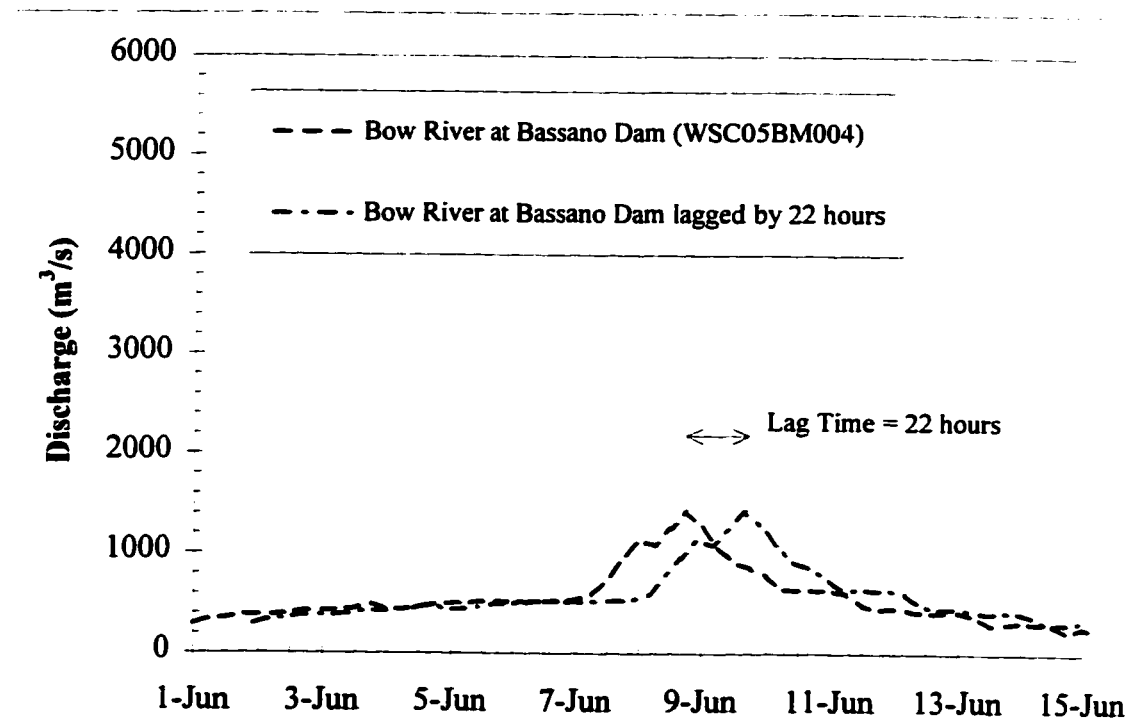
b) Lag Time for the Bow River

Figure 3.25. Travel and lag times for the Oldman/South Saskatchewan River, 1995 event.

91
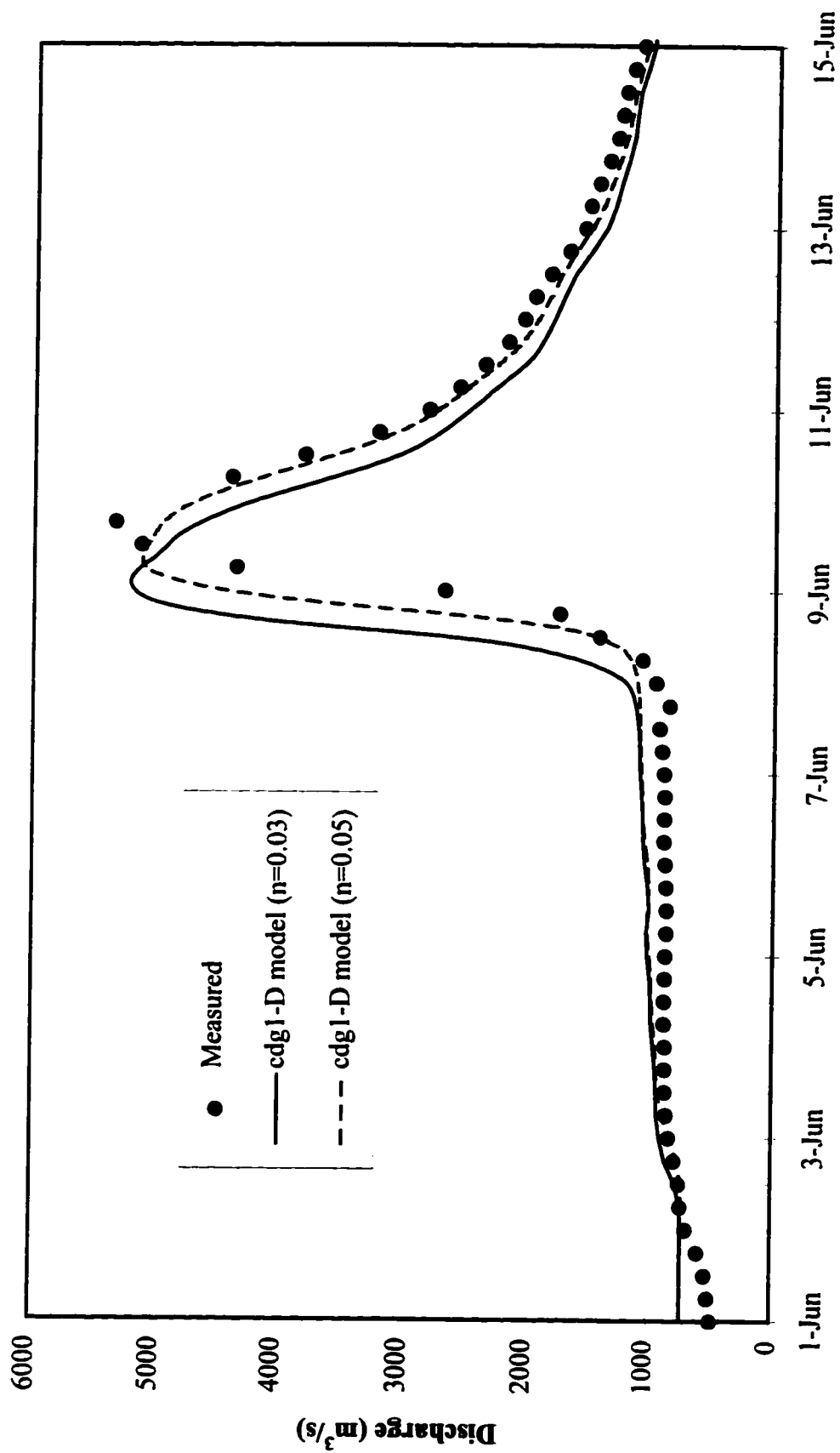
Figure 3.26. Comparison of measured and computed hydrographs at Medicine Hat based on lagging the Bow River hydrograph by 22 hours, 1995.
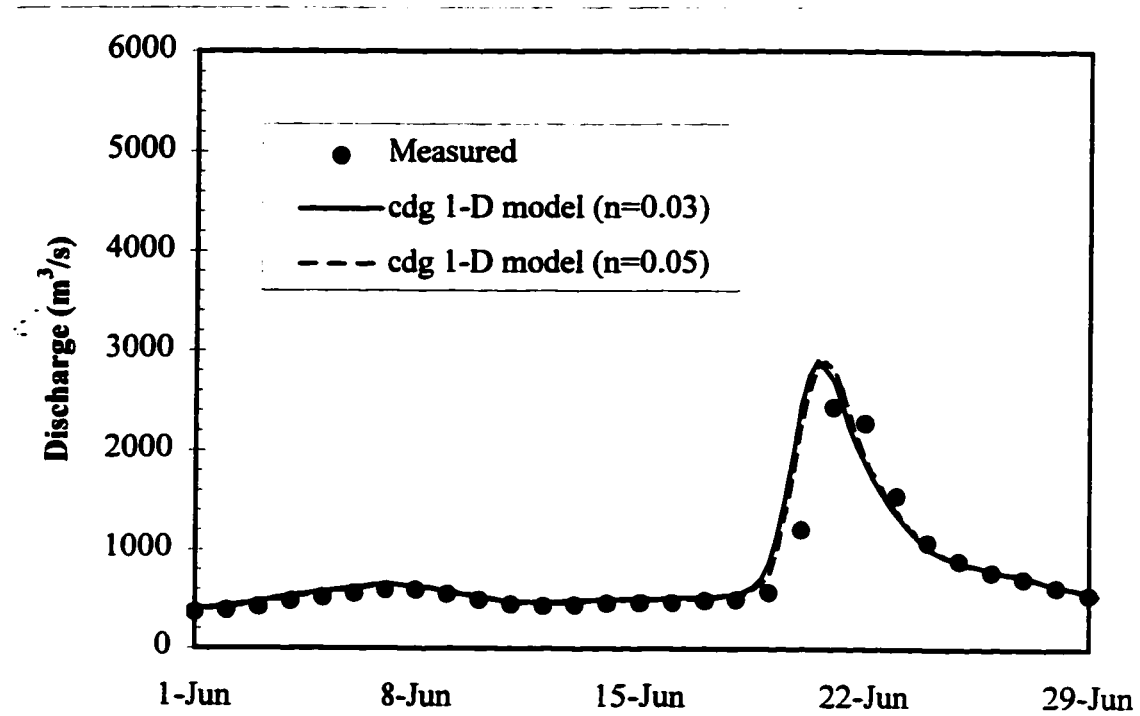
a) Lethbridge
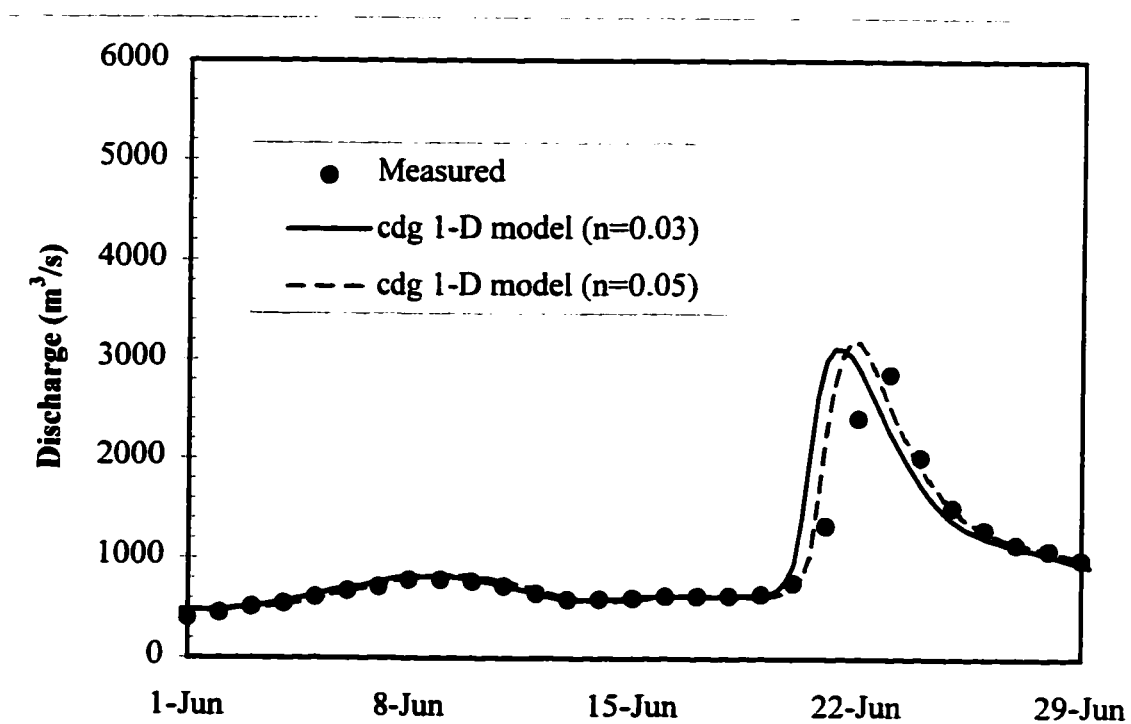
b) Medicine Hat

Figure 3.27. Comparison of measured and computed hydrographs for variable Mannings n, for the 1975 event on the Oldman/South Saskatchewan River.

93
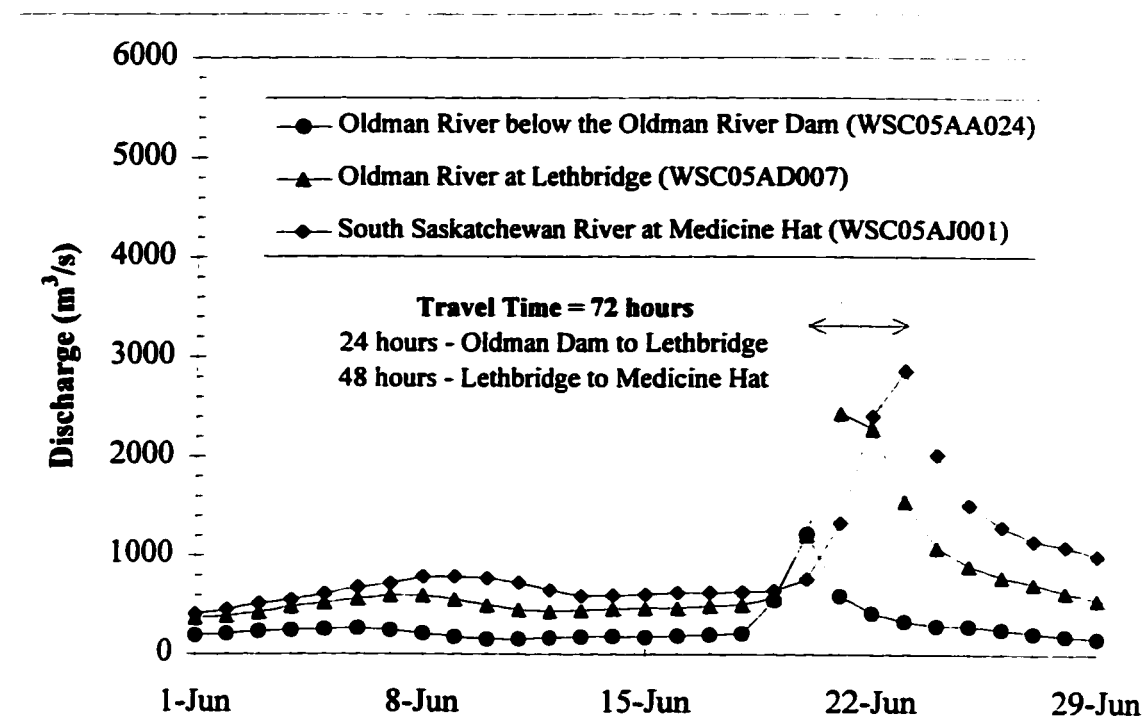
a) Travel time between Oldman River Dam and Medicine Hat
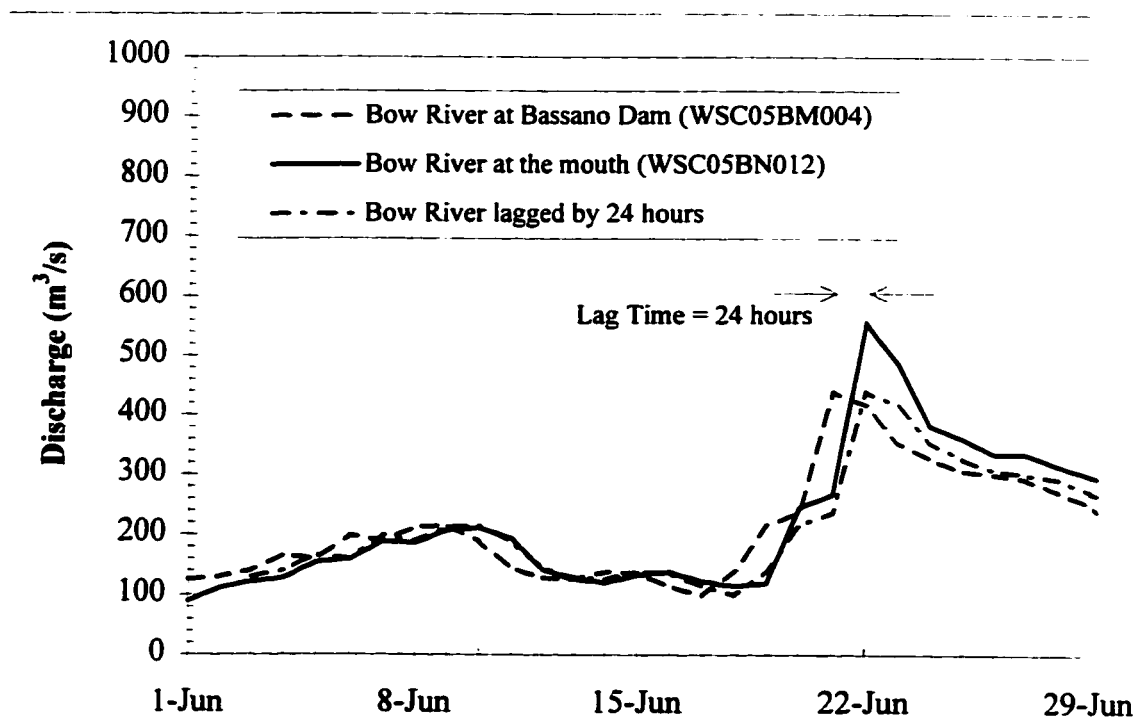
b) Lag time for the Bow River

Figure 3.28. Travel and lag times for the Oldman/South Saskatchewan River, 1975 event.
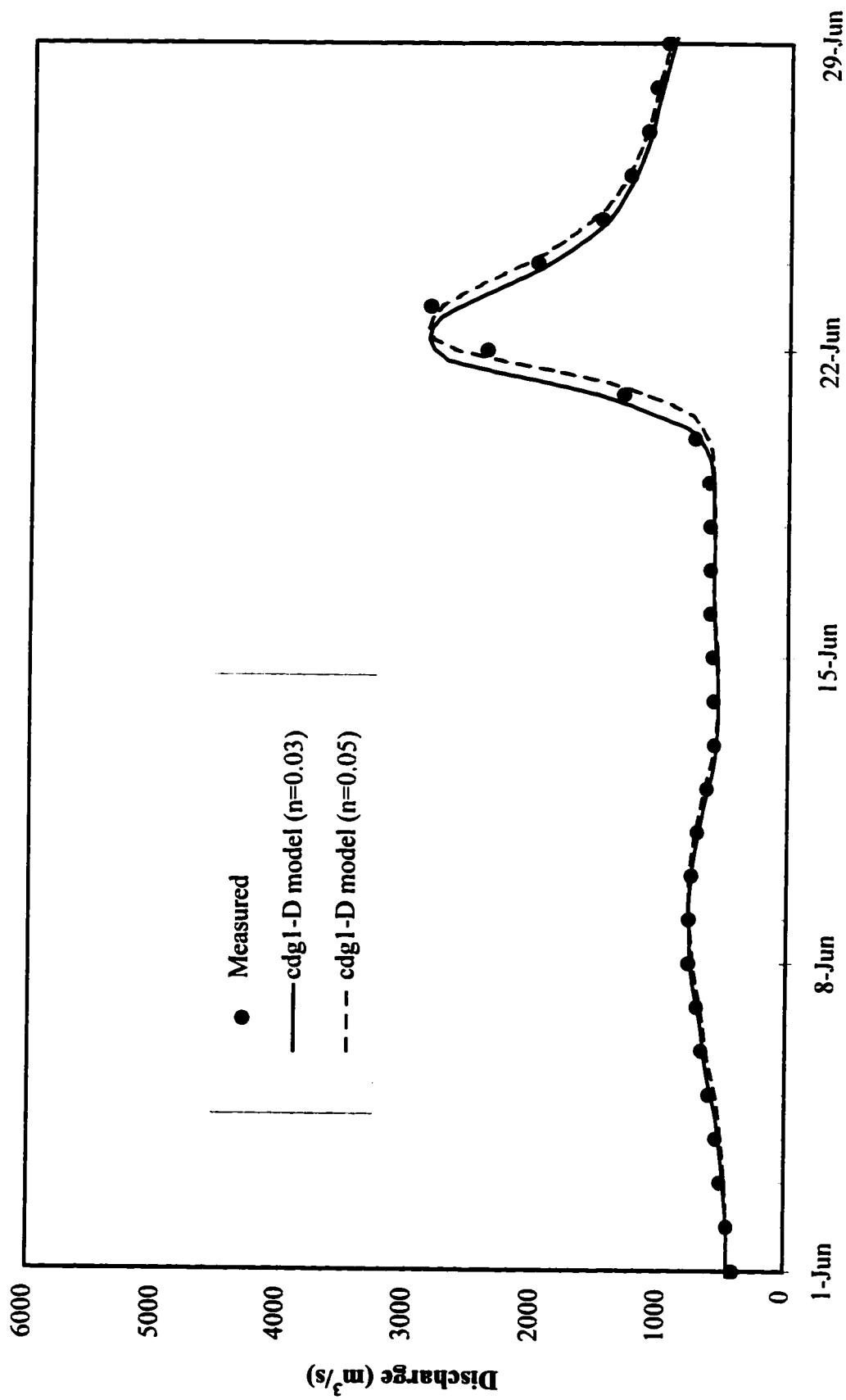
Figure 3.29. Comparison of measured and computed hydrographs at Medicine Hat when the flood was routed from Lethbridge, 1975.

95
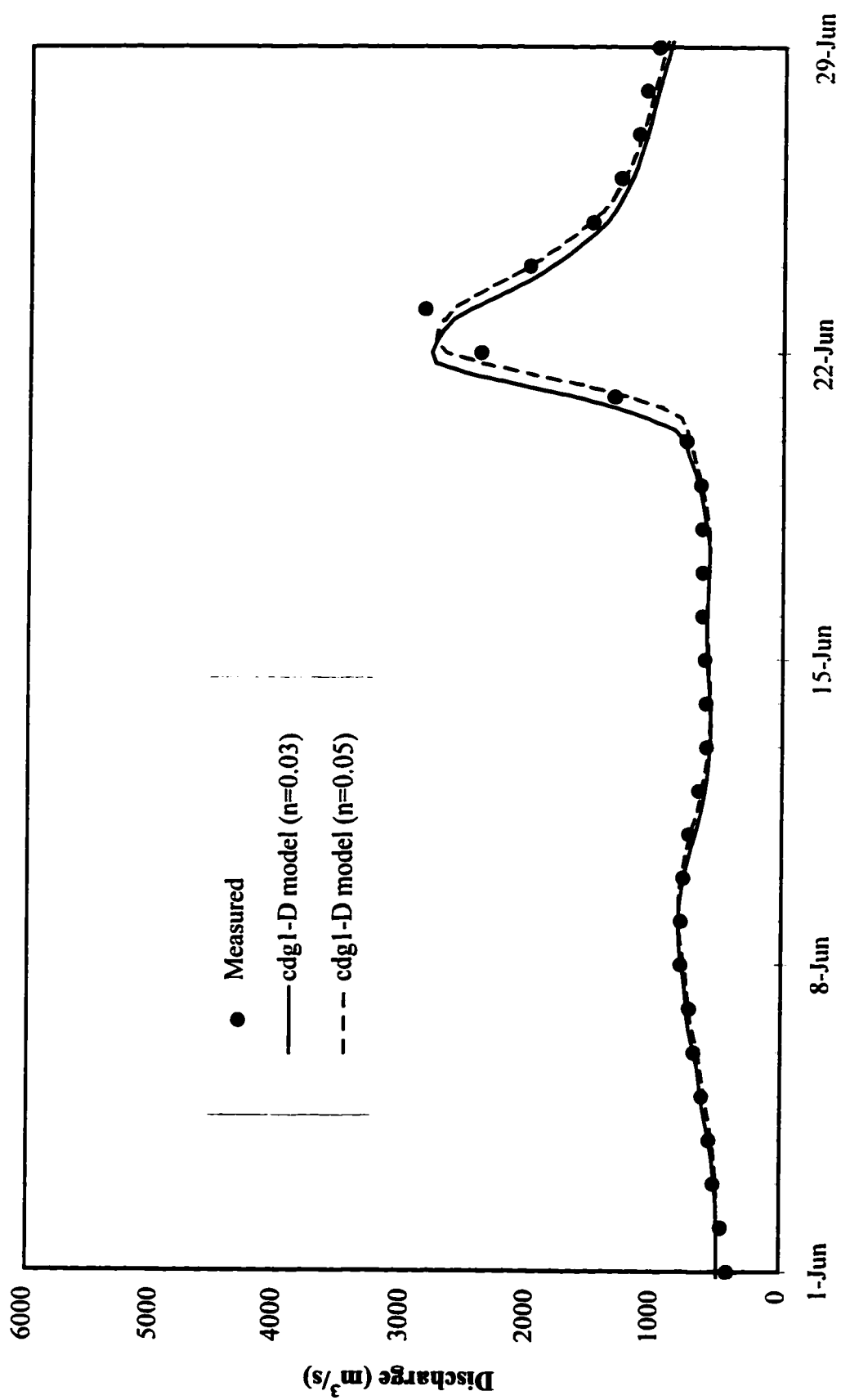
Figure 3.30. Flood routing from Lethbridge to Medicine Hat using the WSC gauge on the Bow River below Bassano Dam for tributary inflow data, 1975.

Figure 3.31. Flood routing from Lethbridge to Medicine Hat using the WSC gauge on the Bow River below Bassano Dam with a lag time of 24 hours for tributary inflow data, 1975.

97
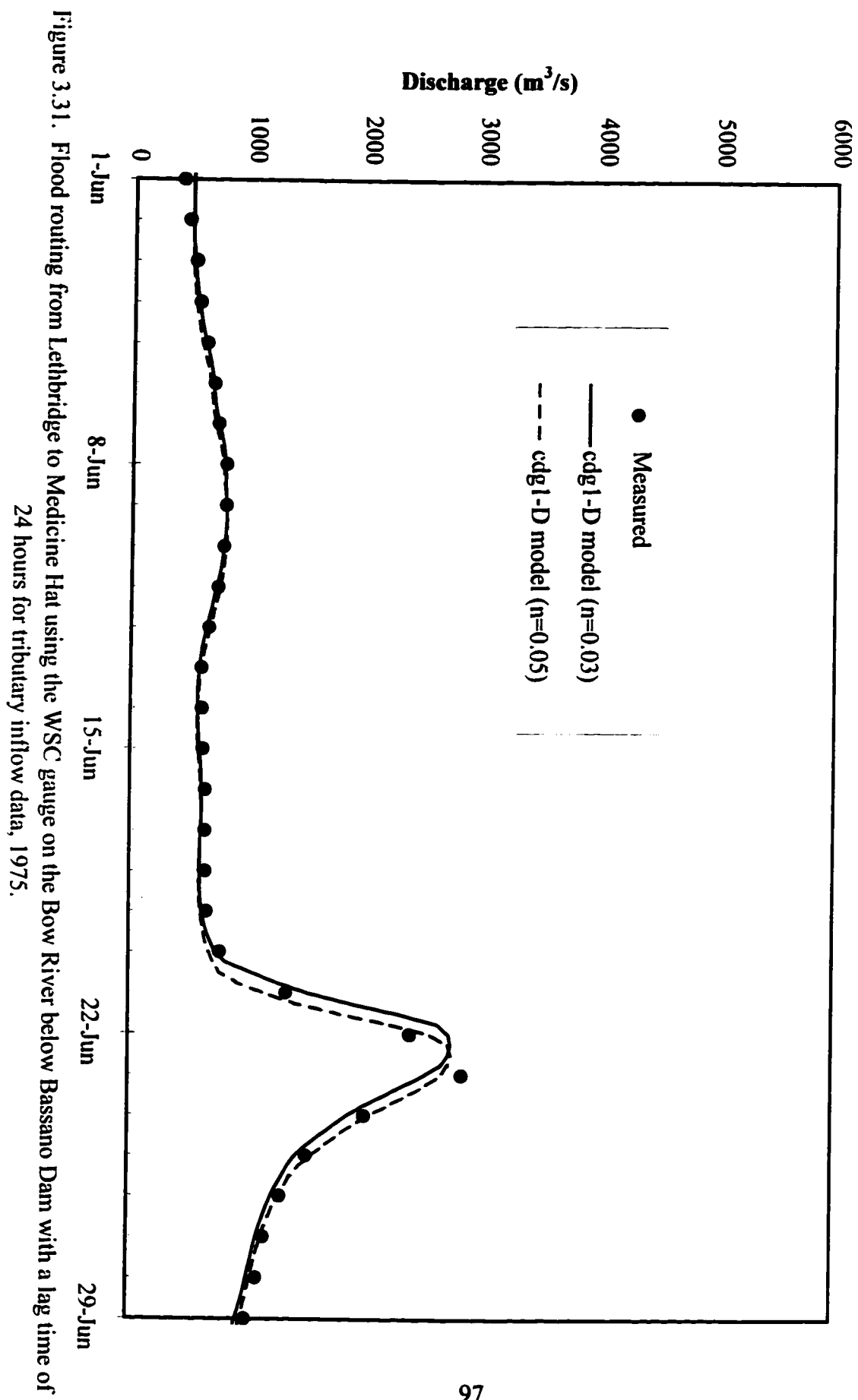
CHAPTER 4

VERIFICATION OF HYDRAULIC FLOOD ROUTING WITH MINIMAL HYDROLOGIC AND GEOMETRIC DATA[3]

4.1   INTRODUCTION

The purpose of this study was to verify the accuracy of hydraulic flood routing techniques when minimal geometric and hydrologic data was available for the study reach. This was accomplished by creating not only a synthesized geometric database. but a synthesized hydrologic database as well since all the tributaries were ungauged.

The following chapter describes the procedure used in developing both the geometric and the hydrologic databases. It looks at the model calibration required for the Porcupine River study reach and it reviews the results obtained through assuming various approximations to the ice conditions which occur during break up.

---

[3] This chapter is an edited version of McKay, K. and F.E. Hicks. 1996. Ice jam Surge Modelling on the Porcupine River, Yukon. Water Resources Engineering Report 96-H1, Civil Engineering Department, University of Alberta, Edmonton, Alberta, Canada, which was written for Department of Indian Affairs and Northern Development (DIAND), Canada, Whitehorse, Yukon, Canada.

4.2   DESCRIPTION OF THE STUDY REACH

4.2.1   BACKGROUND

Figure 4.1 illustrates the study reach which extends upstream of the town of Old Crow a distance of 80 km past the confluence with the Bell River, and downstream of the town of Old Crow to the Alaska border. There are three Water Survey of Canada (WSC) gauges on the Porcupine River in this reach: WSC 09FB001, located 24 km downstream of the confluence with the Bell River; WSC 09FD001, just downstream of the town of Old Crow; and WSC 09FD002, at the international boundary.

Figure 4.2 illustrates the sub-catchments draining to the river, and its tributaries, within the study reach. At the town of Old Crow, the Porcupine River basin drains an area of 55,400 square kilometres (km²) (Water Survey of Canada, 1993). The catchment is bounded on three sides by mountain ranges: the British Mountains to the north; the Richardson Mountains to the east; and the Ogilvie Mountains to the south (Jasek, 1996). There are eight tributaries on the Porcupine River in the study reach, none of which are gauged.

The river is entrenched throughout the majority of the study reach (20 to 40 metres below the plain valleys). The channel varies between a straight single channel and an irregular meandering channel with occasional islands and sand bars. The bed material is sand.

Spring flooding due to rapid snowmelt and ice jam releases has been a frequent

problem for the residents of the town of Old Crow, situated on the bank of the Porcupine River, in the northern part of the Yukon Territory. For example, one of the most severe flooding events in recent history occurred during the 1991 break-up, when an ice jam formed downstream of Old Crow, causing water levels at the town to rise between 1 and 2 metres (m) (Jasek, 1996).

Of particular concern, however, are the surges created by ice jams releasing upstream of the town, as these events can result in rapid, and much more dramatic, water level increases, especially when they are associated with a large snowmelt runoff event. An event of this type was observed and documented by the Department of Indian Affairs and Northern Development (DIAND) staff during the spring of 1995 when water levels rose dramatically in Old Crow. The propagation of the snowmelt flood wave with its associated ice jam surges through town resulted in water levels increases between 4 and 5 m (Jasek, 1996).

4.2.2 DESCRIPTION OF THE 1995 SPRING BREAKUP EVENT

Jasek (1996) provides a description of the breakup event which lead to the flooding at the town of Old Crow in May 1995. Snowmelt runoff from the Richardson Mountains caused a rapid increase in stage on the Porcupine River, triggering the 1995 breakup. As a result, multiple ice jams formed along the study reach. Four of these ice jams are shown on the maps of the study reach in Figures 4.3 to 4.5. The first one (A) had already released when it was first observed between Berry Creek and Old Crow, on May 2 at 14:00. Within three hours the surge arrived in Old Crow,

100

causing a noticeable increase in water levels. The second jam (B), which was 15 km in length had formed by May 3. Its toe was located 18 km downstream of the confluence of the Bell and Porcupine Rivers, in a narrow bend. It released at 16:20 on May 3, and the resulting flow peak arrived in Old Crow approximately 15 hours later. Jasek (1996) states that ice surging from the Bell River causes the release of this ice jam. On May 3, there were also two other jams: C (19 km long) and D (11 km long) located 48 and 19 km upstream of the Bell River confluence, respectively. The time of release and the total travel time to Old Crow is uncertain. However based on gauge records, the peak travel time between the Bell River (WSC 09FB001) and Old Crow (WSC 09FD001) gauges was about 14 hours.

4.2.3 AVAILABLE GEOMETRIC DATA

4.2.3.1 Channel Distances

River stations, or locations along the channel length, were based on the system established by DIAND. Stations, specified in kilometers downstream of the confluence of Whitestone and Miner Rivers, were obtained from a 1:50,000 scale N.T.S. map as described in Section 2.5.4, starting at Station 90 km. This location for the upstream boundary of the modelled reach was selected to encompass the 1995 ice jams (and their estimated backwater region).

All of the surveyed cross sections were referenced to this stationing system, as were all major tributaries and key sites of interest. Table 4.1 presents the location of these

key sites along the Porcupine River.

Table 4.1. Location of key sites along the Porcupine River

Location	Station (km)
Nukon Creek confluence	130
Bell River confluence	170
Porcupine River below Bell River (WSC 09FB001)	**194**
Berry Creek confluence	202
Driftwood River confluence	235
Lord Creek confluence	279
Old Crow River confluence	315
Town of Old Crow	317
Porcupine River at Old Crow (WSC 09FD001)	**320**
Bluefish River confluence	360
Caribou Bar Creek confluence	381
Porcupine River near the International Boundary (WSC 09FD002)	**400**

4.2.3.2 Water Surface Slopes from the N.T.S. maps

Table 4.2 provides the water surface elevations obtained from the 1:50,000 and 1:250,000 scale N.T.S. maps. Table 4.3 presents the estimates of the water surface slopes determined from this data.

4.2.3.3 Available Cross Section Surveys

Figure 4.6 illustrates the data available for the study reach which includes:

- a water surface profile and thalweg elevations at cross sections surveyed in

102

1992 (Jasek, 1993)[+] ;

- water levels and thalweg elevations at cross sections surveyed in 1972 (DIAND, 1976);

- high water marks and ice scar data from 1991 and 1992 (Jasek, 1993); and

- the water surface profile obtained from the N.T.S. maps.

Table 4.2. Water surface elevations from the N.T.S. maps

Station (km)	Contour Elevation
32	300 m
168	900 ft (270 m)
238	875 ft (270 m)
252	850 ft (260 m)
283	825 ft (250 m)
317	800 ft (240 m)
375	775 ft (240 m)
386	750 ft (230 m)

[+] The water surface profile for 1992 was surveyed over a period of one week. During this time the water level dropped by approximately 0.25 m. Correspondingly, the discharge varied between 240 m³/s and 170 m³/s. Therefore, each water level was corrected by the difference between the water level at the WSC gauge near Old Crow (09FD001) at the time of survey and the water level anticipated for the average discharge of 212 m³/s over the period at the same gauge (Jasek, 1993).

103

There are also four surveyed cross sections near the WSC gauge below Bell River (09FB001), which extend upstream of the gauge by about 5 km and downstream by about 2 km. However, these could not be included in this figure, or used in the determination of the effective bed profile, as they have not been tied in to Geodetic Survey of Canada monuments. As Figure 4.6 illustrates, the lack of geometric data has to be considered a serious limiting factor in this investigation.

Table 4.3. Water surface slopes based on the N.T.S. map data

Reach (km)	Water Surface Slope
32 to 168	0.00019
168 to 238	0.00011
238 to 252	0.00054
252 to 283	0.00025
283 to 317	0.00022
317 to 375	0.00013
375 to 386	0.00069

4.2.4 AVAILABLE HYDROLOGIC DATA

4.2.4.1 WSC Gauge Data Available for the 1995 Event

The Porcupine River gauges at Bell River and Old Crow remained operational throughout the 1995 spring breakup period. Stage data from these gauge records were supplied by DIAND in 5 minutes increments. These data are presented in Figure 4.7. Two flow generating processes are seen in these figures. The first is snowmelt runoff, which provided a large mass flow over an extended duration (two to three

104

weeks). Superimposed on the snowmelt hydrographs are a number of shorter duration events (less than one day), which caused water levels to increase at a much more dramatic rate. These are the ice jam releases, which were triggered by the snowmelt runoff event.

Documentation provided by DIAND facilitates an interpretation of these stage hydrographs in terms of the ice jam release events. The rapid increase in water level seen at the Bell River gauge (09FB001) on May 3 resulted from the release of ice jam B; the peak on May 5 was caused by the release of the remaining ice (jams C and D) from upstream of the Bell River (Jasek, 1996). At the Old Crow gauge (09FD001), the corresponding flow peaks are seen between May 4 and 6. The first peak in the Old Crow stage hydrograph, seen on May 2, is the result of the first ice jam (A) described in Section 4.2.2.

In addition to the gauge record, manual water level measurements were made by DIAND staff at two sites in the town of Old Crow during the flood event. These data are reproduced in Figure 4.8.

4.2.4.2 WSC Gauge Rating Curves

Figure 4.9 illustrates the available stage-discharge data for WSC gauge 09FB001, on the Porcupine River below its confluence with the Bell River, based on WSC discharge measurement summaries dating back to 1963. As the figure illustrates, there is very little data available under ice conditions. Furthermore, ice thicknesses were

not documented in the measurement summaries. Therefore, only an open water rating curve could be developed for this gauge site.

Figure 4.10 illustrates the available stage-discharge data for WSC gauge 09FD001, just downstream of the town of Old Crow, based on WSC discharge measurement summaries dating back to 1961. There are two curves as this gauge was moved in 1972. Once again, there is insufficient data available under ice conditions to define ice cover rating curves.

4.3 MODELLING THE 1995 BREAKUP EVENT

4.3.1 INTRODUCTION

The hydraulic flood routing model implemented for the study requires two types of input data: geometric and hydrologic. The geometric data required includes details of the effective bed profile, channel top widths and hydraulic resistance characteristics of the river channel. The hydrologic data must provide the necessary boundary conditions, including upstream and downstream boundary conditions, as well as details of the lateral inflows.

As well as establishing the geometry and boundary conditions an hydraulic model has to be calibrated. This involves varying the channel roughness until modelled stage-discharge rating curve matches an established stage-discharge rating curve or until computed and measured water surface profiles correspond.

4.3.2 GEOMETRIC DATABASE

There is a reasonable minimum to the amount of survey data required to achieve a reliable hydraulic flood routing model. Therefore, a key question arising from an examination of the available data for this case study was whether or not there was sufficient information with which to develop an effective bed profile.

The calculated effective bed elevations at each cross section and their corresponding water levels are plotted in Figure 4.11 along with the water surface profiles surveyed in 1992 and determined from the N.T.S. maps. The effective bed used for the modelled reach was estimated graphically by lowering the water surface profile from the N.T.S. maps until it passed through the effective bed elevations for the cross sections at Old Crow. Figure 4.11 illustrates this effective bed profile.

4.3.3 BOUNDARY AND INITIAL CONDITIONS

4.3.3.1 Introduction

The solution of the non-linear partial differential system of equations (2.15 and 2.16) requires specification of two boundary conditions, as well as any lateral inflows. The initial conditions, stage and discharge at every computational node, must be specified as well. Since the flow in the modelled reach of the Porcupine River is subcritical, one of these two boundary conditions must be specified at the upstream end of the modelled reach, and one must be provided at the downstream end. In general, this upstream boundary condition is a discharge hydrograph, while at the downstream

boundary it is may be a stage or discharge hydrograph, or a stage-discharge rating curve.

4.3.3.2 Boundary Conditions

Upstream Boundary Condition

As mentioned, the upstream boundary condition is generally the inflow (discharge) hydrograph to the modelled reach. One could attempt to specify a stage hydrograph as the upstream boundary condition. However, it has been found in earlier investigations (and confirmed in this one) that this is an unstable upstream boundary condition for a subcritical flow.

For the Porcupine River study, the upstream boundary was taken at 194 km. where the WSC gauge on the Porcupine River below the Bell River (09FB001) is located. The discharge hydrograph measured at this gauge provided the boundary condition.

Downstream Boundary Condition

Practically speaking it is often the case, especially in a forecasting situation, that the downstream boundary condition is unknown. In this case, the most downstream data available for the 1995 event was WSC gauge record at Old Crow. However, this data is unsuitable for use as the downstream boundary condition, as this is the area of interest in this study and, therefore, the Old Crow gauge data is required for a comparison to the modelled output. If the downstream boundary is located far enough below of the most downstream point of interest, then a constant stage may be

assumed for the downstream boundary condition. The required distance is that which is sufficient to ensure that backwater and drawdown effects resulting from the assumed boundary condition would not affect the model's output at the site of interest.

For this model, the downstream boundary was located 66 km downstream of the WSC gauge at Old Crow, just downstream of the confluence of the Porcupine River and Caribou Bar Creek (386 km). A sensitivity analysis was conducted to verify that the effect of the chosen station and stage for the downstream boundary on the modelled output was negligible.

Lateral Inflow Boundary Conditions

Four tributaries contributed flow to the study reach: Berry Creek, Driftwood River. Lord Creek and the Old Crow River. Since none of these tributaries are gauged. another method had to be developed to estimate these lateral inflows. The Old Crow River, the fourth tributary shown in Figure 4.1, was neglected as it contributes little flow to the Porcupine River, due to large wetland and lake storage within its basin (Jasek, 1996).

In order to estimate inflow hydrographs for the remaining three tributaries, the volume of water passing the two Porcupine River gauges (WSC 09FB001 and 09FD001) was calculated using two methods. The first involved integrating the discharge hydrographs from May 1 to 30, 1995. The difference between the volumes of water passing each gauge represents the amount of water contributed from the

tributaries. In the absence of other information, this volume was apportioned to the three tributaries based on their basin area. Figure 4.2 shows various small basins adjacent to the Porcupine River which also contribute a significant quantity of water to the Porcupine River. These were accounted for by assuming the inflows occurred only at the confluences of Berry Creek, Driftwood River, and Lord Creek with the Porcupine River and including the areas of the small basins with the tributary basin area immediately downstream.

The discharge hydrograph for each tributary was found by averaging the volume apportioned to each tributary over the 30 days runoff period. This assumes that the inflows from the tributaries were constant over the runoff period, which does not account for the timing of runoff, or any ice jam events which may have occurred. The absence of gauge data for these tributaries is considered a serious data limitation for the flood forecasting model.

The second method for estimating lateral inflows was based on the discharge hydrograph measured at Old Crow and a constant (carrier) discharge established from the measured stage hydrograph at the WSC gauge below Bell River (09FB001). The difference between the constant discharge at the upstream gauge, below Bell River, (WSC 09FB001) and the discharge immediately prior to the event at the Old Crow gauge (WSC 09FD001) was assumed to be contributed by lateral inflow. It was apportioned to the three tributaries previously mentioned based on their basin area. Once again, the discharge hydrograph for each tributary assumed constant inflow over

110

the runoff period, neglecting runoff timing and ice jam events.

4.3.3.3   Initial Conditions

Before beginning an unsteady flow simulation, the initial conditions (stage and discharge at every computational node) must be established. These are determined by using the cdg1-D model to calculate a gradually varied flow profile for a constant inflow and tributary discharges, based on observed flows on the day the simulation began.

4.3.4   MODEL CALIBRATION

The calibration of channel resistance may be accomplished by two methods. The first requires that a water surface profile modelled over a given reach match the measured water surface profile over the same reach, for a known discharge. The second method involves calibrating theoretical stage-discharge relationships with the measured rating curve at a given site (typically at a gauge site). The former approach is preferable. since it facilitates consideration of gradually varied flow effects. This typically cannot be done in the second approach, since data is available at a single point only, necessitating a uniform flow approximation.

A water surface profile was surveyed over a 20 km reach on the Porcupine River near Old Crow for a discharge of approximately 1500 m^3/s (Jasek, 1996) and, as discussed above, cross section data was also available for this reach. Water surface profiles were computed at this discharge for various channel roughnesses using the U.S. Army

111

Corps of Engineers gradually varied flow analysis program, HEC-2. Each simulation assumed a constant roughness height for the bed, k_b, as it was considered impractical to model variations within this 20 km reach, given the fact that roughnesses would be estimated in the remaining 300 km where data for calibration was not available. Figure 4.12 shows the calculated water surface slopes obtained using k_b values of 0.05 and 0.1 m. The roughness height of 0.1 m was considered to give the better overall fit to the measured water levels. In comparison, Jasek (1993) determined the equivalent roughness height of the bed, k_b, to be 0.2 m near the town of Old Crow, based on a calibration at a discharge of 212 m^3/s. This might be considered a large difference, given that roughness height should be independent of discharge unless there is a significant change in bed form regime. However, both calibrations were conducted using the HEC-2 program, which does not use the Chezy equation (and therefore the roughness height) explicitly, but rather converts the input k_b values to Mannings n values using the Strickler equation. Consequently, calibrations at different discharges result in different roughness heights. This is a significant limitation of the HEC-2 model if roughness height is the preferred roughness parameter as the values obtained by this method may not be representative of the actual values.

As discussed earlier, there are four surveyed cross sections in the upstream reach, near the WSC gauge on the Porcupine River below Bell River (09FB001). However, there was not sufficient data for a water surface profile calculation. Therefore the second approach, calibration of a rating curve, was employed. In this case, a measured water

112

surface slope was available from these four cross sections, improving the approximation slightly. The water surface slope determined from these cross sections was 0.000094, which compares favorably with the water surface slope of 0.00011 obtained from the N.T.S. maps. Based on a calibration of the rating curve at the gauge, the bed roughness was determined to be 0.002 m.

The difference between the calibrated roughness heights for the Old Crow reach and at the WSC gauge below the Bell River (09FB001) is cause for some concern, especially since the bed material known to exist through the entire reach is sand. For example, considering the corresponding Mannings n values, 0.023 and 0.012, respectively, the value at the WSC gauge near the Bell River seems unreasonably low. However, without additional hydrologic data, further investigation to determine the roughness could not be conducted.

In order to determine how to apportion these calibrated roughnesses through the study reach, a geomorphological evaluation of the Porcupine River was conducted using aerial photographs supplied by DIAND. Figure 4.13 illustrates the various planform patterns identified, which vary between a straight single channel to irregular meandering channel with occasional islands and sand bars. Using this information, it was decided that, for this preliminary investigation, the bed roughness height determined based on the data at the Bell River gauge (09FB001) would be used downstream to 240 km, and the bed roughness height determined for the Old Crow reach would be used for the remaining reach.

4.4   MODELLING TESTS

The objective of the Porcupine River study was to verify hydraulic flood routing techniques in a reach with minimal data. In order to accomplish this both the channel geometry and the tributary inflows were approximated. As well, since this was a breakup event some consideration had to be made for the ice conditions occurring in the channel.

This section reviews three options used in accounting for the ice affected portions of the upstream boundary condition. The first assumes that open water conditions exist at the WSC gauge below the Bell River (09FB001) throughout the entire event. The second and third options apply an estimated ice rating curve to the ice affected gauge data. For the last two options, the ice conditions are assumed to exist until the ice at the gauge moves or until all ice has cleared the reach at the gauge.

After the ice conditions at the upstream boundary have been determined, two methods of approximating the tributary inflow are studied. First, the lateral inflow is approximated by integrating the discharge hydrographs available at the Old Crow and Bell River gauges along the Porcupine River to find the volume of flow which has passed each gauge. The difference between the two volumes supplied the volume of tributary inflow. The second method is based on the difference between a constant carrier discharge assumed at the upstream gauge and the discharge immediately prior to the event at the downstream gauge.

114

4.4.1 ICE CONDITIONS

As the gauge on the Porcupine River below the Bell River (WSC 09FB001) measures stage, an inflow hydrograph had to be calculated from the gauge record to provide the upstream boundary condition for this analysis. Although most of the ice cover had cleared between the upstream gauge and the town of Old Crow by this time there was solid ice at the Bell River gauge (WSC 09FB001) until May 3 at 15:00, and ice from the releasing jams passing through until midnight on May 6. Three methods for determining the effects of this ice were considered and compared to determine the best approximation of the effects of ice conditions on this discharge hydrograph. In the first method, the resistance effects of the ice cover were considered negligible and the gauge's open water rating curve was used. In the second approach, the effects of ice on the gauge data were considered until the solid ice cover at the Bell River gauge moved (May 3 at 15:00), after that the open water rating curve was used. Finally, in the third approach, ice effects were considered until the gauge section was free of ice (May 6, at midnight). Again, after that the open water rating curve was used. These three approaches for determining the inflow discharge hydrograph from the measured stage data at the gauge on the Porcupine River below the Bell River are denoted as "Option I", "Option II" and "Option III", respectively, in the ensuing discussion.

In order to implement Options II and III, the effects of ice on the rating curve at the this upstream gauge (WSC 09FB001) had to be approximated. Based on the very limited data available (as illustrated by Figure 4.8) two alternative rating curves were

estimated, first by adding 0.75 m to the stage values in the open water rating curve. and then by adding 1.0 m to the open water rating curve. These approximations of ice rating curves are shown in Figure 4.14. It is acknowledged that this is a crude approach, especially considering that the ice data available at the gauge was not taken during breakup or during 1995. However, as there is no data on the thickness or roughness of the intact or moving ice covers available for the 1995 event, the approximation at least facilitated the determination of the importance of this missing information to the modelling attempt. Figure 4.15 illustrates a comparison of the effects of these approximate ice rating curves on the discharge hydrograph obtained at the Bell River gauge (WSC 09FB001). The difference between the two ice rating curves is not considered significant given the approximate nature of the estimate. as discussed above. Therefore, further discussions are based only on the estimated ice rating curve obtained by adding 1.0 m to the open water rating curve. Figure 4.16 illustrates the discharge hydrographs determined for the Bell River gauge using the three options for including the effects of intact and moving ice during the event. As the figure illustrates, the inclusion of ice effects has a significant impact on the discharge hydrograph obtained.

4.4.2 LATERAL INFLOW BASED INTEGRATION OF AVAILABLE HYDROGRAPHS

Given the lack of ice data for the intact or moving ice covers, it was logical to pursue Option I first. As an initial assessment of the approximate geometry model, the discharge hydrograph obtained from the measured stage data using Option I was

116

input into the cdg1-D model. The time step used for these simulations was 300 seconds (a Courant number of 0.75). Although it was previously recommended to use a Courant number of 0.5 or less a sensitivity analysis comparing a time step of 200 seconds and 300 seconds showed a negligible difference in output (less than 0.001%). The resulting stage hydrograph computed by the model at the upstream boundary was then compared to the measured stage hydrograph. As Figure 4.17 shows, the cdg1-D model reproduced the measured stage well, despite the rectangular channel approximation.

Figure 4.18 shows the discharge and stage hydrographs modelied at the WSC gauge near Old Crow (09FD001) compared to the measured data. Here again, for consistency, the discharge was obtained using the open water rating curve (from Figure 4.9, for the gauge at Old Crow). As the figure illustrates, the cdg1-D model accurately models the wave speed, which is remarkable considering the lack of available geometric data. The peak discharge predicted by the cdg1-D model is 12% lower than the peak obtained based on the measured stage and the open water rating curve. In this case, we cannot necessarily attribute this difference to modelling error, given the approximate way in which the tributary contributions were estimated. The importance of the tributary inflows becomes clear when comparing the shapes of the hydrographs measured at the two gauges, or in looking at the modelled results versus measured data for the gauge at Old Crow as there is clearly a tributary event following the peaks which could not be included in the analysis. Tributary

contributions throughout the breakup period could account for part of the difference at the time of the peaks, as well.

4.4.3 LATERAL INFLOW BASED ON A CONSTANT CARRIER DISCHARGE

In an attempt to estimate the tributary contributions more accurately, lateral inflows were determined using the second method described in Section 4.3.2.2. Since Option I produced the best results, the discharge hydrograph, estimated using the open water rating curve at the WSC gauge near Bell River (09FB001), was used for the upstream boundary condition in this modelling scenario. The discharge hydrograph modelled with the new tributary inflows at the WSC gauge near Old Crow (09FD001) is also shown in Figure 4.18. In this case, the timing of the event is accurately predicted by the cdg1-D model. The modelled peak discharge is 3% higher than the peak obtained based on the measured stage and the open water rating curve.

The location of the wave peak is shown, with respect to time, for this simulation. in Figure 4.19. As mentioned, the upstream boundary for this simulation was the WSC gauge (09FB001) on the Porcupine River below Bell River (194 km). The peak of the wave was caused by a snowmelt runoff event and the release of jams C and D, which were located at 151 km and 122 km, respectively. After traveling 43 to 72 km, the flood wave had diffused. The wave speed calculated from Figure 4.19 was 1.39 m/s between 194 km and 210 km and 3.15 m/s downstream from 210 km, giving average channel velocities of 0.93 m/s and 2.20 m/s. These velocities were compared

to average channel velocities calculated knowing the peak discharge and cross sectional area at various points along the study reach. The comparison showed that in the downstream reach, where some cross sectional data was available and characteristics of the river channel remained relatively constant, that these velocities were within 5%. However, in the upstream reach, where no cross section data was available and the channel characteristics were highly variable, these velocities could not be compared with any reliability.

4.5   DISCUSSION OF RESULTS

The primary objective of this study was to evaluate hydraulic flood routing techniques where limited hydrologic and geometric data were available. Thus the cdg1-D model was applied to the 1995 spring breakup event which occurred on the Porcupine River.

The data available for this river was extremely sparse. Specifically:

1. The survey data in the 300 km long modelled reach of the Porcupine River is concentrated over a 20 km distance through the town of Old Crow. The cross sections at the WSC gauge below Bell River (09FB001) are not tied into Geodetic Survey of Canada elevations, and therefore could not be used in developing the effective bed profile.

2. There are 8 tributaries in the study reach, 4 of which are between the two gauges that remained operational during the 1995 event. None of these tributaries are

119

gauged. In addition, it is known that an ice run on at least one of these tributaries affected the release of the modelled ice jam event.

3. There is insufficient data to establish ice affected rating curves at either gauge.

4. Roughness calibrations were only possible for open water conditions, and at only two points within the modelled reach.

Despite this critical lack of data, encouraging results were obtained with this case study. The timing of peak arrival was almost exact and the peak was low by only 12% when lateral inflows were quantified by integrating the discharge hydrographs at the two WSC gauges (09FB001 and 09FD001). Since the Porcupine River is entrenched, overbank flooding does not occur. Therefore, at least part of this difference must be attributed to the fact that tributary hydrographs were unknown. indicating that neither the limited geometry nor the lack of ice data. are significant to the quality of modelling results for this event. This is consistent with the results obtained in Chapter 3 on the Peace and Oldman/South Saskatchewan Rivers and is further demonstrated when the second method for quantifying lateral inflows was used. The timing in this case was exact and the peak was high by 3%. Therefore. properly quantifying the contributions from these tributaries is extremely important. Measured hydrographs would provide much more accurate results.

It is important to remember that the application in this context is for flood routing over long distances with limited channel geometry. When limited channel geometry is available, the quantification of the corresponding local flood levels is

inaccurate. Therefore, any comparison of measured and computed water levels will only demonstrate whether the model results appear consistent with the measured data in terms of the timing and relative stage changes observed. The computed values tend to be vertically offset because the effective bed level in the model is different from the actual bed level. Natural variations in bed level are large and consequently, the effective bed used in the limited geometry model can be several metres different from the surveyed bed at a given point. This difference is not significant in terms of flood routing over hundreds of kilometers, as has been shown in the previous chapter. However, in the context of determining water levels at specific sites, these differences are important.

One noticeable factor evident from the results presented in Figure 4.18 is that despite the extremely low bed roughnesses used and the fact the ice effects on the flow have been neglected both in interpreting the measured water levels and in propagating the flood wave, the predicted peak discharge is low. Including ice effects would widen this margin. This may be considered further evidence of the importance of the missing tributary data. Given this lack of data, the complicated nature of the ice cover timing (given the various ice runs) and the approximate nature of the estimated ice rating curve, any attempt to include ice effects would have to be considered purely speculative at this time.
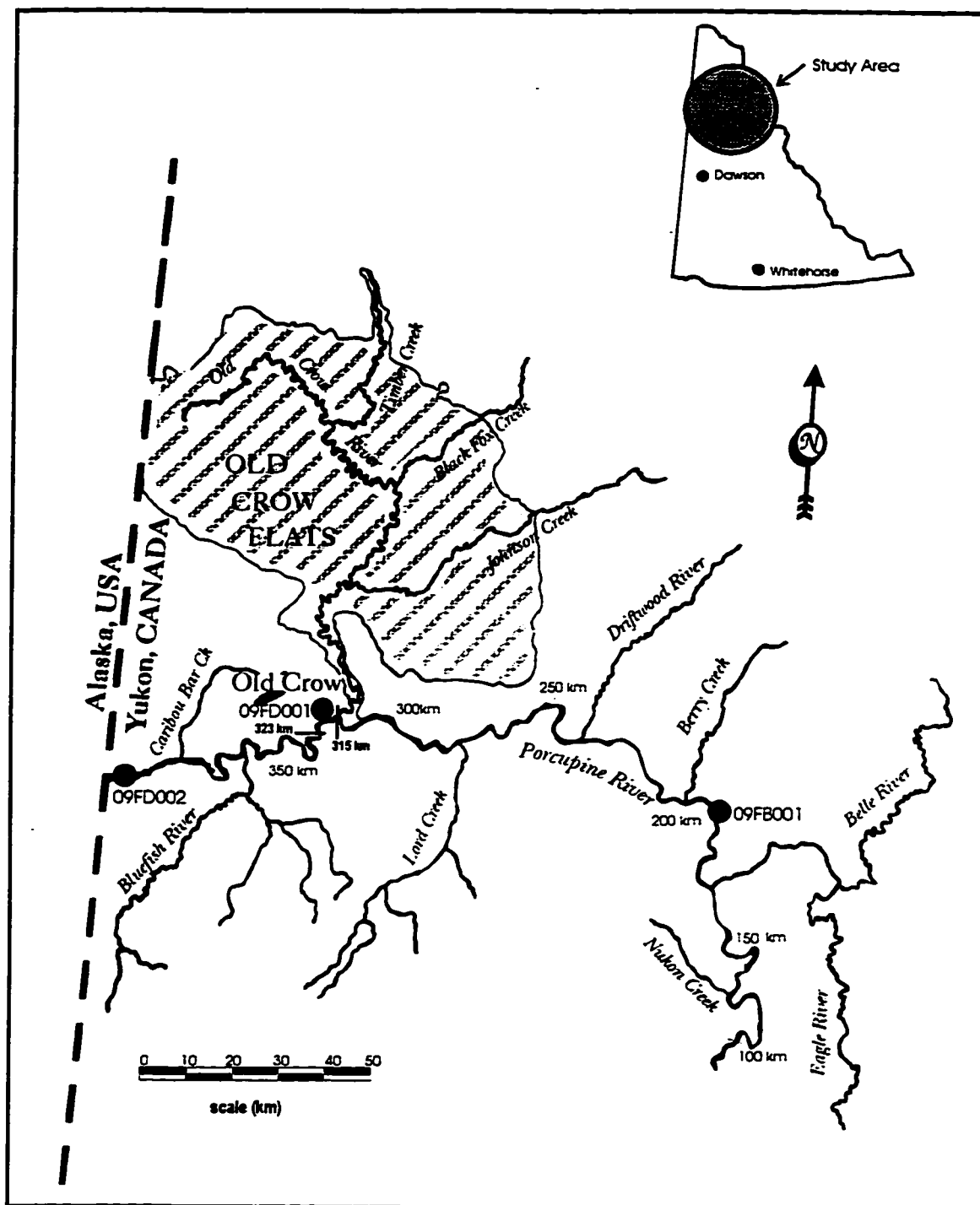
Figure 4.1. Location sketch for the Porcupine River study reach.
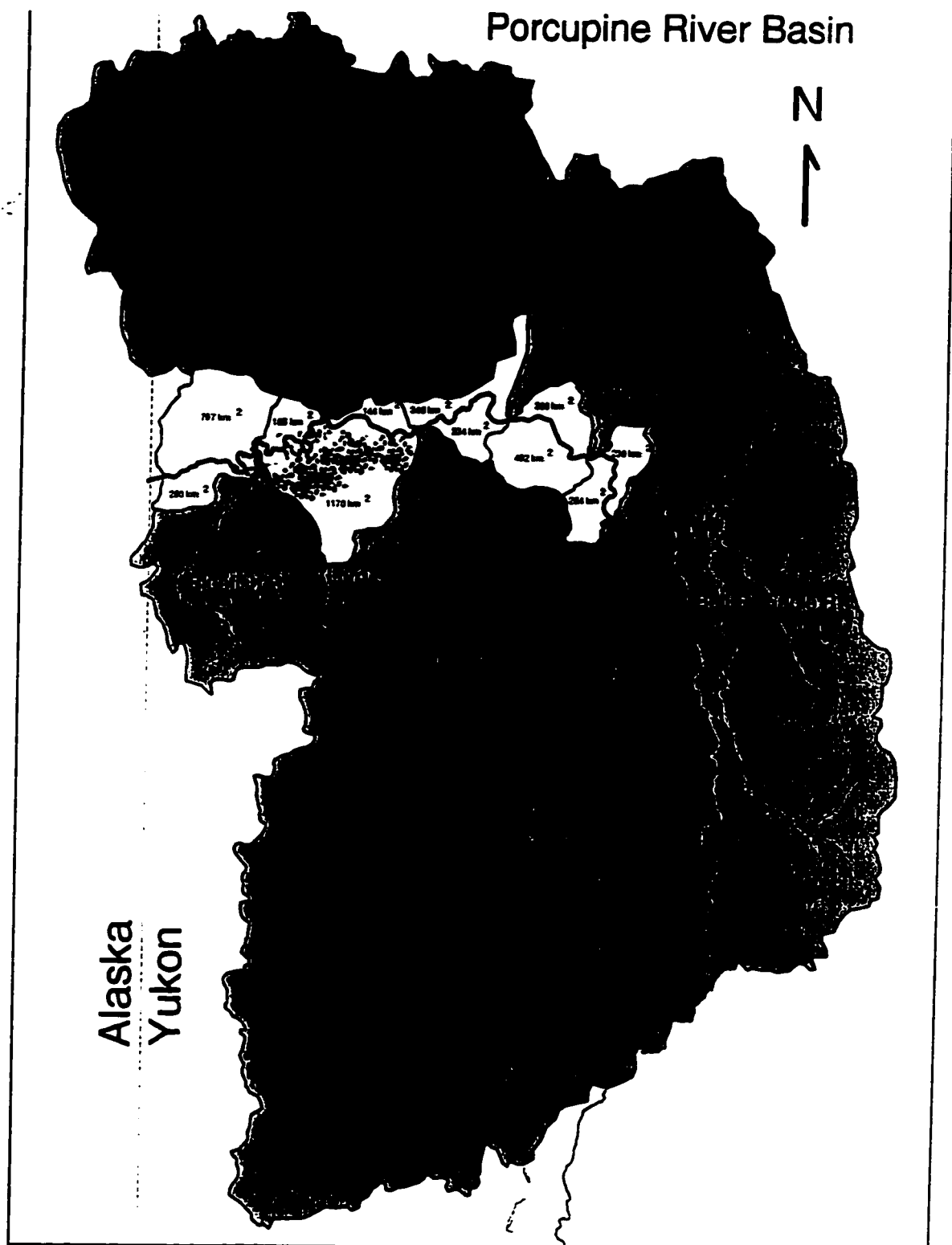
Figure 4.2. Drainage catchments within the Porcupine River basin.
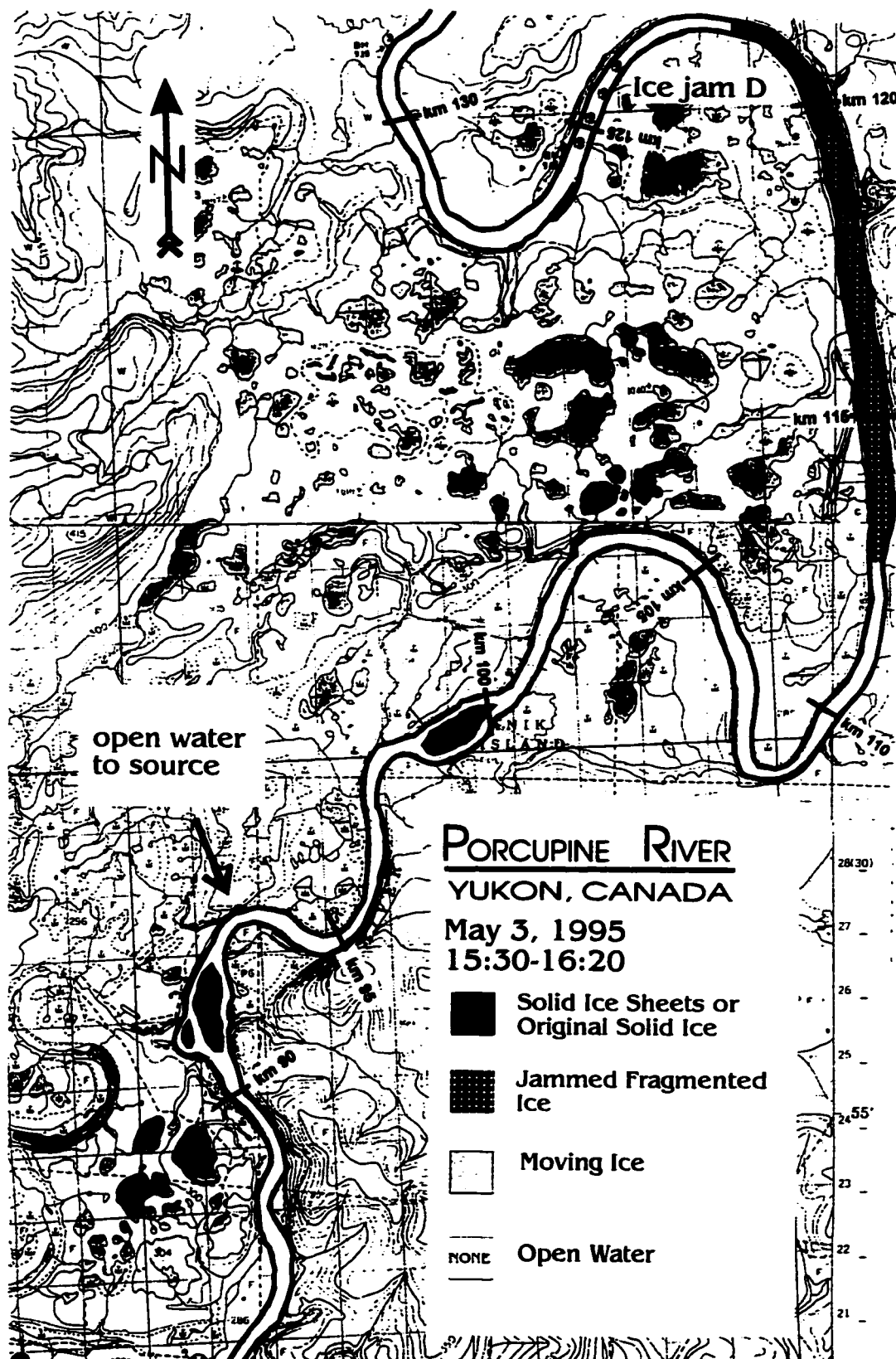
Figure 4.3. Ice covered and open water areas between km 90 and km 130.
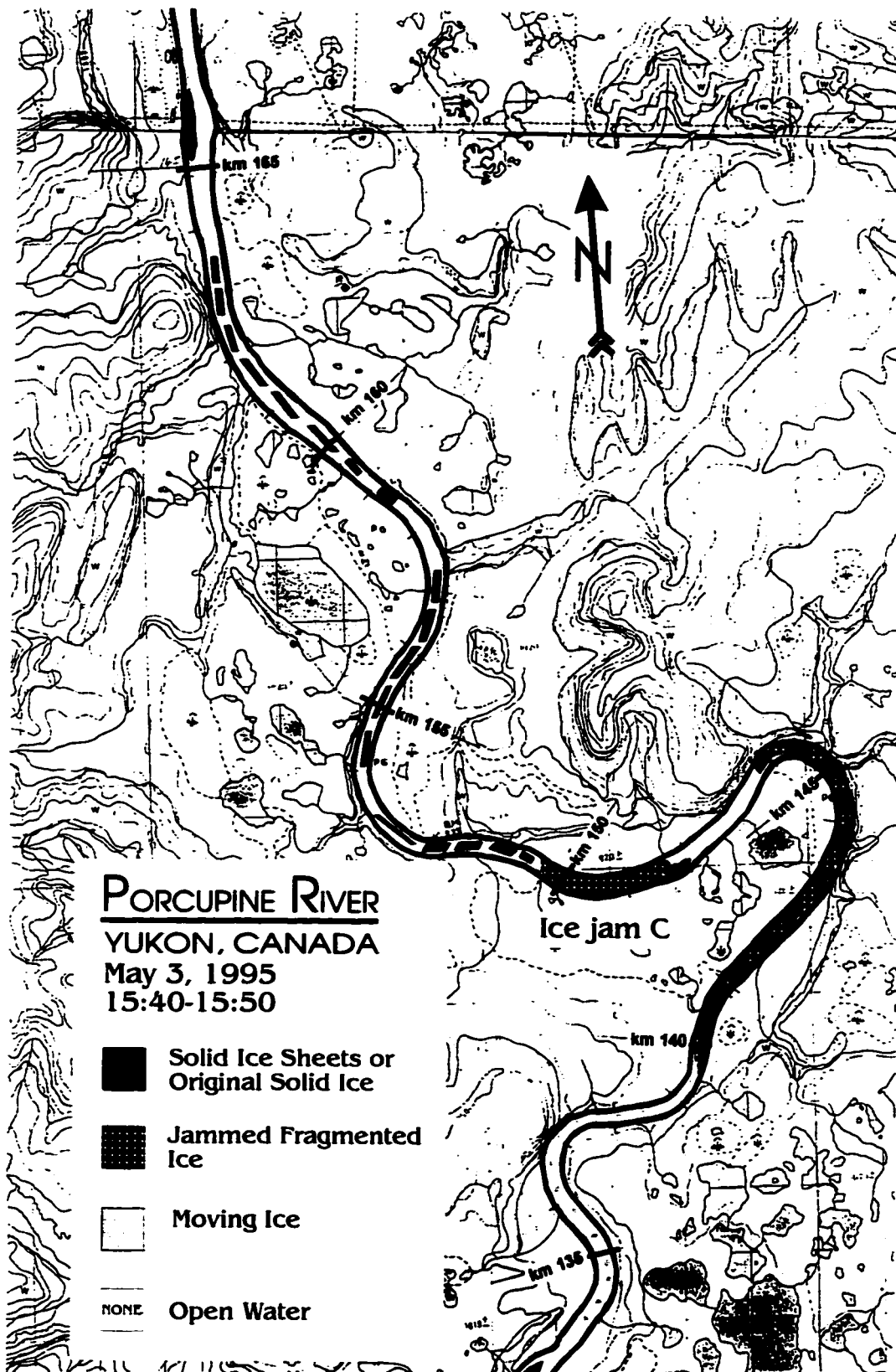
Figure 4.4. Ice covered and open water areas between km 130 and km 170.
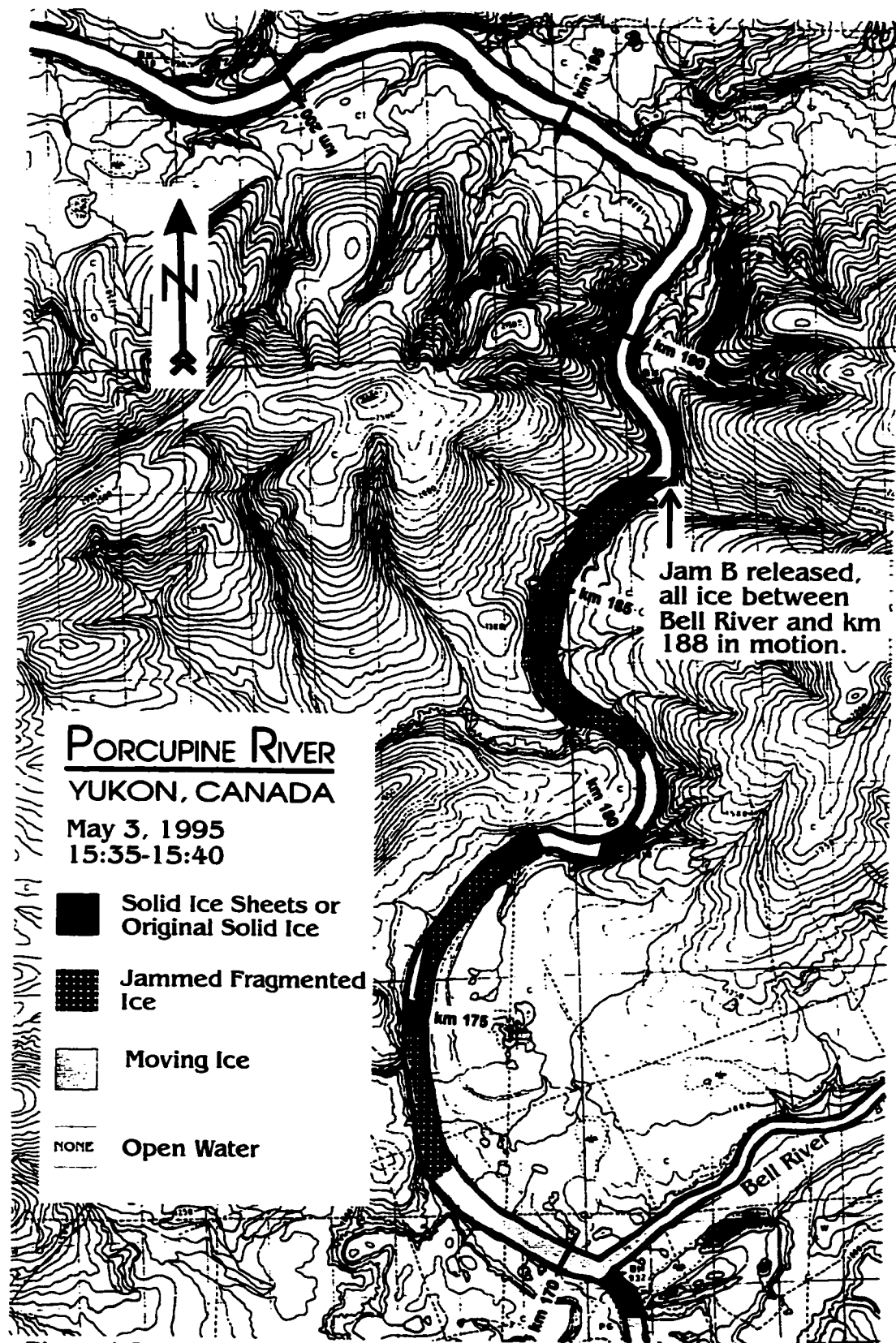
Figure 4.5. Ice covered and open water areas between km 170 and km 200.
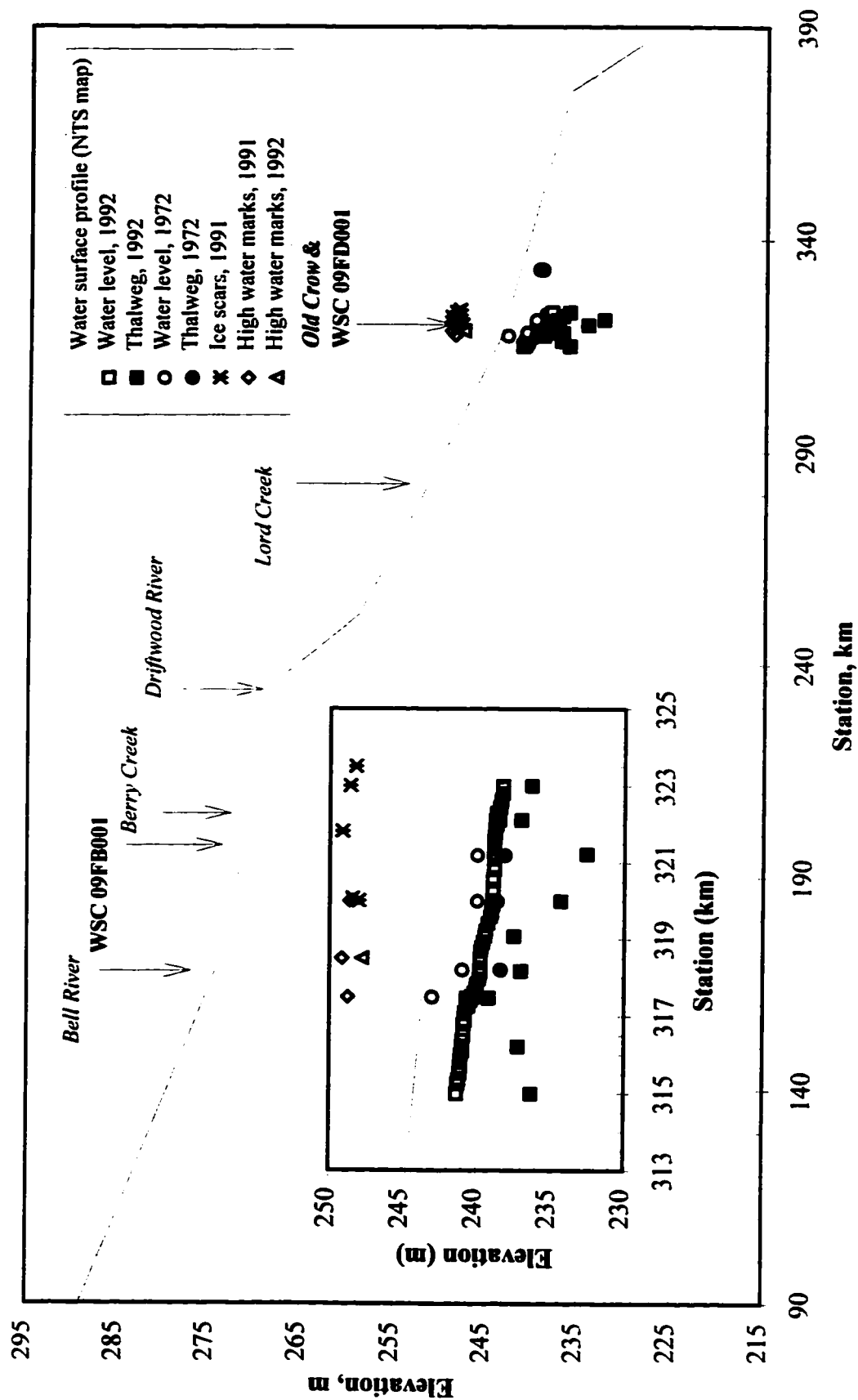
Figure 4.6. Available data for the Porcupine River.
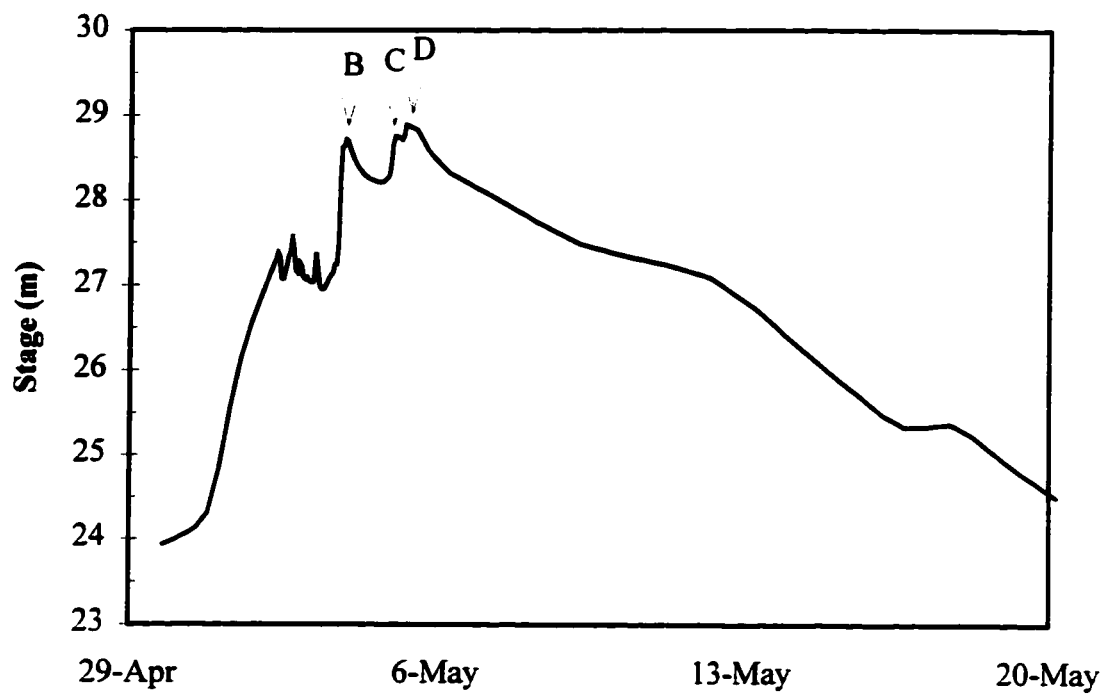
a) WSC gauge below the Bell River (09FB001)
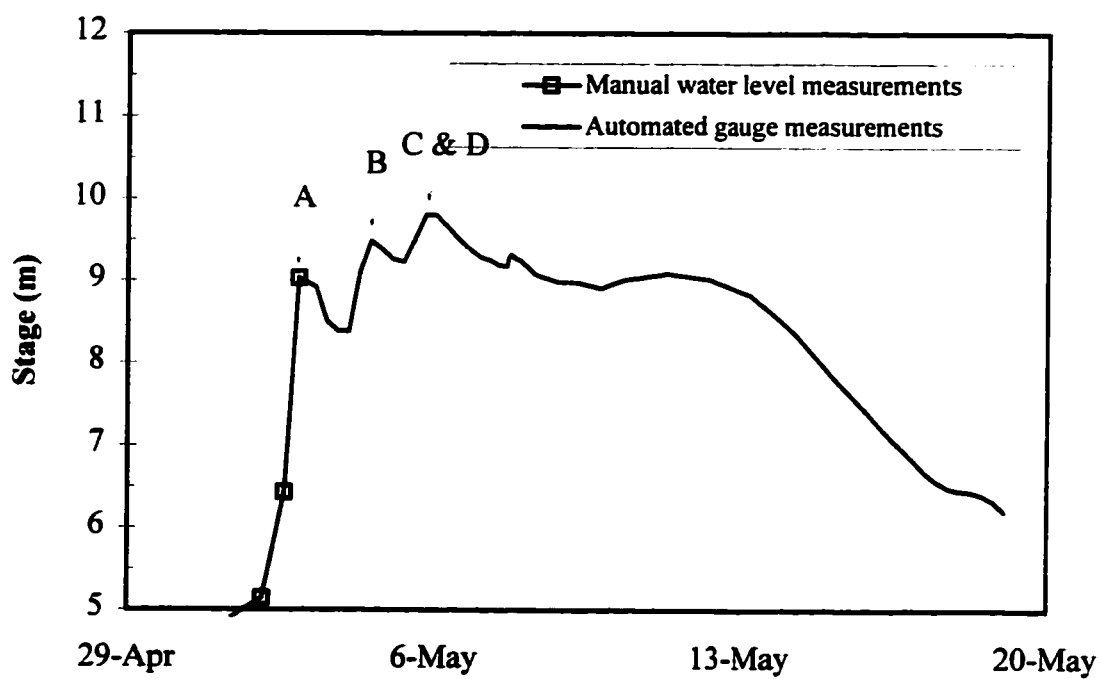
b) WSC gauge at Old Crow (09FD001)

Figure 4.7. Stage hydrographs measured on the Porcupine River during breakup 1995.

128
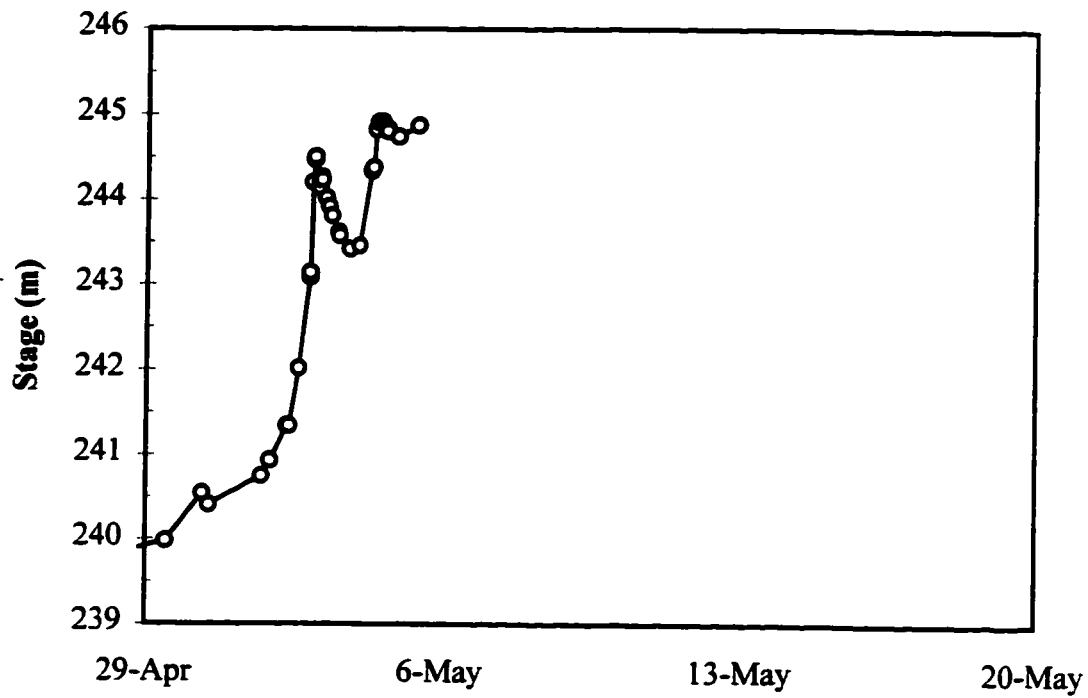
a) measurements at 317.75 km
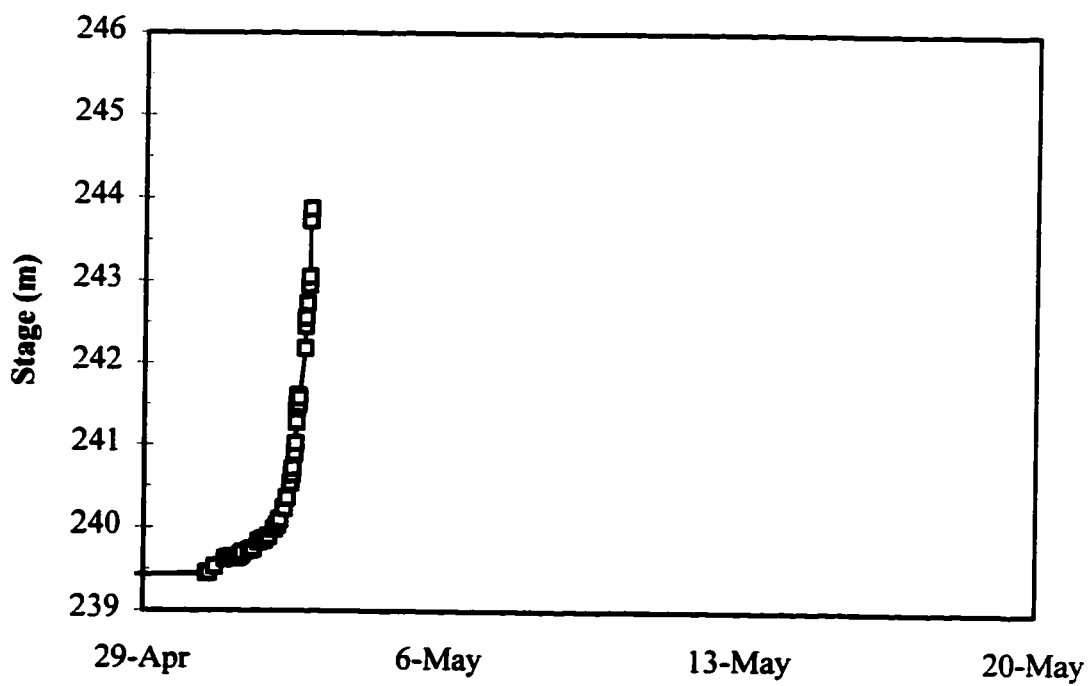
b) measurements at 320 km

Figure 4.8. Manual water level measurements in the town of Old Crow during breakup 1995.
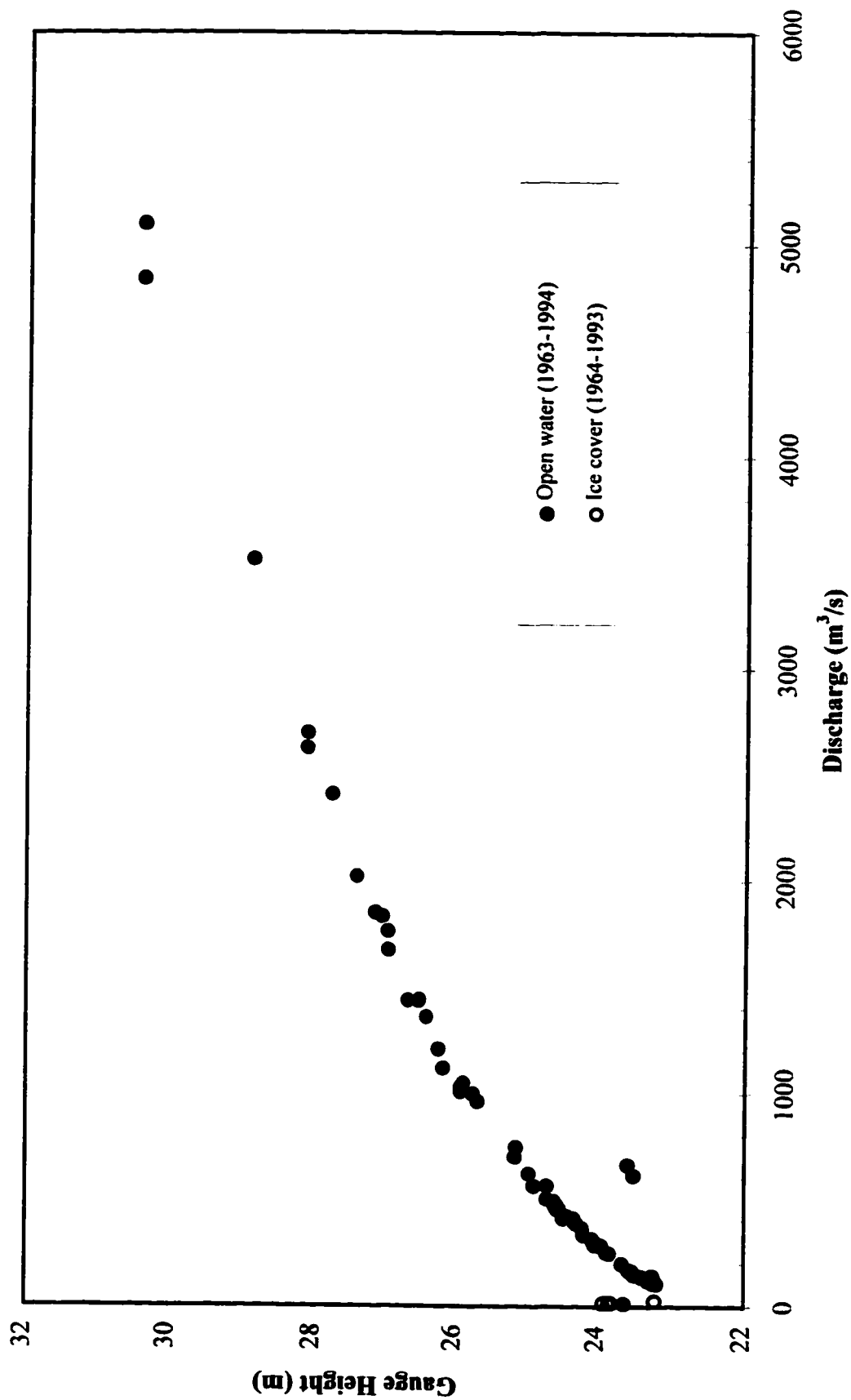
Figure 4.9. Available stage-discharge data at WSC gauge below Bell River (09FB001).

130
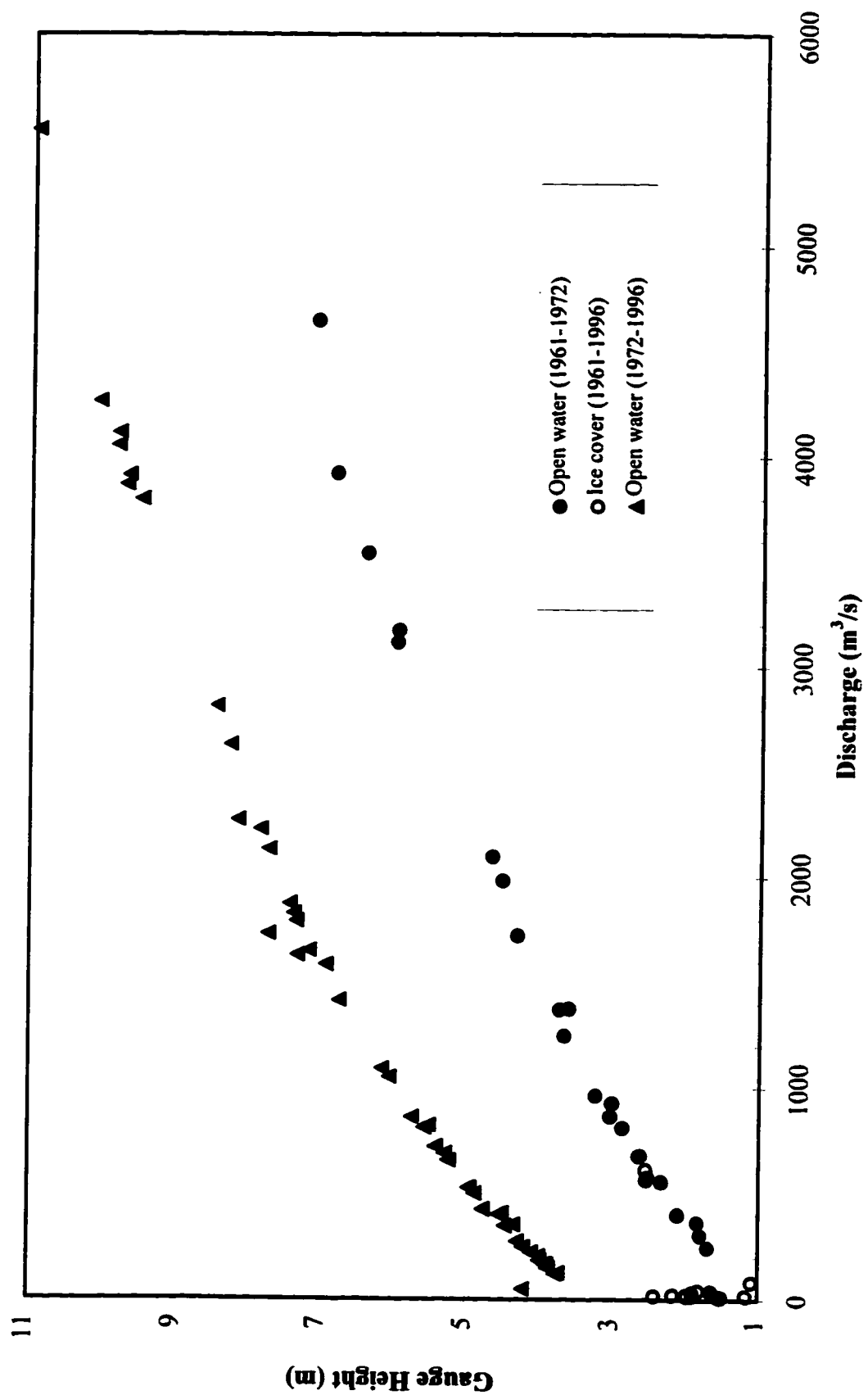
Figure 4.10. Available stage-discharge data at WSC gauge at Old Crow (09FD001).

●Open water (1961-1972)
○Ice cover (1961-1996)
▲Open water (1972-1996)

Discharge (m^3/s)

Gauge Height (m)

131
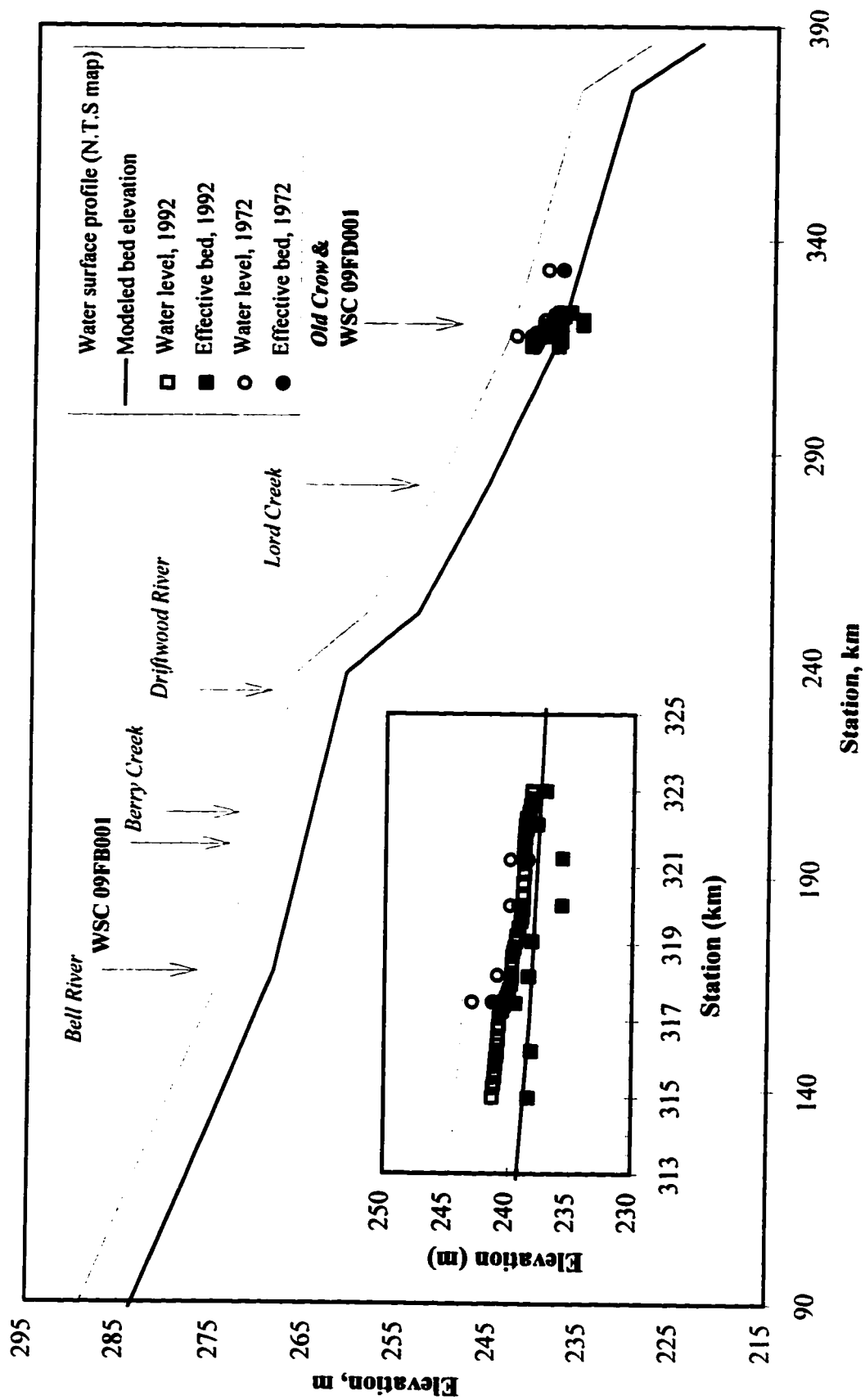
Figure 4.11. Effective bed used in the flood routing model on the Porcupine River.
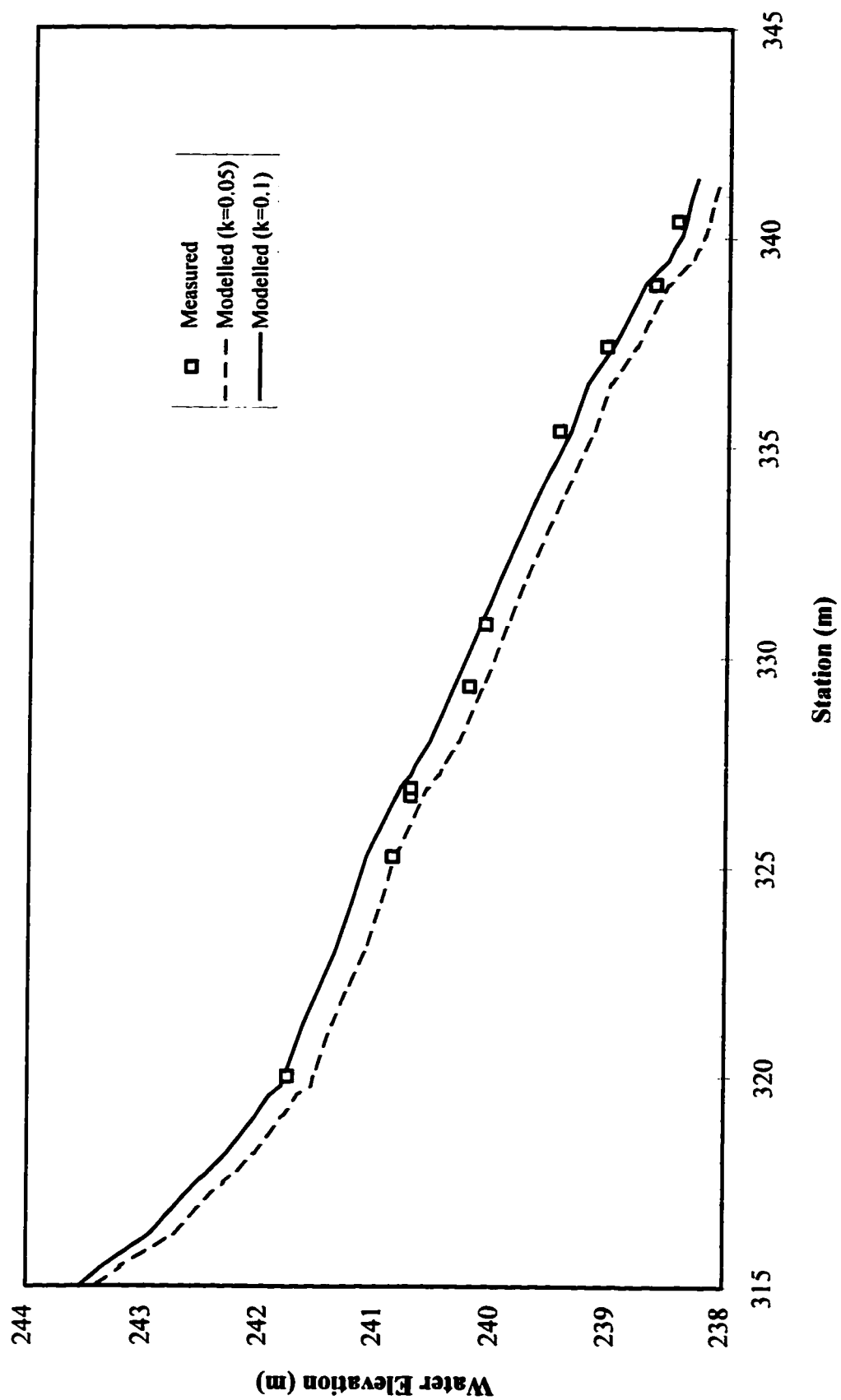
Figure 4.12. Calibration of roughness height at Old Crow.
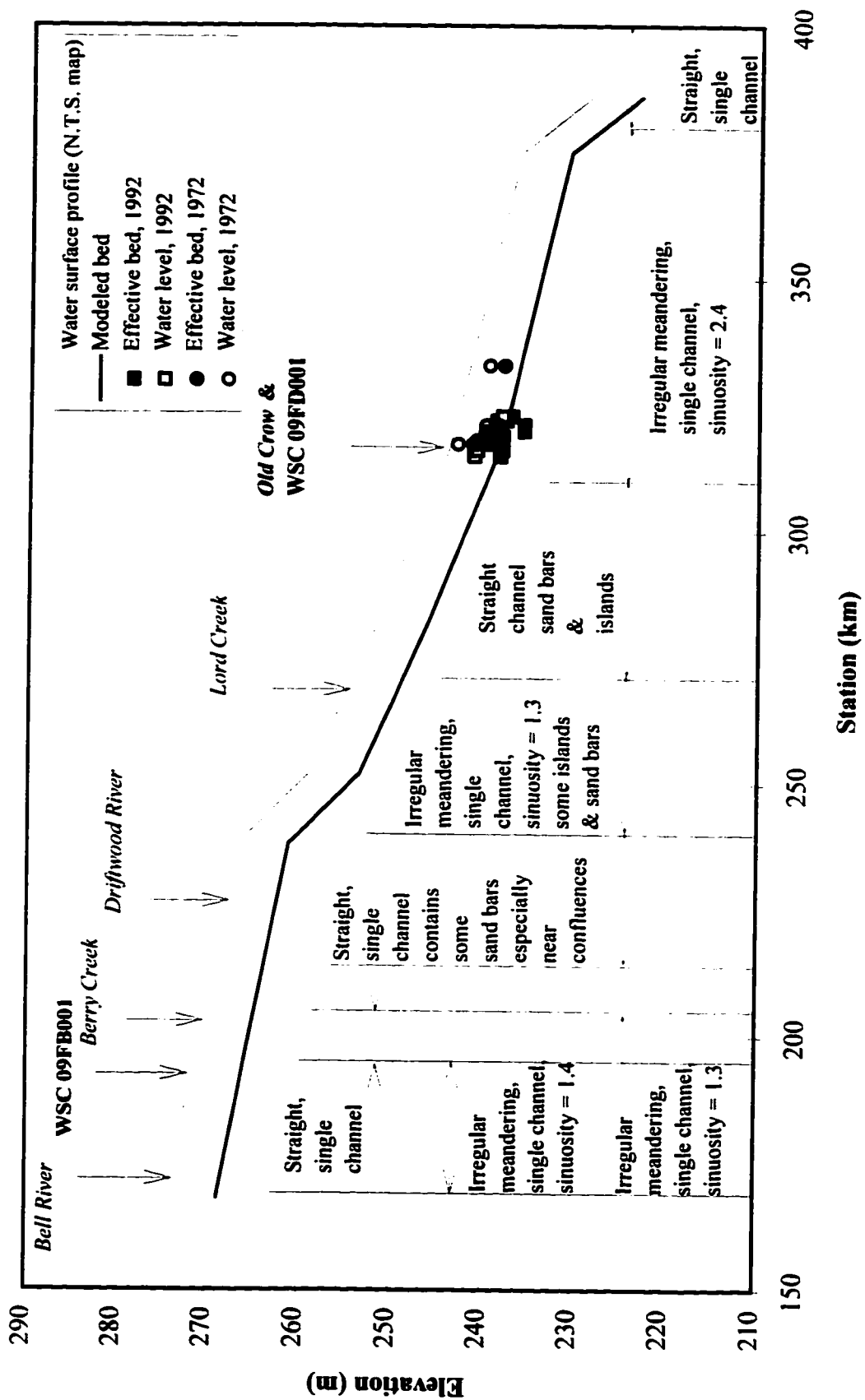
Figure 4.13. Geomorphological changes on the Porcupine River.

134
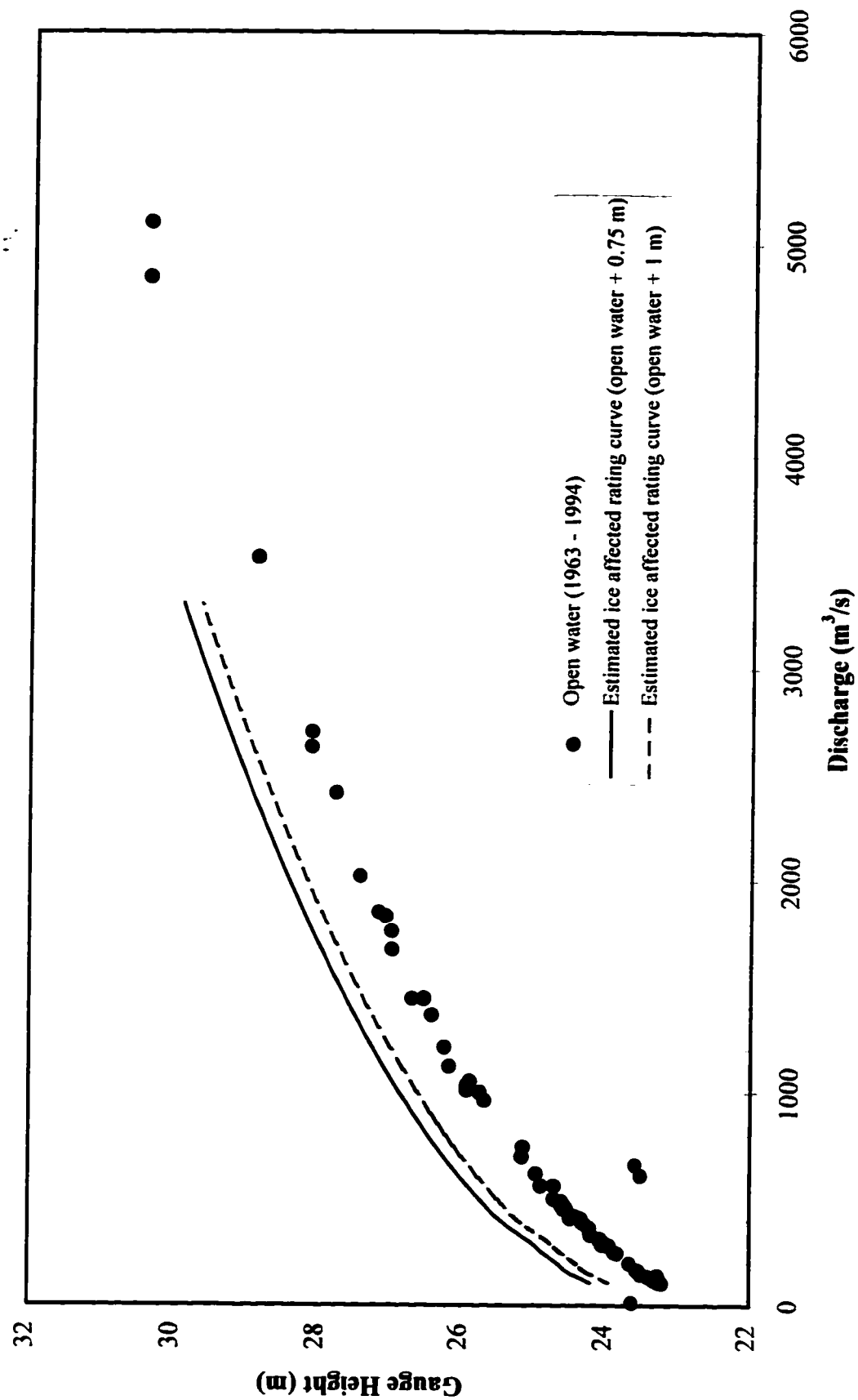
Figure 4.14. Estimated ice affected rating curves at the WSC gauge below Bell River (09FB001).
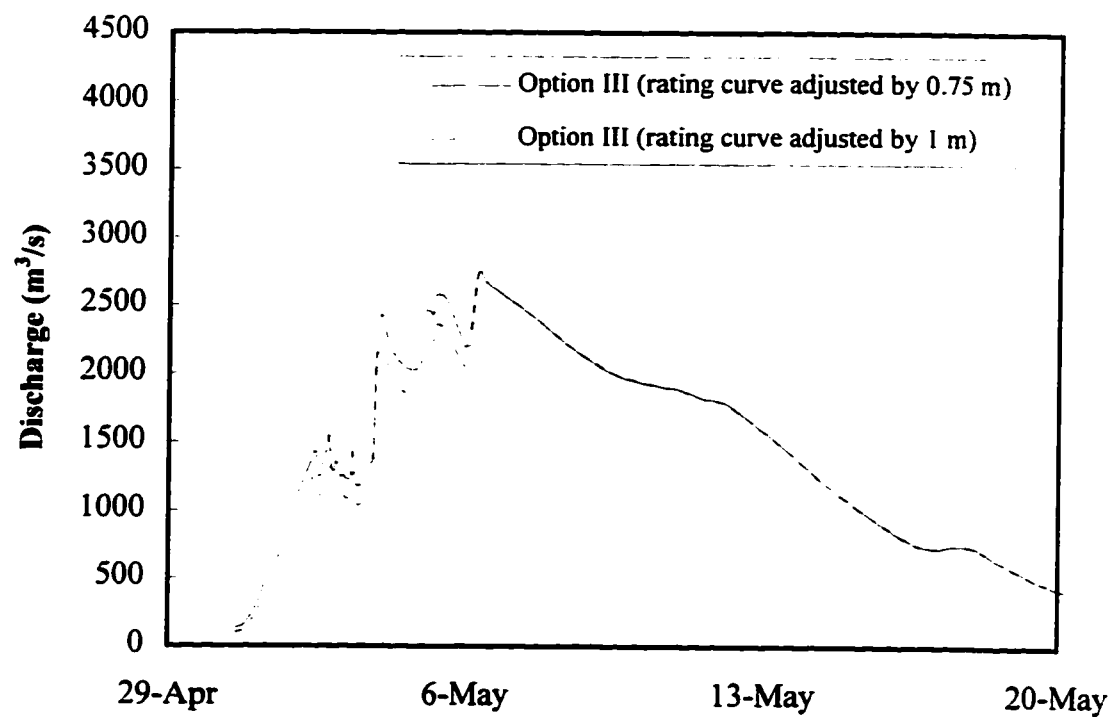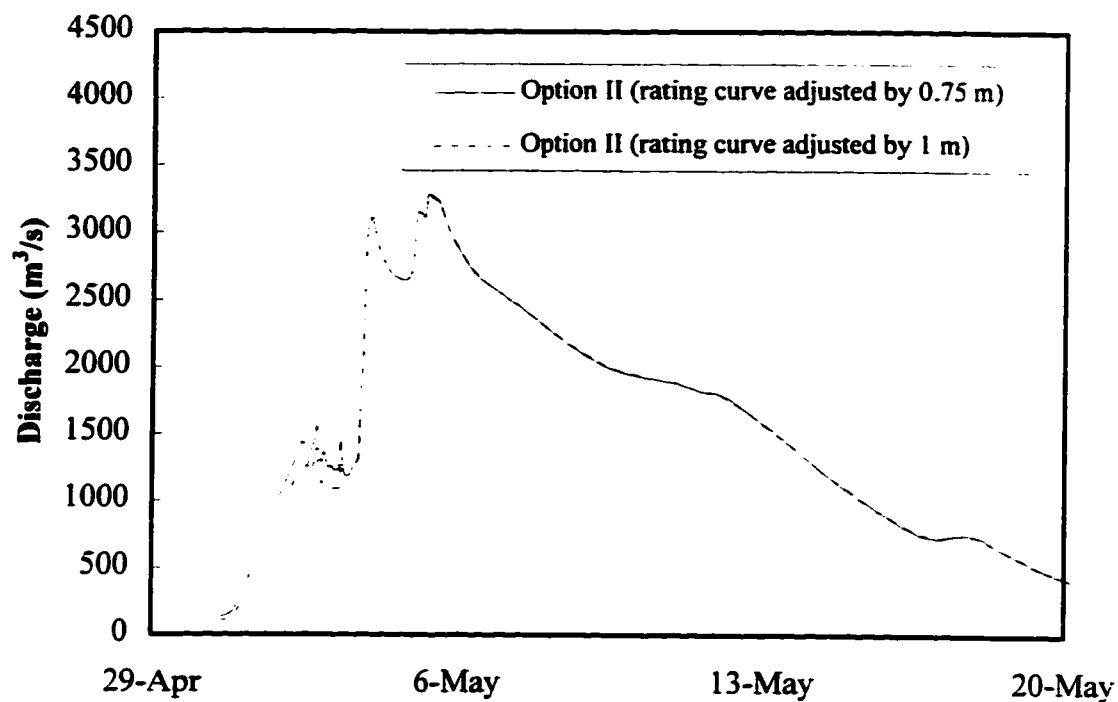
Figure 4.15. Comparison of the effects of the estimated ice affected rating curves for the Porcupine River gauge below Bell River.
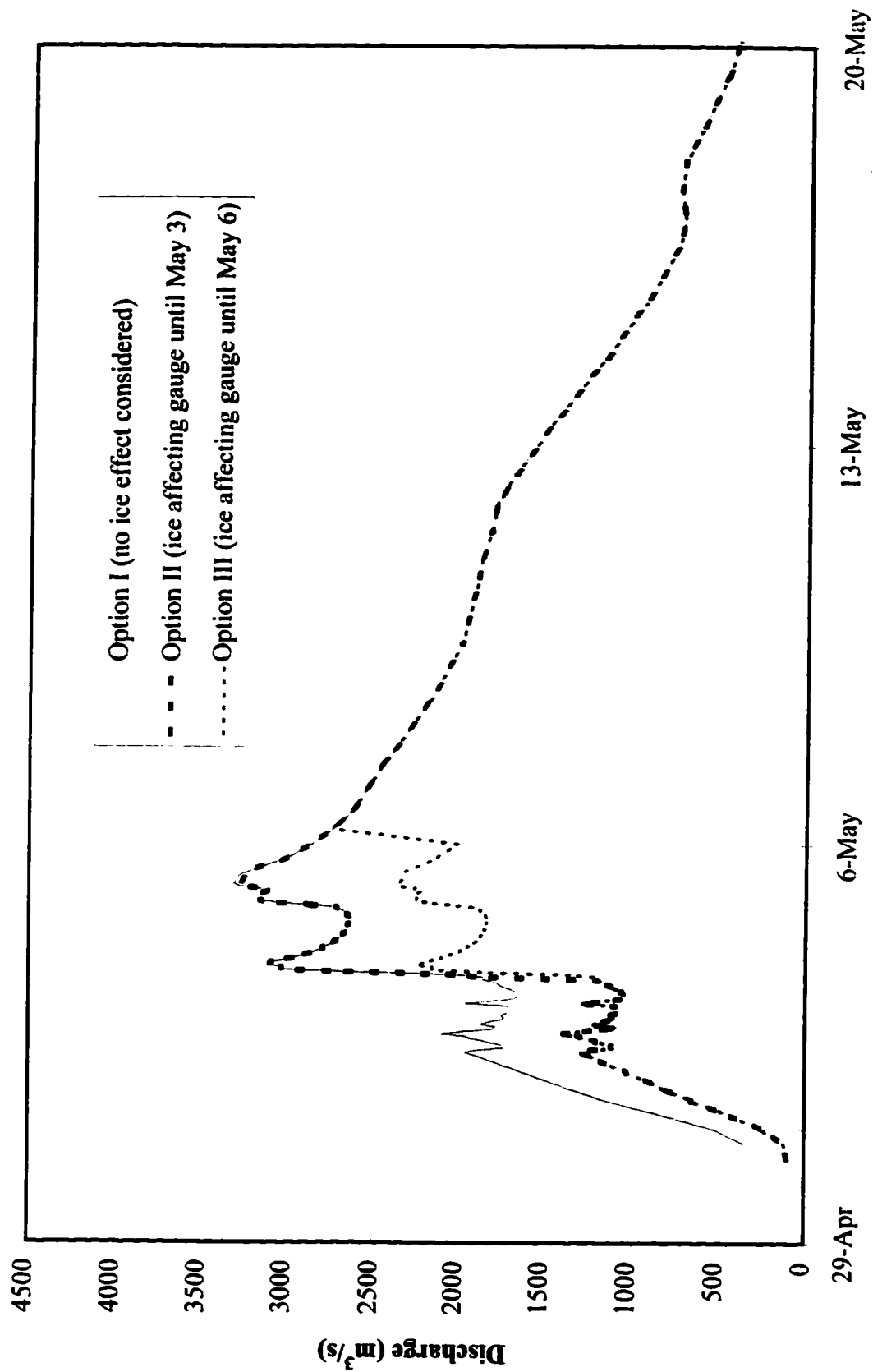
Figure 4.16. Discharge hydrographs determined for the WSC gauge on the Porcupine River below Bell River by the three methods.

137
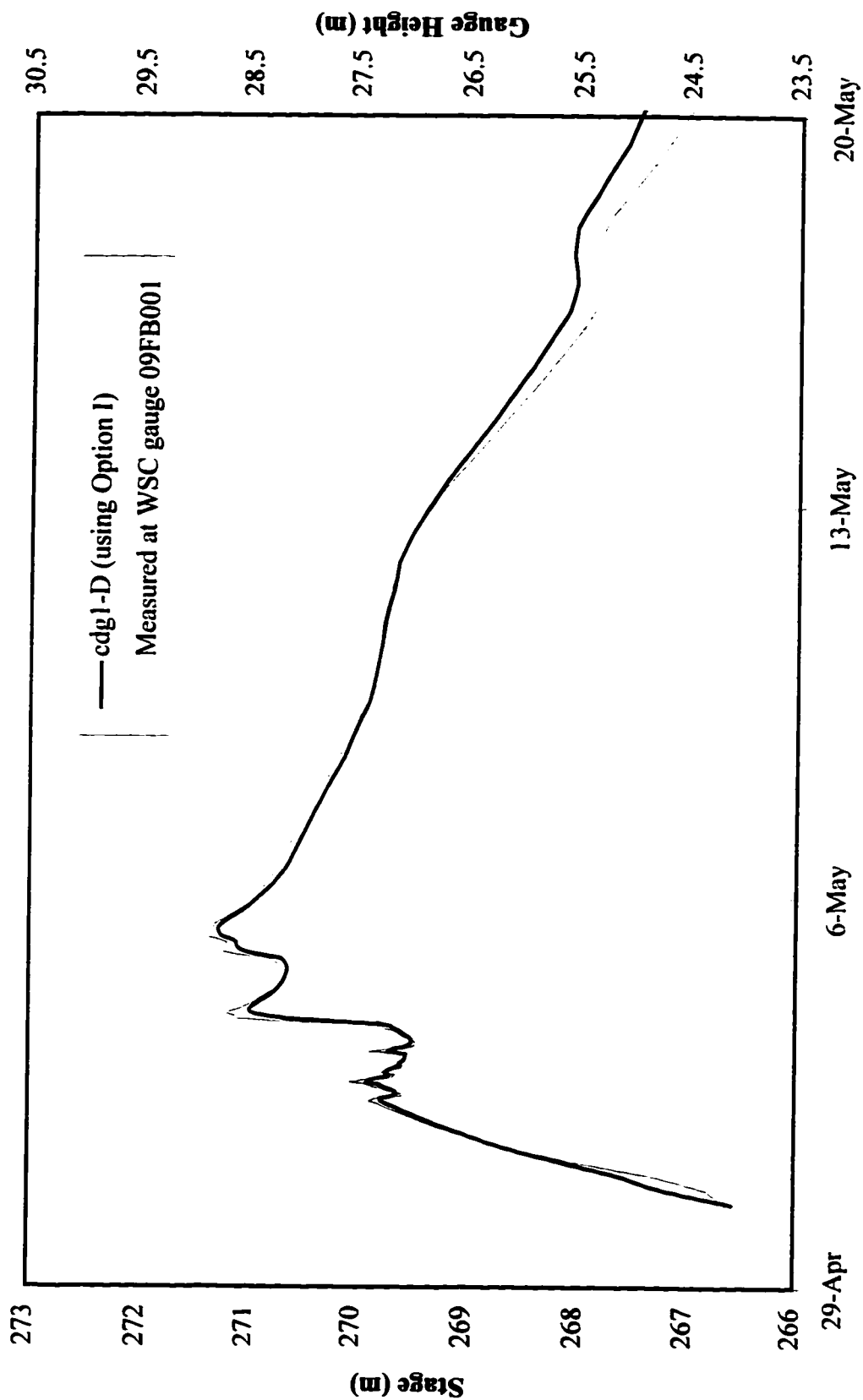
Figure 4.17. Comparison of measured and computed stage hydrographs at the gauge on the Porcupine River below Bell River using Option I.

138
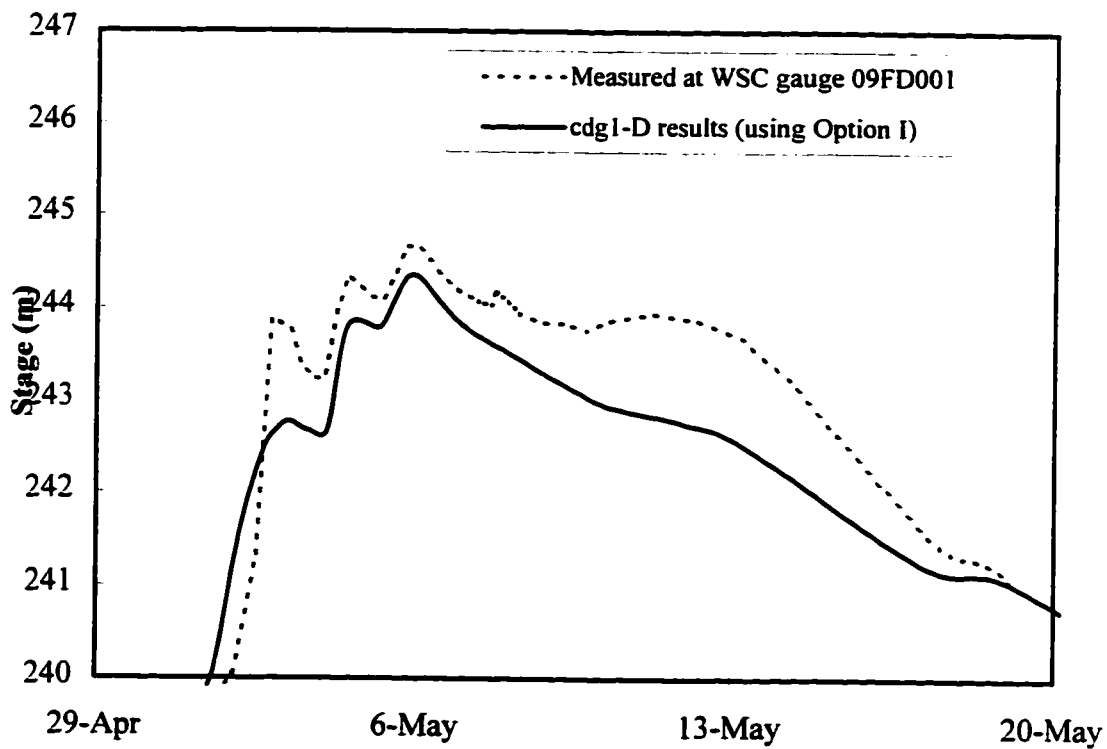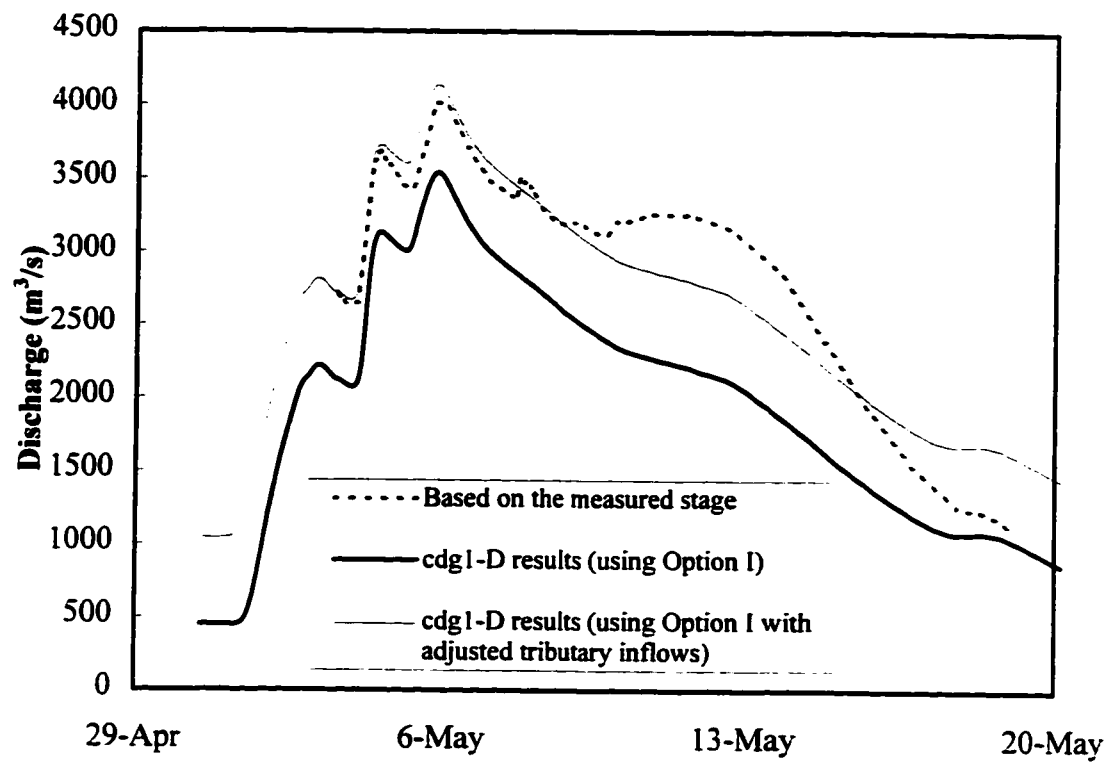
Figure 4.18. Simulation results for the Porcupine River gauge at Old Crow.
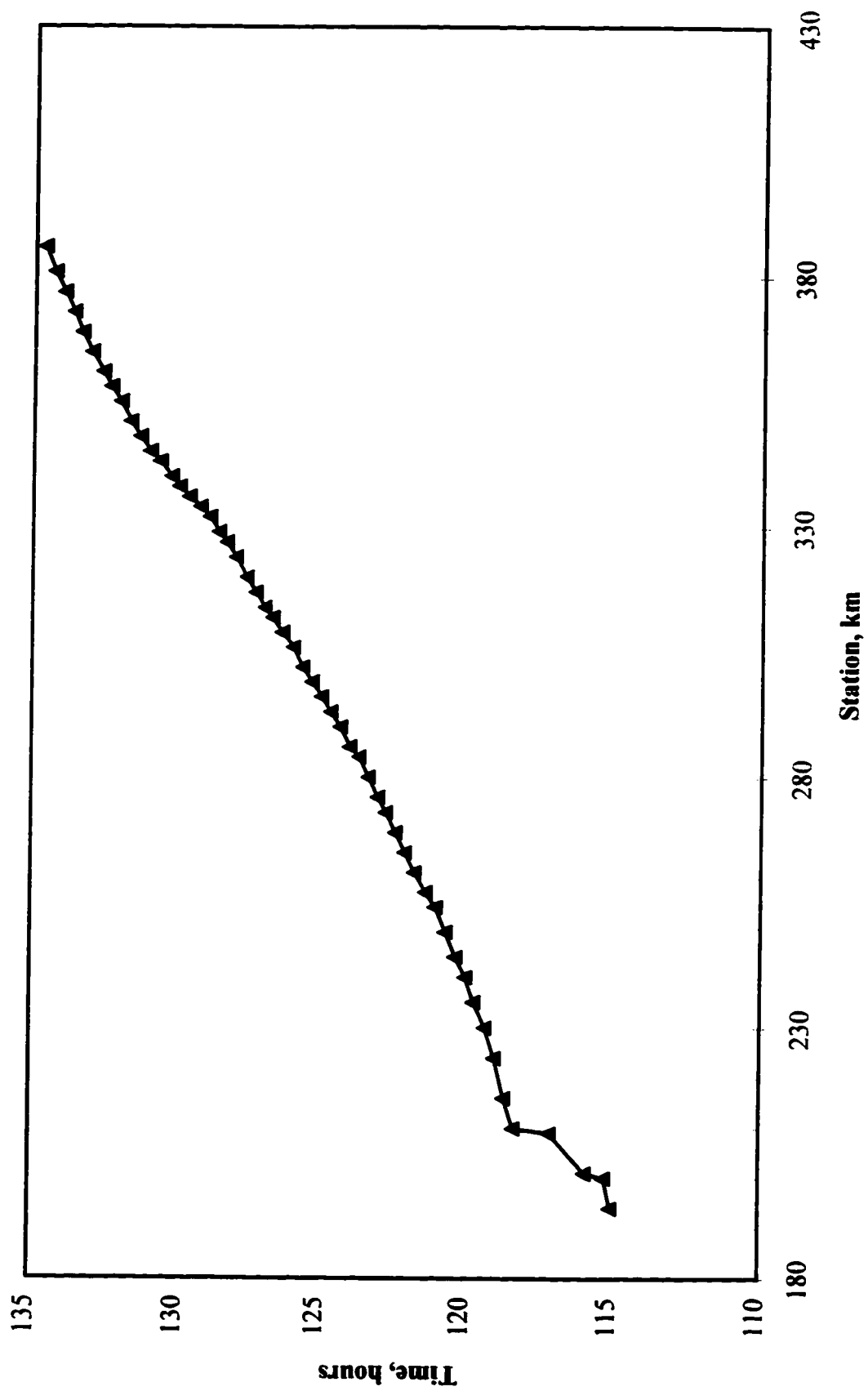
Figure 4.19. Location of the surge peak with respect to time for the 1995 event on the Porcupine River.

CHAPTER 5

EVALUATION OF DYNAMIC FLOOD ROUTING WITH ABUNDANT GEOMETRIC DATA

5.1 INTRODUCTION

The objective of this chapter is to evaluate the accuracy of the dynamic hydraulic flood routing model when the geometric data describing the study reach are abundant. This is accomplished by verifying three aspects involved in flood forecasting a dynamic event (an ice jam surge release) which occurred on the Saint John River, New Brunswick. The first is the rectangular channel approximation. Given the abundance of survey data for the study reach, this case study provided an excellent opportunity to justify the importance of the channel slope over that of the natural channel geometry. This would enforce the reliability of the geometric databases used in the previous studies.

Secondly, the Saint John River study looks at the importance of the channel geometry in predicting water levels rather then discharges. Since only a measured stage hydrograph is available for comparison to the computed hydrographs, all of the computed hydrographs are stage hydrographs.

Finally, this chapter reviews the equilibrium jam approximation to a large measured jam. This is accomplished by comparing the equilibrium ice jam profile to that of an

ice jam measured during the breakup event, as well as comparing the stage hydrographs modelled by routing each jam configuration.

5.2   DESCRIPTION OF THE STUDY REACH

5.2.1   BACKGROUND

Figure 5.1 shows the study reach of the Saint John River.   The river is approximately 700 km in length traveling from the Little Saint John Lake in Maine to the Bay of Fundy at the city of St. John, New Brunswick.   There are three hydroelectric power stations along the river: Grand Falls, Beechwood, and Mactaquac (Humes & Dublin, 1988).   The dams at these sites create the head for a run-of-river hydropower operation which provide little backwater effects on the upstream reaches (Ismail & Davis, 1992).

The reach of the Saint John River extends along the international boundary between the United States and Canada, from Fort Kent, Maine to the dam at Grand Falls, New Brunswick, a distance of approximately 100 kilometres.   The backwater from this dam affects the downstream 10-20 kilometres of the reach (Beltaos, Burrell, and Ismail, 1994).

The Saint John River has experienced many major flood events which have been documented as far back as 1696 (Kindervater, 1985)   The majority (69%) of these were ice related (Humes & Dublin, 1988).   These events cause millions of dollars in damage to the communities which lie   along the river's banks.   In 1987 alone,

flood damages were estimated to be $30,000,000 (Humes & Dublin. 1988).

The hydrologic details of the ice related event which occurred at Sainte-Anne-de-Madawaska, along the Saint John River, in 1993, were well documented. The ice jam profile, shown in Figure 5.2, was measured during this event. The water levels obtained at Saint Leonard, 5 km below the head of the ice jam, following the release of the jam, are shown in Figure 5.3. Both of these pieces of information were supplied by the National Water Research Institute (NWRI). As well, two Water Survey of Canada (WSC) gauges on the Saint John River in the study reach recorded streamflow during the event. These are at Fort Kent (WSC 01AD002) and Grand Falls (WSC 01AF002), which can be seen in Figure 5.1. Since the data available from these gauges is only published as mean daily flows, NB Power supplied hourly discharge data recorded during the event for both Fort Kent and Grand Falls gauges. The stage hydrograph from Grand Falls is shown in Figure 5.3. and the discharge hydrographs at Fort Kent and Grand Falls are found in Figure 5.4.

5.2.2   AVAILABLE GEOMETRIC DATA

5.2.2.1   Channel Distances

River stations, or locations along the channel length, were determined in kilometres downstream of Fort Kent on the 1:50,000 scale N.T.S. maps. Station 1.32 km was the WSC gauge in Fort Kent. This location for the upstream boundary of the model was selected as it provided an inflow hydrograph for the boundary condition and it

143

encompassed the 1993 ice jam at Sainte-Anne-de-Madawaska and its estimated backwater effects. All of the surveyed cross sections were referenced to this stationing system, as well as all of the key sites of interest. Table 5.1 presents the location of these key sites along the St. John River.

Table 5.1. Location of key sites along the Saint John River

Location	Station (km)
Fort Kent (WSC 01AD002)	1
Edmunston (WSC 01AD004)	33
Sainte-Anne-de Madawaska	62
Head of Jam	*49*
Toe of jam	*69*
Saint Leonard	**74**
Grand Falls (WSC 01AF002)	**95**

5.2.2.2   Available Cross Section Surveys

The available cross section surveys, which were tied into the stationing system. were supplied by NWRI and NB Power. The abundance of available surveys is shown in Figure 5.5.

5.2.2.3   Water Surface Slopes

Table 5.2 provides the water surface elevations found from the 1:50,000 scale N.T.S. maps. Table 5.3 presents the water surface slopes calculated from the data in Table 5.2.

144

Table 5.2. Water surface elevations from the N.T.S. maps

Station (km)	Contour Elevation
24	460 ft. (140m)
28	450 ft (140 m)
34	440 ft (130 m)
95	130 m
95	120 m
95	110 m
96	90 m

Table 5.3. Water surface slopes based on the N.T.S. map data

Reach (km)	Water Surface Slope
24to 28	0.00092
28 to 34	0.00046
34 to 95	0.00007
95 to 95	0.06667
95 to 95	0.20000
95 to 96	0.01600

5.2.2.4 Channel Resistance

The channel resistance for this study was obtained from data, shown in Table 5.4. supplied by NB Power. From these values, Mannings n was taken as 0.02 for the downstream portion of the reach and 0.025 for the upstream section.

Table 5.4. Mannings *n* Roughness Coefficient for the Saint John River upstream of Grand Falls Reach

Flow (m³/s)	Reach	
	1 - 33 (upstream)	33 - 95 (downstream)
140	0.0299	0.0247
280	0.0286	0.0237
1700	0.0260	0.0215
2850	0.0247	0.0204
5700	0.0241	0.0199

5.2.3 DETAILS OF THE DOCUMENTED ICE JAM RELEASE EVENT

The 1993 ice jam release modelled in this case study provided the dynamic event used to evaluate the hydraulic flood routing techniques applied by the cdg1-D model. The event was described by Beltaos, *et al.* (1994). On April 13, the ice jam formed at 69.2 km near Sainte-Anne-de-Madawaska, as shown in Figure 5.1. The profile measured along the jam April 13 and 14 extended upstream to 49.2 km. The water levels behind the jam rose, causing the closure of the TransCanada Highway at various locations along the banks of the Saint John River, including at Riviere Verte, 15 km upstream of Ste-Anne-de-Madawaska. This increase in stage is more evident when an M1 backwater curve is approximated as a horizontal line. The jam shown in Figure 5.2 affects approximately 40 km of the study reach.

At 09:00 on April 15th the jam released. The surge peak arrived in Saint Leonard (74.26 km), approximately 5 kilometers downstream of the toe of the jam, 48

minutes after this release. The ice from the jam entered Saint Leonard 35 minutes after the jam release and continued to flow past for 90 minutes.

5.3 MODELLING THE ICE JAM SURGE RELEASE PROPAGATION

5.3.1 INTRODUCTION

As with the previous studies, the hydraulic flood routing model implemented in this study requires two types of input data: geometric and hydrologic. The geometric data required includes the effective bed profile, channel top widths, and channel hydraulic roughness throughout the entire study reach. The boundary and initial conditions for the model, supplied by the hydrologic data, include upstream and downstream boundary conditions as well as details of lateral inflows.

Several approaches were studied in modelling the ice jam surge release propagation. The first looked at the effect of the bed profile. In order to accomplish this, two geometric databases were constructed; one which was based on the effective bed calculated from the surveyed cross sections and the other which employed a smoothed bed profile. The second approach evaluated the equilibrium ice jam assumption by conducting the simulations for the measured jam profile as well as for an equilibrium jam.

5.3.2 GEOMETRIC DATABASE

5.3.2.1 Introduction

As mentioned, two geometric databases were required for this study. However, since the cross section survey data available on the St. John River is abundant, both databases were created based solely on the available survey data without any supplemental data from the topographic maps. The data required for the creation of the databases included the channel widths, which were the same for both cases, and the effective bed profiles.

5.3.2.2 Channel Widths

The channel widths used in the hydraulic model were calculated from the surveyed cross sections assuming bank full conditions. Since the spacing of the cross sectional surveys was so irregular, additional computational nodes were required. Therefore, the top widths for the additional nodes were obtained by interpolating between the two surveyed cross sections encompassing the extra node.

5.3.2.3 Effective Bed Profile

As was previously mentioned, the geometric data available along the Saint John River, shown in Figure 5.5, was abundant. However, since the cdg1-D model assumes a rectangular cross section, the effective bed had to be determined at each of the surveyed cross sections.

The calculated effective bed is shown in Figure 5.6. The initial effective bed profile for the modelled reach was left as calculated to see the effect of the irregular bed profile on the cdg1-D model's ability to predict water levels. A second effective bed profile was estimated by graphically smoothing the previous profile. The smoothed effective bed profile is also shown in Figure 5.6. The NTS water surface profile is also shown in this figure to demonstrate that in the previous case studies the NTS water surface slopes provides an adequate approximation to the effective bed slopes. However, fitting the slope to effective bed calculated from the survey data provides a much better approximation.

5.3.3 BOUNDARY AND INITIAL CONDITIONS

5.3.3.1 Introduction

Two boundary conditions and all lateral inflows must be specified in order to solve the non-linear partial differential equations used in the hydraulic flood routing model. As well, initial conditions, stage and discharge, must be specified at every computational node. The boundary conditions must be specified at the upstream and downstream ends of the reach, as the flow in the modelled reach of the St. John River is subcritical. In general, the upstream boundary condition is a discharge hydrograph. The downstream boundary condition may be a stage or discharge hydrograph, or a stage-discharge rating curve.

149

5.3.3.2 Boundary Conditions

Upstream Boundary Condition

Since a measured ice jam was to be superimposed on the flow to generate the surge being modelled in this study, the upstream boundary had to extend far enough upstream to ensure that the model included the jam head and toe, as well as any backwater effects the jam may have caused. Therefore, the upstream boundary was taken at 1.32 km, where the WSC gauge on the St. John River near Fort Kent is located. This location was also appropriate for the upstream boundary as the hydrograph measured at this gauge accounted for the snowmelt runoff event, and the previous ice related events, associated with the ice jam surge release being modelled.

Downstream Boundary Condition

Quite often in flood forecasting, the downstream boundary condition is unknown. In this case, the downstream boundary was taken as the upstream face of the dam located at Grand Falls (95.3 km), since this structure provided a discontinuity in the flow, which would prevent surge propagation further downstream. The boundary condition at this location assumed a constant stage, estimated from the stage hydrograph measure the WSC gauge at Grand Falls. The accuracy of this assumption was verified by using the measured stage hydrograph which, as shown in Figure 5.3, was relatively constant.

150

Figure 5.1 shows a few of the tributaries which flow into the Saint John River within the study reach. For this investigation, the lateral inflow contribution was considered negligible in comparison to magnitude of the event which occurred in the main channel, especially since the ice jam profile was routed over an extremely short reach. Reviewing the WSC gauge data for the tributaries confirms this assumption. The tributary that flowed into the 6 kilometre reach, Grande Riviere, contributed only 2% of the total flow. As well, the tributary inflows upstream of the ice jam were accounted for in the measured ice jam profile.

5.3.2.3   Initial Conditions

The initial conditions (stage and discharge) must be specified at every computational node prior to beginning an unsteady flow simulation. For the Saint John River case study these were established in three steps. The first involved using the cdg1-D model to calculate a gradually varied flow profile for constant inflow and tributary discharges, based on the flows observed on the day the simulation began. Once the steady flow conditions were determined, the discharge hydrograph at Fort Kent, which was available for April 10 through 16, 1993, was routed until the time when the jam released, April 15 at 09:00. At this point, the ice jam profile, whether measured or computed based on the equilibrium jam assumption, was superimposed on the flow, thus establishing the antecedent conditions for the ice jam surge release. In routing both the equilibrium and   measured ice jam releases, the jam being

151

studied was simply imposed by adjusting the water levels to match the jam profile. However, the discharge was not varied, which may cause some limitations in the accuracy of routing ice jam surge releases.

5.3.2.4 Model Calibration

Hydraulic models are calibrated by varying the model features to obtain a coincidence between measured and modelled hydrographs. With cdg1-D the roughness is the parameter which is varied. For open channel events, the roughness of the bed, banks and floodplains must be accounted. For this study, a sensitivity analysis showed that the value of roughness had minimal effect on the water surface profile produced for the initial conditions. Therefore, the initially chosen values of roughness were used throughout this study. These are found in Section 5.2.2.4.

Ice roughness also becomes important when modelling ice jam surge releases using the equilibrium jam option of the cdg1-D model, as this option requires the specification of the jam location, length, and roughness, in order to establish the antecedent conditions for the ice jam surge release. Since an ice jam profile is available in this case, the ice roughness was calibrated using the cdg1-D model and was found to be 5 m. This roughness corresponds to a Mannings n for the ice jam of 0.045 which is comparable to the findings of others (Ohashi and Hamada, 1970). The calibration can be seen in Figure 5.7.

5.4 MODELLING TESTS

In order to evaluate the effectiveness of hydraulic flood routing techniques for modelling dynamic events where abundant data was available, two key approaches were taken. The first involved comparing the results of two simulations where different effective bed profiles were used, to evaluate the accuracy of the rectangular channel approximation. The second reviewed the possibility of using an equilibrium jam profile over a measured jam profile when modelling a ice jam surge propagation for a large jam.

For each simulation a time step increment of 40 seconds was used in order to ensure a Courant number of 0.5 or less throughout. The results of these simulations, which were obtained by comparing the measured and computed events at St. Leonard Bridge, approximately 6 km downstream of the toe of the jam, are discussed here.

5.4.1 VARIABLE EFFECTIVE BED PROFILES

As previously discussed, two geometric databases were created for modelling the 1993 break up event on the Saint John River. The first one used an effective bed calculated directly from the surveyed cross sections. The second used an effective bed smoothed through the effective beds from the surveyed cross sections.

The results of these two simulations can be seen in Figure 5.8. In both cases, the timing of the event peak arrival was exact. The accuracy in modelling the peak was found by determining the ratio of the difference between the measured and computed

water level to the change in water level for the computed run. Using this method. the magnitude of the peak was modelled within 40 cm (15%) for the effective bed from the surveyed cross sections and within 7 cm (2.5%) for the smoothed bed.

Even though the smoothed bed approximation seems to provide a better approximation to the measured bed, it is important to realize that this is solely based on where the bed elevation happened to be specified. Therefore, in order to have a better comparison of the two simulations the change in stage for each simulation was plotted versus time in Figure 5.9. These were not compared to a measured change in stage as the base flow stage was not available for the measured stage hydrograph at St. Leonard Bridge.

The wave front location is plotted with respect to time for the simulation based on the effective bed profile from the surveys in Figure 5.10. The wave front location was chosen over the wave peak location for Figure 5.10 due to the dynamic nature of the event and to the formation of the flood wave resulting from the release of the ice jam. Subsequent to the jam release, multiple wave peaks join to form one wave prior to its propagation downstream, as shown in the discharge profiles in Figure 5.11. The wave front locations plotted for Figure 5.10 can be seen in the water surface profiles of Figure 5.12.

The wave speed calculated from Figure 5.10 was 9.07 m/s. From the cdg1-D results the average channel velocity was found to be 1.29 m/s. The dynamic ($V_w=U+c$) and diffusive ($V_w=\frac{3}{2}U$) wave velocities were 1.93 m/s and 8.38 m/s.

respectively. Beltaos *et al.* (1994) estimated the average velocity as a surface velocity which was based on the movement of the ice from the jam location to St. Leonard. The average channel velocity for Beltaos *et al.* (1994) was 2.9 m/s. The dynamic and diffusive wave velocities were calculated for this channel velocity and were found to be 9.99 m/s and 4.35 m/s. All of these propagation velocities are shown in Figure 5.10 with the computed wave front propagation.

The wave speed computed from the cdg1-D results falls between the dynamic wave speed computed for these results and that computed based on Beltaos *et al.* (1994) estimate of the average channel velocity. The diffusive wave speeds calculated for both the cdg1-D results and Beltaos' average channel velocity are evidently much slower than the wave speed calculated for this event. Therefore, this ice jam release is dynamic.

5.4.2 VARIABLE ICE JAM PROFILES

When a large ice jam occurs on a river reach it is often convenient to describe its profile through the use of an equilibrium jam. Therefore, this study also assessed the applicability of the equilibrium jam approximation. Figure 5.7 shows a comparison of the profile of the modelled equilibrium jam which had a roughness of 5 m (as shown in Section 5.3.2.4.), and the ice jam profile measured on the Saint John River during the 1993 event.

For the case when the equilibrium jam was employed, the geometric database

155

containing the smoothed effective bed profile was used. The computed hydrograph for the equilibrium jam scenario was identical to that modelled with the measured jam, as shown in Figure 5.13. Thus, the equilibrium jam provided an excellent approximation to a large ice jam in this particular case.

5.4.3   VARIABLE DOWNSTREAM BOUNDARY CONDITION

In order to confirm the assumption of a constant water level for the downstream boundary condition the simulation was repeated using a variable downstream boundary condition. The stage hydrograph supplied by New Brunswick Power at Grand Falls was used for this condition. The effective bed calculated from the available survey data was used for this simulation. The results, shown in Figure 5.14. show little variation from the initial run except in the receding limb. The modelled peak is still within 15% and the timing exact, therefore the use of a constant water for the boundary condition in this investigation is justified.

5.5   DISCUSSION OF RESULTS

The objective of the Saint John River case study was to evaluate the ability of hydraulic flood routing techniques in modelling dynamic events where abundant geometric data was available. This was accomplished by evaluating the accuracy of the rectangular channel and the equilibrium jam approximations. In reviewing both approximations, the ability of the cdg1-D model to predict water levels in a well defined channel reach, was evaluated, as the only hydrograph available for

156

comparison to the simulated events was stage hydrograph measured at the St. Leonard bridge.

The results obtained throughout this study were encouraging. Peak water levels were modelled within 15% whether the effective bed profile from available survey data or the smoothed bed is used. The difference between the computed stage hydrographs can only be attributed to the method used in the approximation of the bed profile. Therefore, comparing the change in stage would provide a better evaluation of the models ability to predict water levels. The change in stage could not be calculated for the measured event as the base flow was unknown.

The equilibrium jam option in the cdg1-D model supplied very good results. Provided the ice jam is large and its location, length and roughness may be defined. the equilibrium jam can be used as an approximation to the actual jam configuration. Therefore, measuring the jam profile is not required.

In all of the cases reviewed in this investigation, the modelled events occurred more rapidly than the measured event as shown by the receding limbs in Figures 5.8. 5.13 and 5.14. As described in the description of the event, overbank flooding occurred along and above the ice jam. As well, the ice arrived in St. Leonard 35 minutes after the event and continued flowing for 90 minutes after its initial arrival. Therefore the timing of the water released from storage could not be modelled accurately, since the ice and storage effects on the flow is neglected by the cdg1-D model.

Since the propagation of the ice jam surge was limited by Grand Falls dam, future investigations should concentrate on longer reaches with well defined channel geometry. This would further substantiate the cdg1-D model's ability in routing floods and predicting water levels. As well, a study over a longer propagation reach would confirm when ice and floodplain storage effects can be assumed negligible in routing an ice jam surge release.

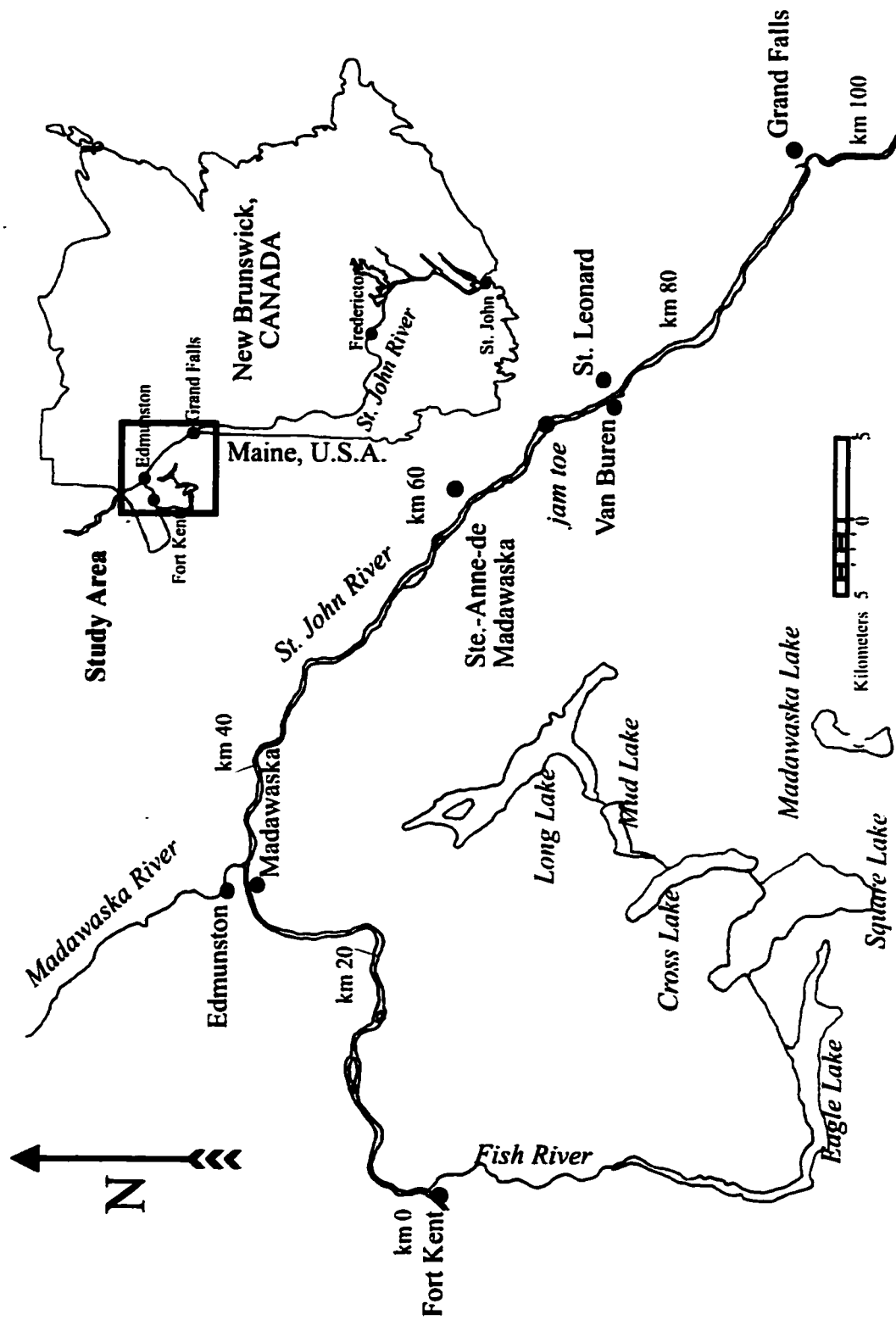Figure 5.1. Location sketch for the Saint John River study reach.
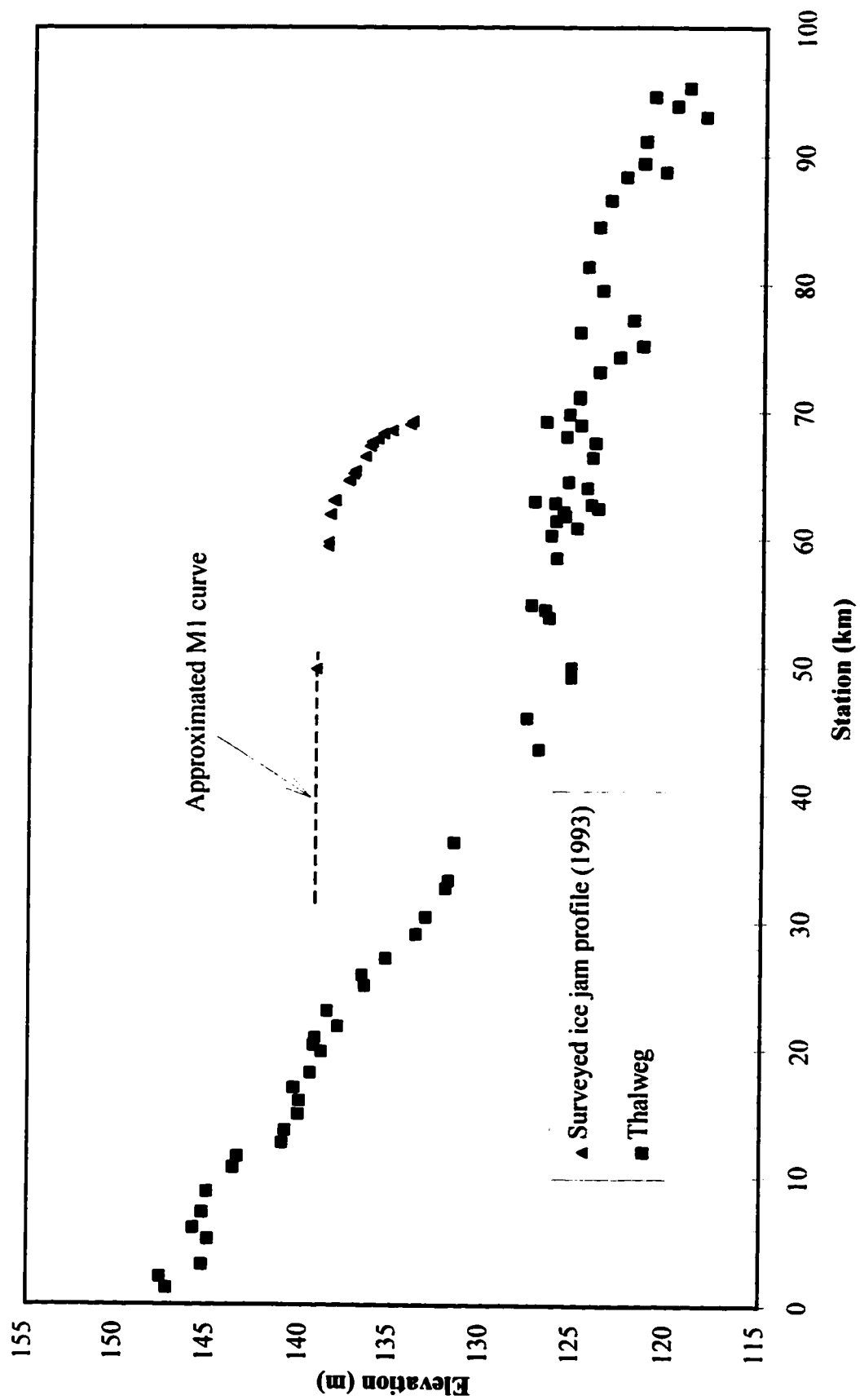
Figure 5.2. Ice jam profile surveyed during 1993 event on the Saint John River.

160
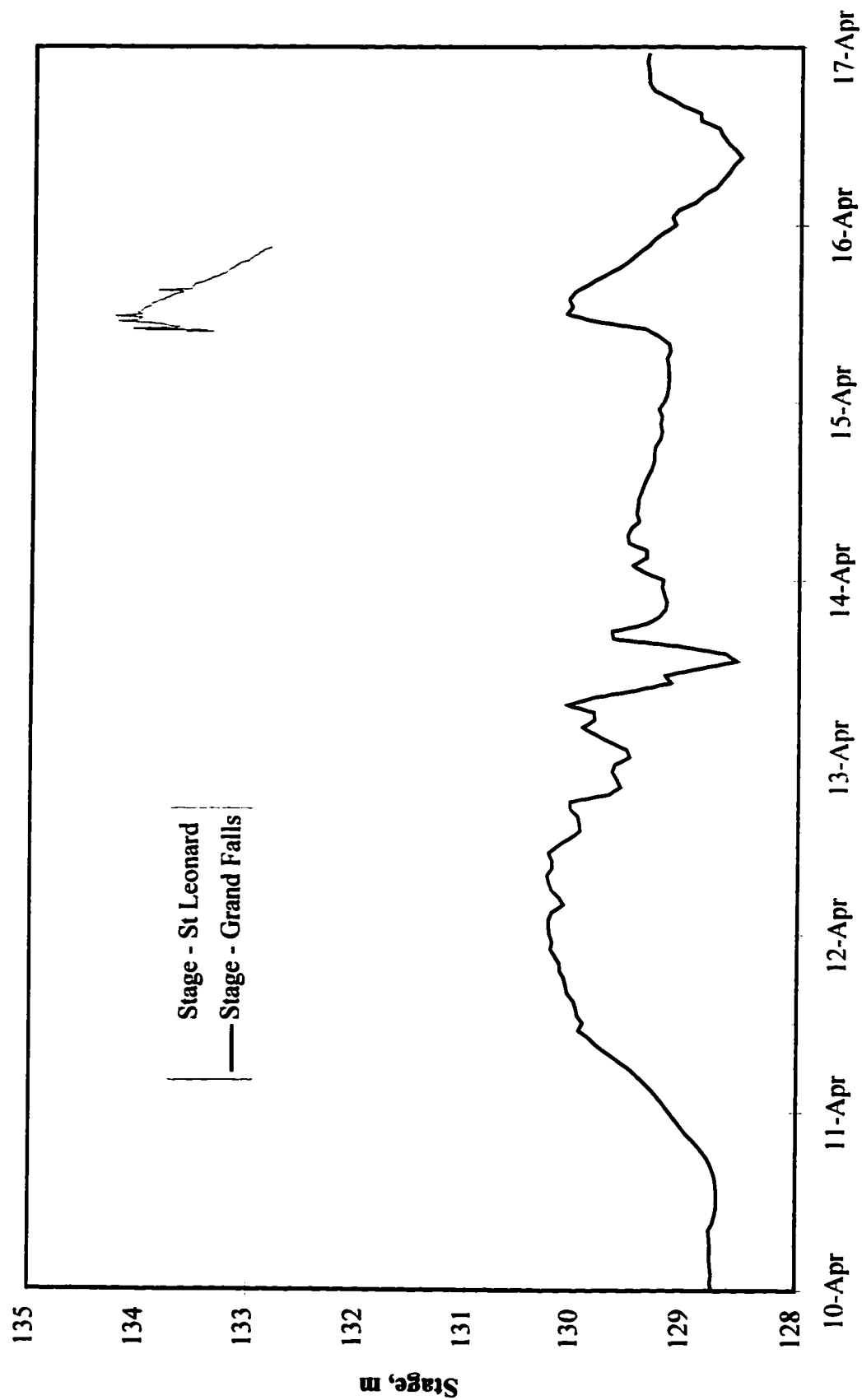
Figure 5.3. Stage hydrographs measured along the Saint John River during the 1993 event.
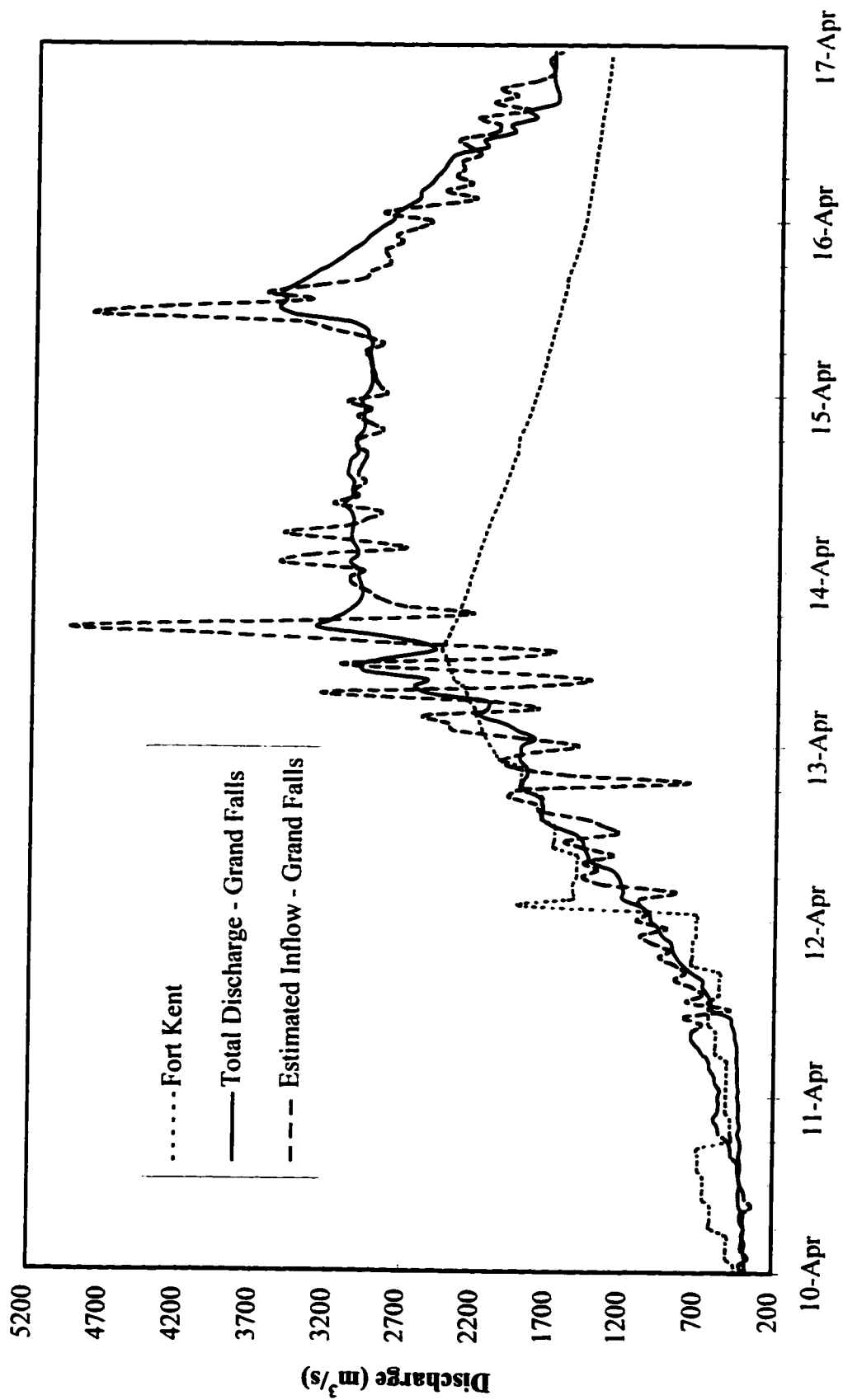
Figure 5.4. Discharge hydrographs for the St John River, 1993.

Legend:
...... Fort Kent
——— Total Discharge - Grand Falls
— — — Estimated Inflow - Grand Falls

Discharge (m³/s)
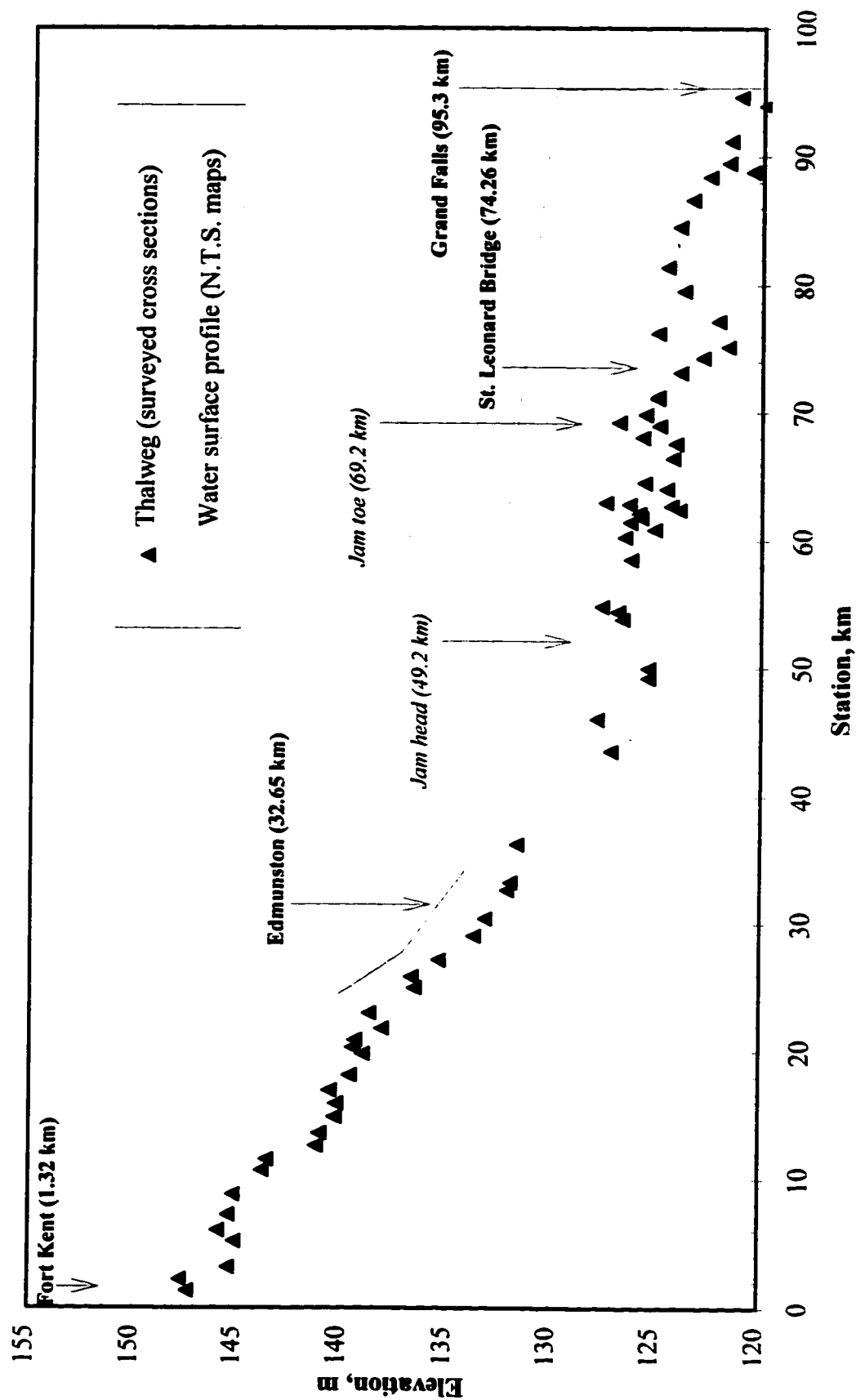
Figure 5.5. Available data for the Saint John River.
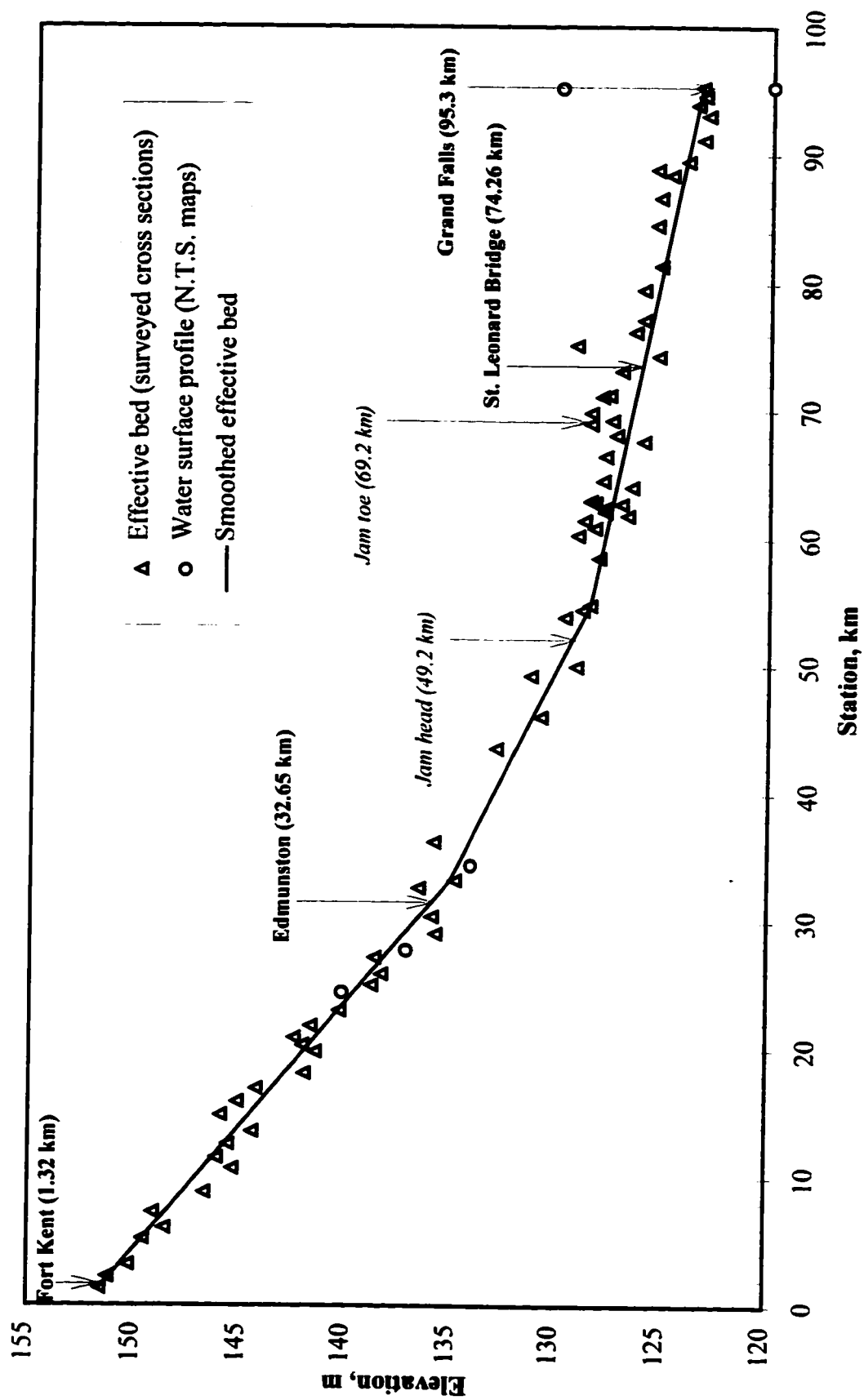
Figure 5.6. Effective bed profiles for the Saint John River.

164
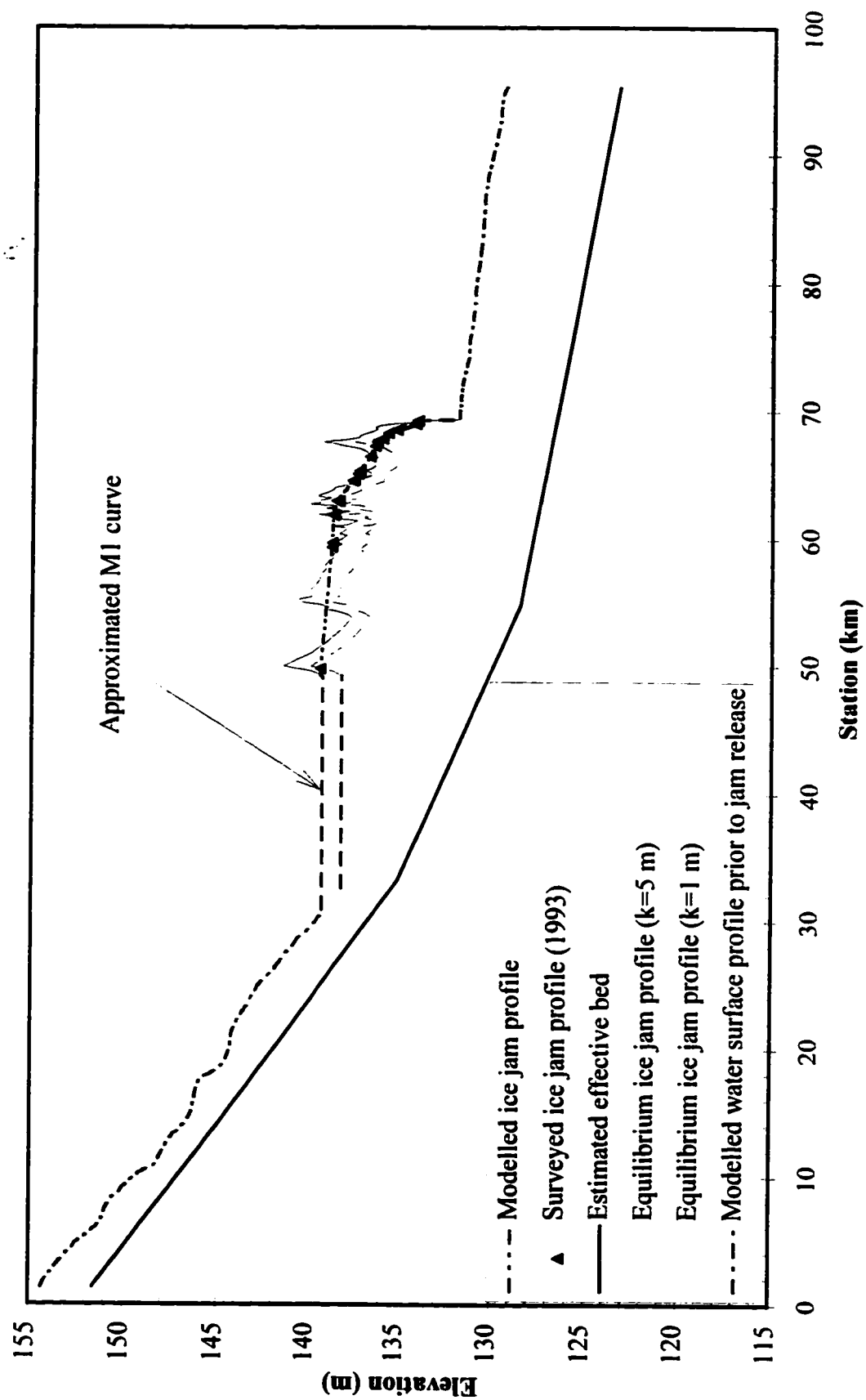
Figure 5.7. Comparison of modelled and measured ice jam profiles.

Figure 5.8. Comparison of measured and modelled stage, using variable bed approximations at St. Leonard Bridge, 6 km downstream of jam toe on St. John River, 1993.

Figure 5.9. Comparison of the change in stage for the estimated bed profiles.

167
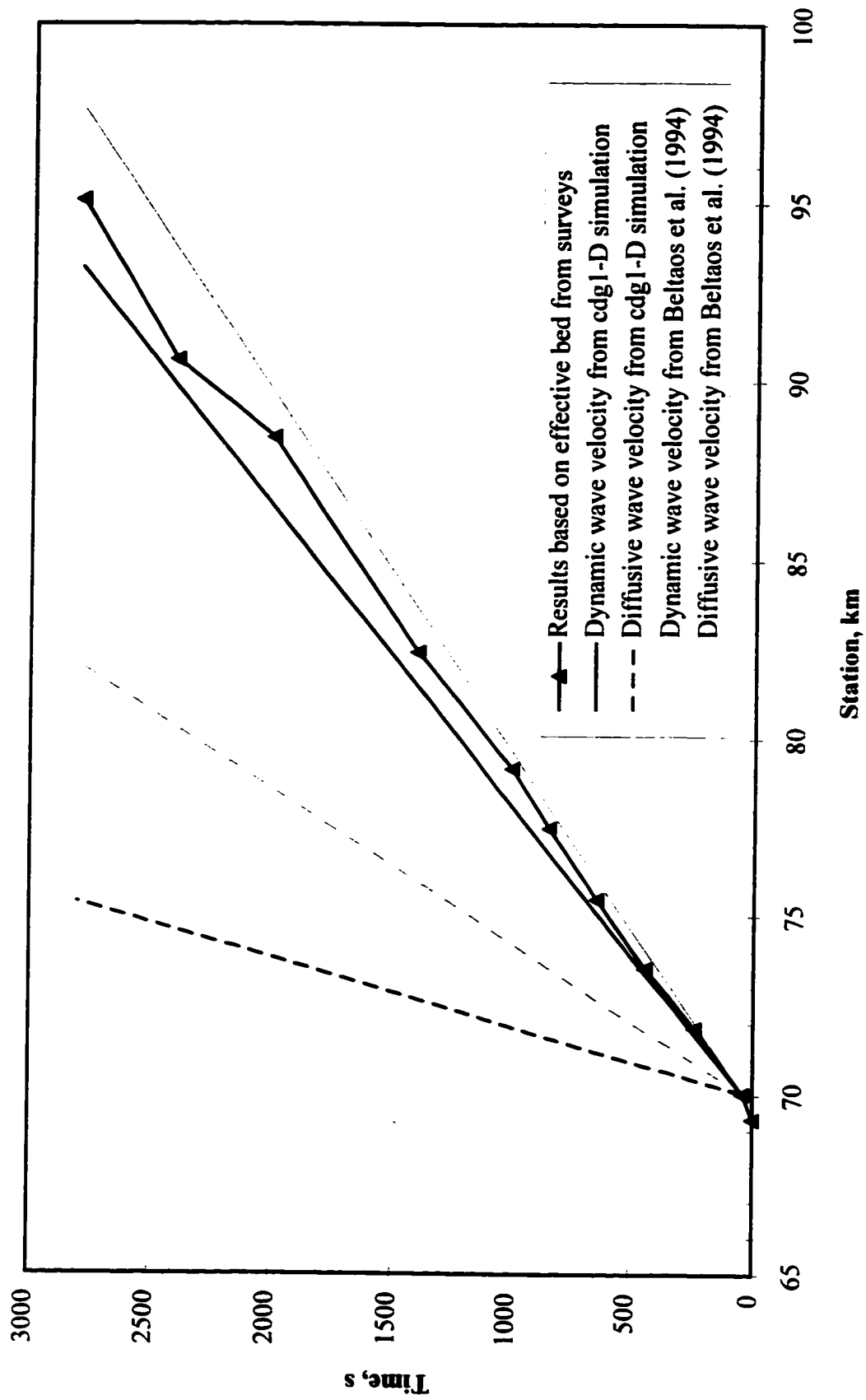
Figure 5.10. Wave front location with respect to time for the 1993 event on the Saint John River.

The figure legend reads:
- Results based on effective bed from surveys
- Dynamic wave velocity from cdg1-D simulation
- Diffusive wave velocity from cdg1-D simulation
- Dynamic wave velocity from Beltaos et al. (1994)
- Diffusive wave velocity from Beltaos et al. (1994)

Axis labels: Station, km (horizontal); Time, s (vertical)
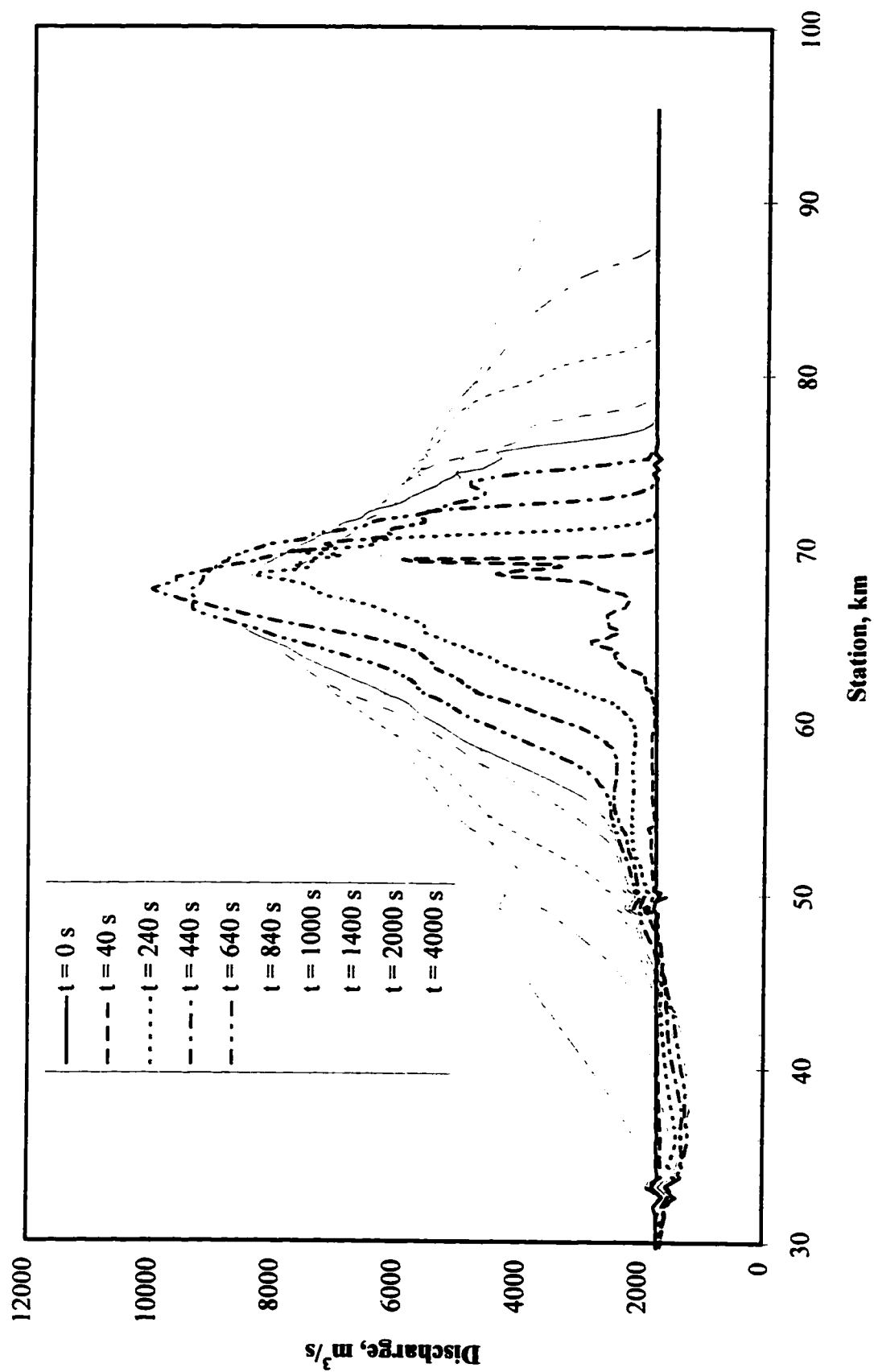
Figure 5.11. Discharge profiles following the release of the 1993 ice jam on the Saint John River.
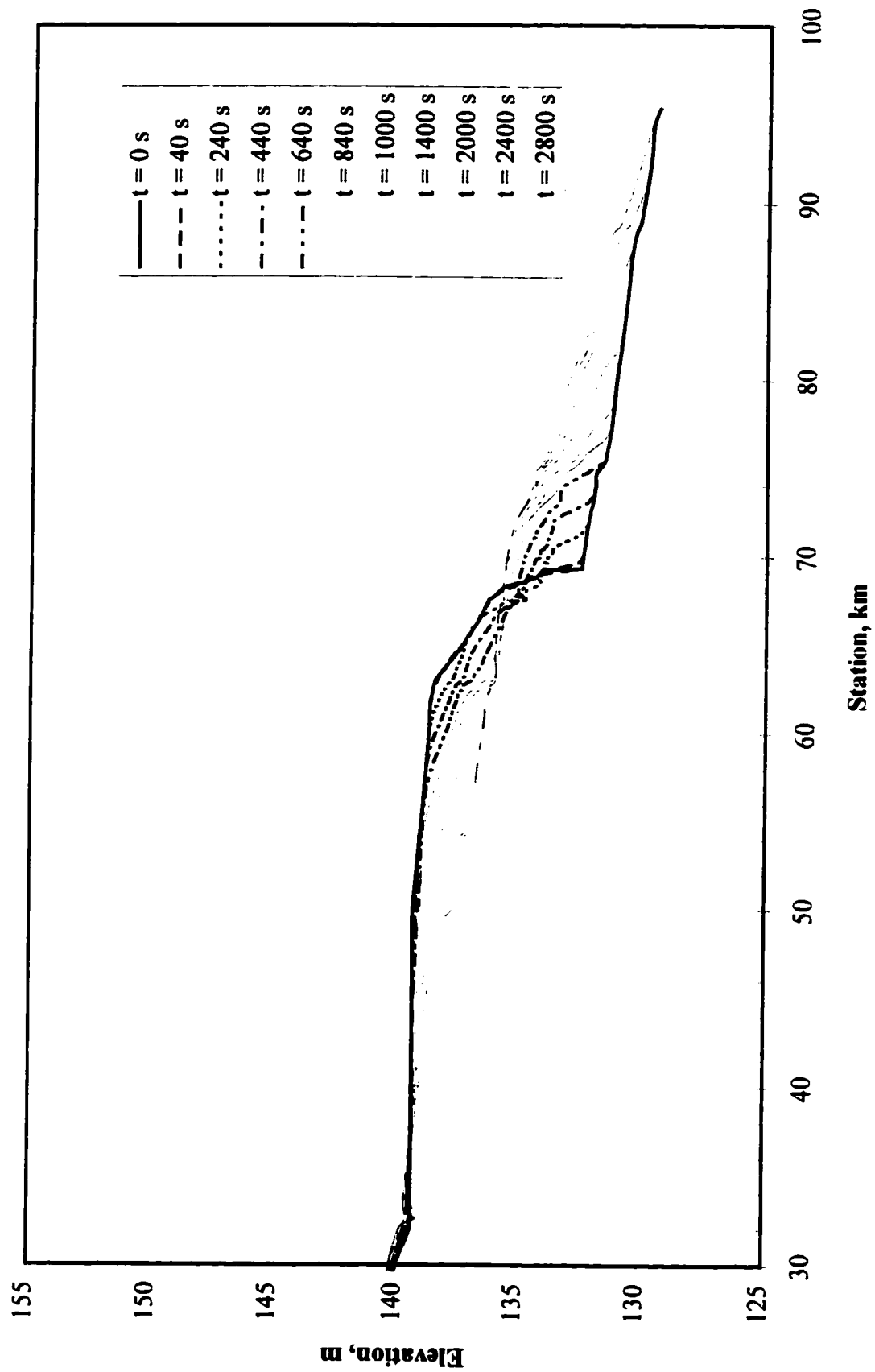
Figure 5.12. Water surface profiles following the release of the 1993 ice jam on the Saint John River.
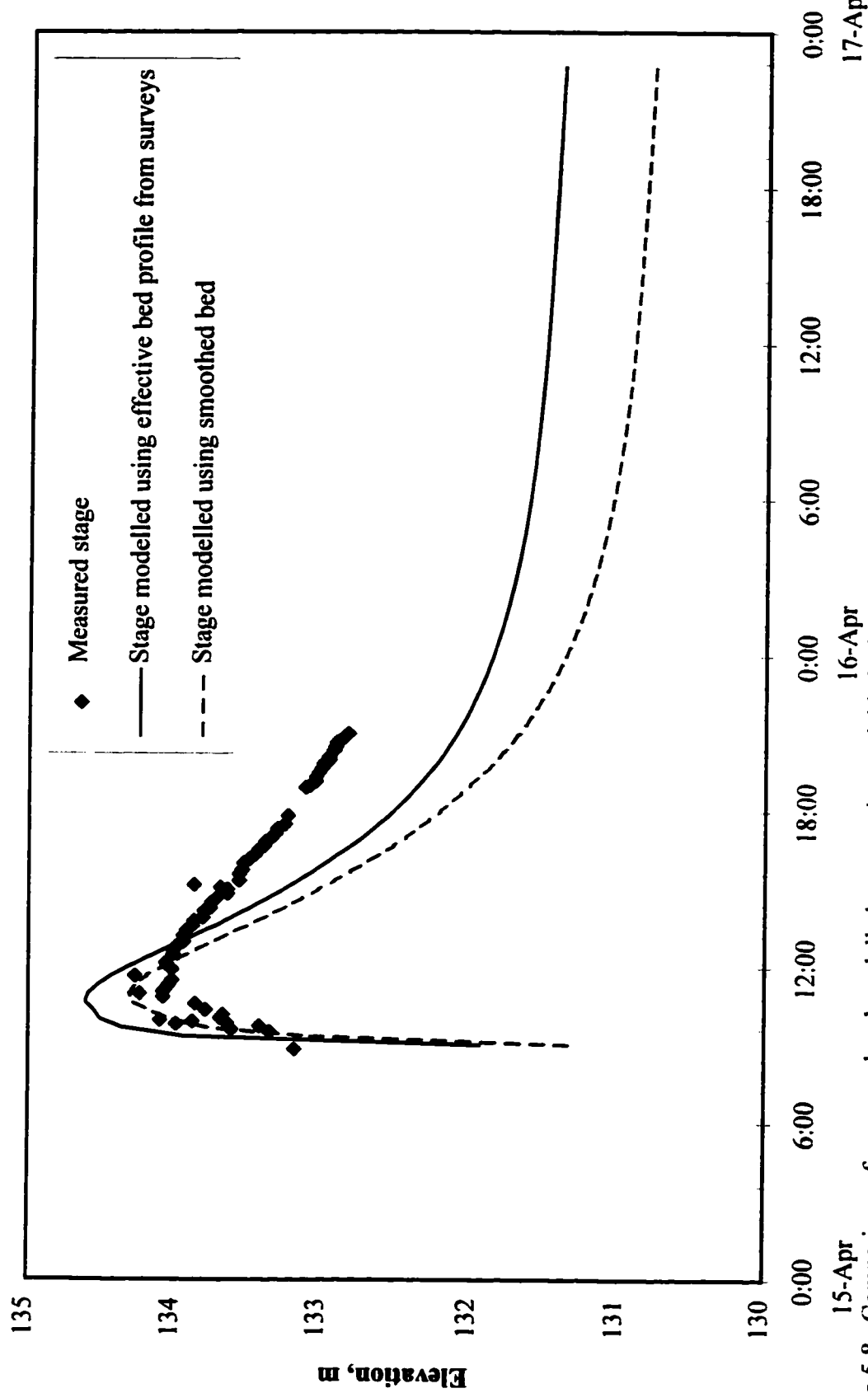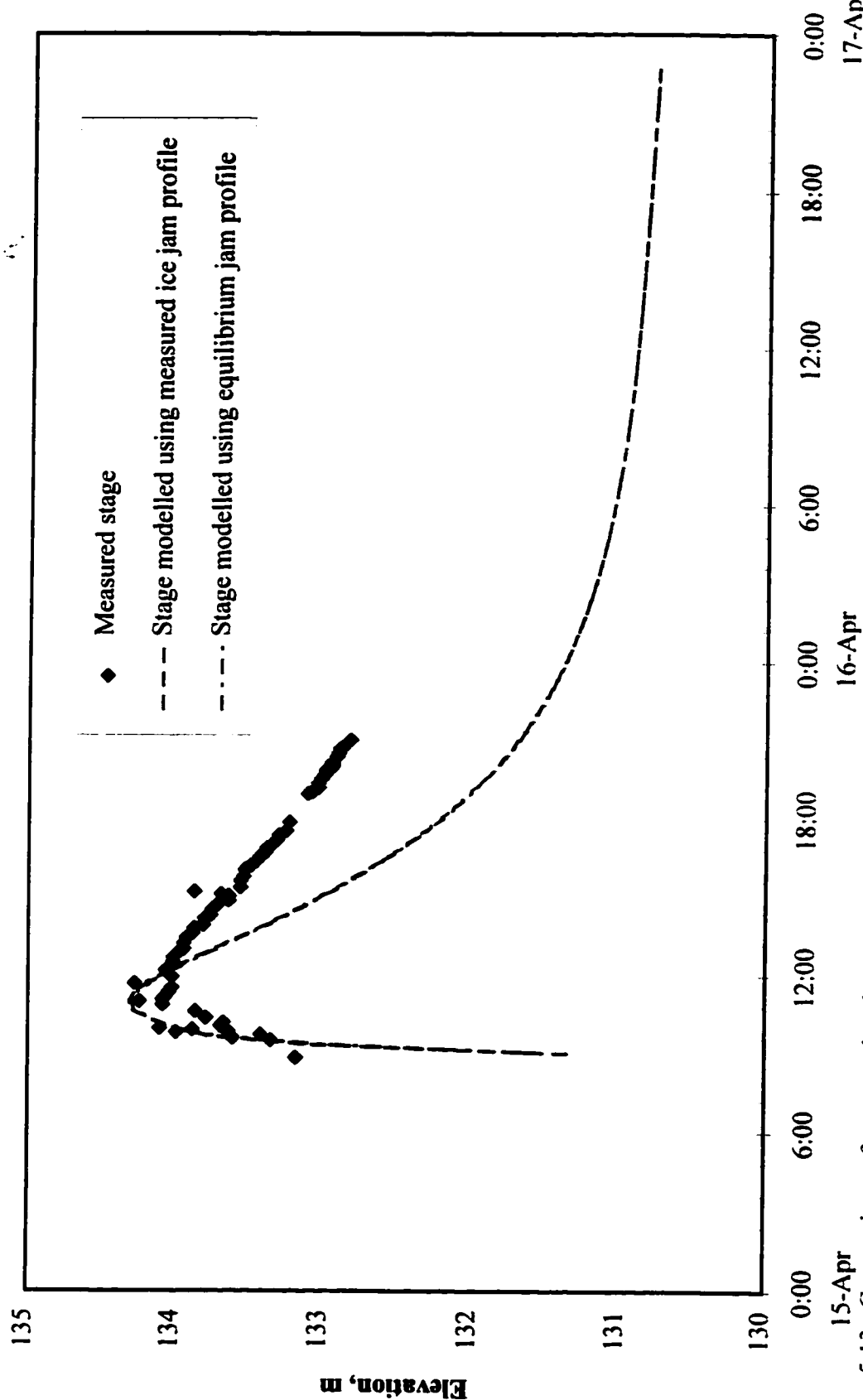
Figure 5.13. Comparison of measured and modelled stage, using variable ice jam profiles, at St. Leonard Bridge, 6 km downstream of jam toe on St. John River, 1993.
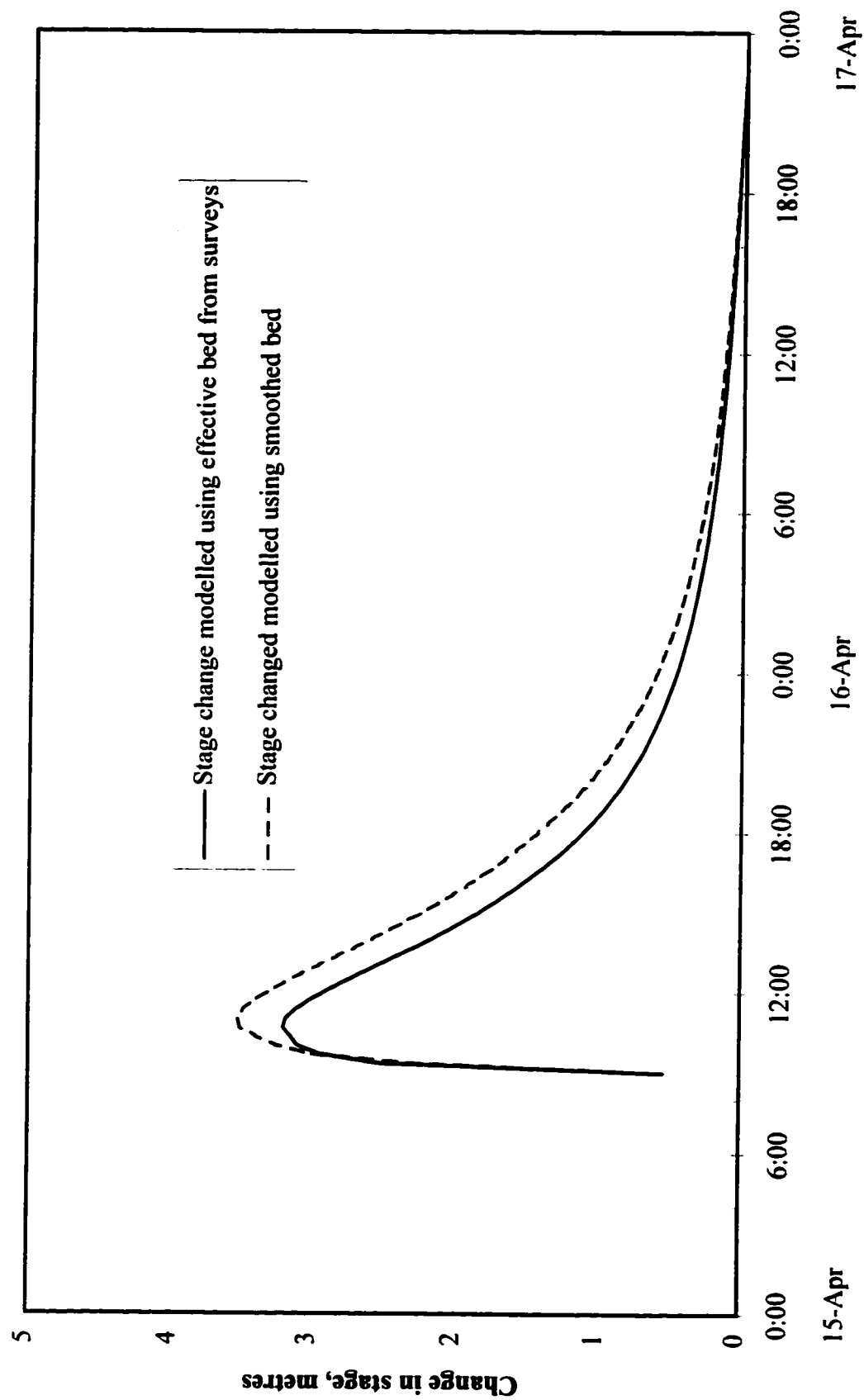
Figure 5.14. Comparison of measured and modelled stage, using variable downstream boundary conditions, at St. Leonard Bridge, 6 km downstream of jam toe on the St. John River, 1993.
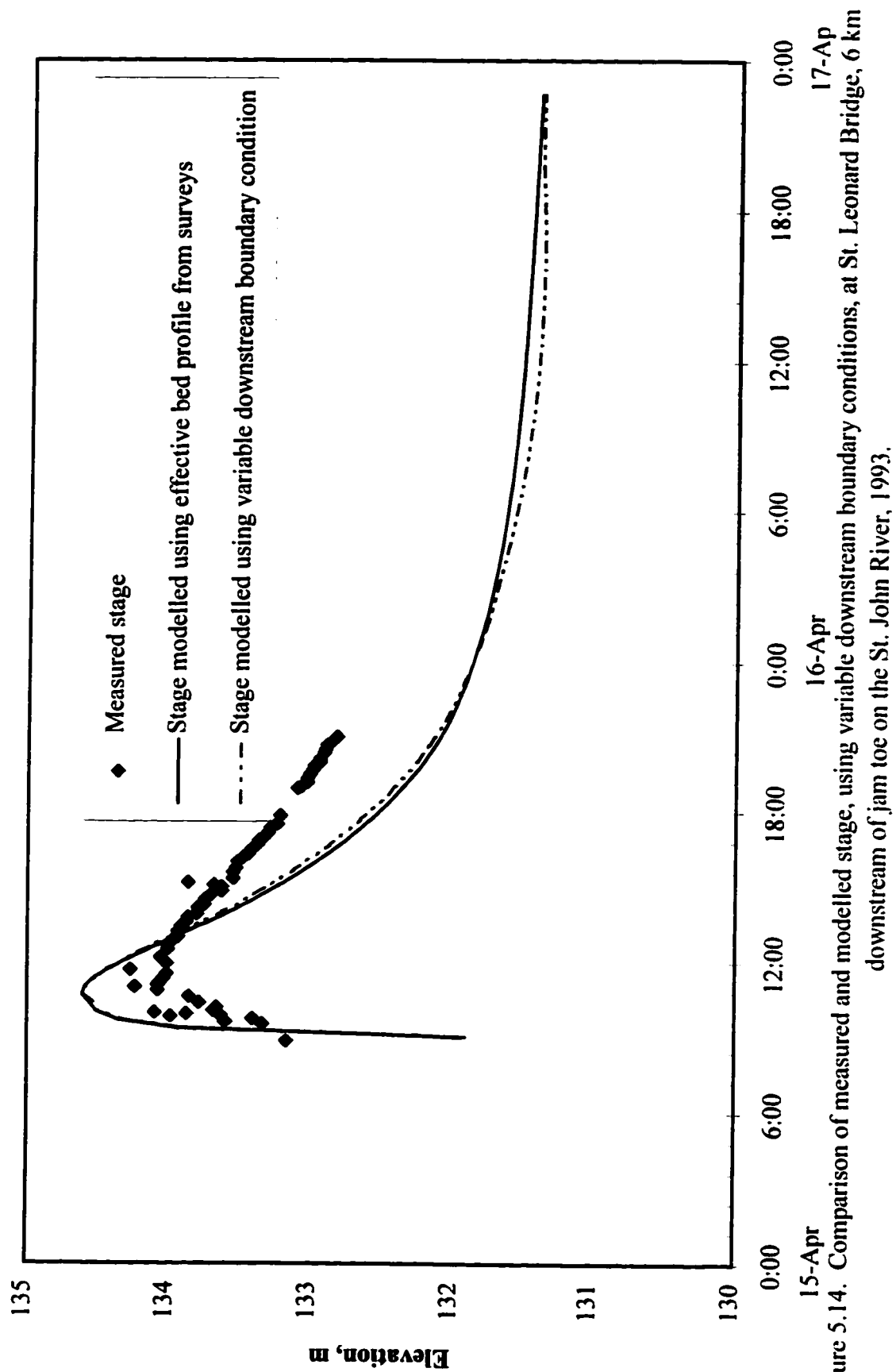
CHAPTER 6

CONCLUSIONS AND RECOMMENDATIONS

Any flood routing technique, whether hydrologic or hydraulic, requires certain basic data. Both models requires streamflow data at the upstream and downstream boundaries of the study reach as well as hydrographs describing the inflow from each tributary within the reach. However, geometric and hydraulic information describing the river channel is only necessary when an hydraulic flood routing technique is employed. Obtaining cross sectional surveys for this purpose is quite costly. Therefore, the purpose of this study was to determine the minimal amount of data required for the use of an hydraulic flood routing model.

In order to accomplish this a limited geometry model was developed for four different study reaches: the Peace River, the Oldman/South Saskatchewan River, the Porcupine River, and the Saint John River. Each model was evaluated by simulating various events which had occurred in each study reach and comparing these simulations to data measured during the event. The Peace River study concentrated on modelling moderate open water events, whereas the Oldman River study reviewed the models abilities for more extreme open water events where over bank flooding occurred. A large snowmelt runoff event with its associated ice jam releases was modelled in the Porcupine River study. In the above three case studies the study reaches were all relatively long (over several hundreds of kilometres). However, the final study, the

173

Saint John River study, examined a dynamic ice jam release event which occurred in a short reach (less than 100 kilometres).

Through the use of these case studies the following discoveries were made concerning the use of limited geometry models for hydraulic flood routing techniques. First, as shown by the Peace River study, the limited geometry model works well over long reaches for moderate open water events, where the flow remains in the main channel throughout the event. It is also reliable for more extreme snowmelt events, like that of the Porcupine River where the river is entrenched. However, as shown by the Oldman/South Saskatchewan River case study, for more extreme open water events over long reaches with overbank flooding, the model is not reliable since it does not account for floodplain storage. In cases like that of the Saint John River, a short river reach with a dynamic event and overbank flooding, the limited geometry model can predict the magnitude and timing of the wave peak. However, for the Saint John River study, the receding limb of the simulated hydrograph was much steeper than the measured limb due to the model's neglect of ice and storage effects.

This study also reviewed the hydraulic flood routing model's ability to predict water levels and average channel velocities. The Peace River study showed that these were highly dependent on the local geometry. Using a rectangular channel approximation when the data was abundant, as in the Saint John River study, further confirmed the importance of natural channel geometry in predicting water levels.

Finally, this study demonstrated the validity of assuming an equilibrium ice

jam profile to approximate a measured jam for the Saint John River reach. This approximation was found to be quite reliable provided the jam location, length and roughness were known, and that the jam was of sufficient length for the development of an equilibrium jam.

Future investigations should focus on the use of hydraulic flood routing models with natural channel geometry or some adaptation to the rectangular channel approximation. Since floodplain storage plays a key role in routing large events, both open water and ice related, a method which accounts for it should be adopted. Natural channel cross sections or an approximation to the additional flood plain area for overbank events are a few possibilities. Modelling with natural channel geometry throughout the entire reach or even at key sites of interest (cities and towns) along the reach would also aid in predicting water levels at these sites. This would be extremely valuable since for the majority of flood events the rise in water level is the main interest of the population residing and working along the river banks.

REFERENCES

Amein, M. 1968. An Implicit Method for Numerical Flood Routing. Water Resources Research, Vol 4, No. 4, pp. 719-726.

Bedient, P.B. and W.C. Huber. 1988. Hydrology and Floodplain Analysis, Addison-Wesley Publishing Company, USA 650 pp.

Beltaos, S. 1983. River ice jams: theory, case studies, and application. Journal of Hydraulic Engineering, Vol. 109 (10): pp. 1338-1359.

Beltaos, S., B.C. Burell, and S. Ismail. 1994. Ice and Sedimentation Processes in the Saint John River, Canada. Proc. of the Twelveth IAHR Symposium on Ice, Trondheim, Norway, pp.11-21.

Beltaos, S. and B.G. Krishnappan. 1982. Surges from ice jam releases: a case study. Canadian Journal of Civil Engineering, Vol. 9 (2): pp. 276-284.

Brooks, K.N., E.M. Davis, D.W. Kuehl. 1972. Program description and user manual for SSARR-Streamflow Synthesis and Resevoir Regulation, North Pacific Division, Corps of Engineers, Portland, Oregon, December.

Chow, T.E. 1959. Open Channel Hydraulics. McGraw-Hill Book Company, Inc.. 680 pp.

CSCE Task Force of River Models, 1987, One Dimensional River Models. Proceedings CSCE Annual Conference, Montreal, Quebec.

Cunge, J.A, F.M Holly, and A. Verwey, 1980. Practical Aspects of Computational River Hydraulics, Pitman Publishing Company, London, England. 420 pp.

Department of Indian Affairs and Northern Development, Northern Natural Resources Branch, Water Management Section, Yukon Territory. Hydrologic and Geomorphic Characteristics of Rivers and Drainage Basins in the Yukon Territory. March, 1976.

Dooge, J.C.I. 1986. Theory of Flood Routing. River Flow Modellling and Forecasting., D.A Kraijenhoff and J.R. Moll, Eds, D. Reidel Publishing Company, Dordrecht, Holland, pp. 39-64.

Doyle, P.F. and D.D. Andres. 1979. 1979 spring breakup and jamming on the Athabasca River near Fort McMurray. Report SWE-79-05, Transportation and Surface Water Engineering Division, Alberta Research Council, Edmonton, Alberta. 44 pp.

Ferrick, M.G. 1985. Analysis of river wave types. <u>Water Resources Research</u>, Vol. 21: pp. 209-220.

Fread, D.L. 1976. Flood Routing in Meandering Rivers with Floodplains. <u>Proceedings of the Symposium on Inland Waterways for Navigation, Flood Control, and Water Diversions, Waterways, Harbours and Coastal Engineering Division</u>, ASCE, pp.16-35.

Fread, D.L. 1988. <u>The NWS DAMBRK Model: Theoretical Background/User Documentation</u>. Office of Hydrology, National Weather Service (NWS), Maryland, U.S.A.

Gerard, R. 1979. River ice in hydrotechnical engineering: a review of selected topics. <u>Canadian Hydraulics Symposium</u> 79, Vancouver, British Columbia, pp. 1-29.

Gerard R., M. Jasek, F.E. Hicks. 1992. <u>Ice jam flood assessment - Yukon River at Dawson</u>. prepared for Indian and Northern Affairs Canada, Whitehorse, Yukon.

Gunaratnam, D.J., and F.E. Perkins. 1970. <u>Numerical Solutions for Unsteady Flows in Open Channels</u>. M.I.T. Hydrodynamics Laboratory Report No.127.

Henderson, F. M. 1966. <u>Open Channel Flow</u>. MacMillan Publishing Co., Inc., New York, N. Y., 522 pp.

Henderson, F.M. and R. Gerard. 1981. Flood waves caused by ice jam formation and failure. <u>Proc. of the IAHR Symposium on Ice</u>, Quebec, Vol. 1: pp. 277-287.

Hicks, F.E. and K. McKay. 1995. <u>Peace/Slave River Flow Modelling</u>. (NRBS Project 1154-D1) Water Resources Engineering Report No. 95-H3. Civil Engineering Department, University of Alberta, Edmonton, Canada.

Hicks, F.E. and P.M. Steffler. 1995. Comparison of finite element method for the St. Venant equations. <u>International Journal for Numerical Methods in Fluids</u>. 20: 99-113.

Hicks, F.E. and P.M. Steffler. 1992. A characteristic-dissipative-Galerkin Scheme for open channel flow. <u>ASCE Journal of Hydraulic Engineering</u>, 118(2): 337-352.

Hicks, F.E. and P.M. Steffler. 1990. <u>Finite Element Modeling of Open Channel Flow</u>. Water Resources Engineering Report No. 90-6, Civil Engineering Department, University of Alberta, Edmonton, Canada, 356 pp.

Hicks, F.E., Steffler, P.M. and R. Gerard. 1992. Finite element modelling of surge propagation and an application to the Hay River, N.W.T. Canadian Journal of Civil Engineering, 19(3): 454-462.

Hicks, F.E., N. Yasmin, and X. Chen. 1994. Peace River Flow Analysis. (NRBS Project 1154-C1) Water Resources Engineering Report No. 94-H2, Civil Engineering Department, University of Alberta, Edmonton, Canada.

Humes, T.M. and J. Dublin. 1988. A Comparison of the 1976 and the 1987 Saint John River Ice Jam Flooding with Emphasis on Antecedent Conditions. Proc. of the Fifth Workshop on Hydraulics of River Ice/Ice jams, Winnipeg, Canada, pp. 43-61.

Ismail, S. and J.L. Davis. 1992. Ice Jam Thickness Profiling on the the Saint John River, New Brunswick. Proc. of the Eleventh IAHR Symposium on Ice, Banff, Canada, pp.383-394.

Jasek, M. 1996. Conversation and Correspondence.

Jasek, M. 1993. Ice Jam Flood Assessment - Porcupine River at Old Crow - Phase 2a, Indian and Northern Affairs Canada, Whitehorse, Yukon.

Joliffe, I.B. 1982. Comparison of Implicit Finite Difference Methods to Solve the Unsteady Open Channel Flow Equations. Water Resources Engineering Report No. 82-1, Civil Engineering Department, University of Alberta, Edmonton, Canada. pp.134.

Joliffe, I. and R. Gerard. 1982. Surges released by ice jams. Proc. of the Workshop on the Hydraulics of Ice Covered Rivers, Edmonton, Alberta, pp. 253-259.

Kellerhals, R., C.R. Neill and D. I. Bray. 1972. Hydraulic and Geomorphic Characteristics of Rivers in Alberta. Research Council of Alberta, River Engineering and Surface Hydrology Report 72-1, Edmonton, Alberta, 54 pp.

Kindervater, A.D. 1985. Flooding Events in New Brunswick - An Historical Perspective. Water Planning and Management Branch, Inland Waters Directorate, Atlantic Region, Dartmouth, N.S. (Report IWD-AR-WPMB-84-65).

Krishnappan, B.G. 1983. MOBED User Manual Update I. Hydraulics Division, National Water Research Institute, Burlington, Ontario.

Krishnappan, B.G. and N. Snider. 1977. Mathematical modelling of sediment-laden flow in natural streams. Scientific Series No. 81, Inland Directorate, Canada Centre for Inland Waters, Burlington, Ontario. 48 pp.

178

Liggett, J.A. 1975. Basic Equations of Unsteady Flow. <u>Unsteady Flow in Open Channels</u> K. Mahmood and V. Yerjevich, Eds., Vol. 1, Water Resources Publications, Fort Collins, Colorado, pp. 29-62.

McKay, K. and F.E. Hicks. 1996. <u>Ice Jam Surge Modelling on the Porcupine River, Yukon</u>. Water Resources Engineering Report No. 96-H1, Civil Engineering Department, University of Alberta, Edmonton, Canada. 42 pp.

McKay, K., S. Mikolajczyk and F.E. Hicks. 1996. Application of hydraulic flood routing techniques to the 1995 flood in Southern Alberta. <u>Proc. of the CSCE Annual Conference</u>, Edmonton, June 1996.

Miller, W.A. and J.A. Cunge. 1975. Simplified Equations of Unsteady Flow. <u>Unsteady Flow in Open Channels</u>, K. Mahmood and V. Yevjevich, Eds., Vol. 1, Water Resources Publications, Fort Collins, Colorado, pp. 183-257.

Ohashi, K. and T. Hamada. 1970. Flow measurements of ice-covered rivers on Hokkaido. <u>IAHR Ice Symposium</u>, Reykjavik, Iceland.

Saade, R.G., S. Sarraf, and N. El-Jabi. 1993. Numerical modelling of surges resulting from ice jam releases. <u>Proc. of the CSCE Annual Conference, Eleventh Canadian Hydrotechnical Conference</u>, Fredricton, New Brunswick. Vol.1: pp.633-641.

Taggart, J. 1995. <u>The Peace River Natural Flow and Regulated Flow Scenarios - Daily Flow Data Report</u>. Surface Water Assessment Branch, Alberta Environmental Protection, Edmonton, Alberta.

Water Survey Canada. 1993. <u>HYDAT</u>

Watt, W.E., K.W. Lathem, C.R. Neill, T.L. Richards, J. Rouselle. 1989. <u>Hydrology of Floods in Canada: A Guide to Planning and Design</u>. National Research Council of Canada, Ottawa, Ontario. 245 pp.

Wong, J., S. Beltaos, and B.G. Krishnappan. 1985. Laboratory tests on surges created by ice jam releases. <u>Canadian Journal of Civil Engineering</u>, Vol. 12 (4): pp. 930-933.